The trending Ornstein-Uhlenbeck Process and its Applications in Mathematical Finance

Dr Christian Thierfelder

Hertford College

University of Oxford

A thesis submitted for the degree of

Mathematical Finance

April 12, 2015

Acknowledgements

First of all, I would like to thank Dr Johannes Ruf for pointing me in the direction of this project and for his patience, help and guidance while I was working on this thesis.

I also thank my former employer d-fine AG for the opportunity to participate in the Oxford Math Finance programme.

Above all I thank Martina for her endless support.

Contents

Chapter 1

Introduction and Scope

One of the first and most lasting questions of financial econometrics is whether asset prices are predictable. Perhaps because of the obvious analogy between financial investments and games of chance, mathematical models of asset prices have an unusually rich history that predates virtually every other aspect of economic analysis. The fact that many prominent mathematicians and scientists have applied their considerable skills to forecasting financial securities prices is a testament to the fascination and the challenges of this problem. Indeed, modern financial economics is firmly rooted in early attempts to beat the market. An endeavor that is still of current interest, discussed and debated in journal articles, conferences and at cocktail parties [CLM97]. There is now a large amount of evidence that the the predictability of financial asset returns. Despite the lack of consensus as to the sources of such predictability - some attribute it to inefficient markets or irrational investors - there is a growing consensus that predictability is a genuine feature of many financial asset returns.
The aim of this thesis is to analyse and extend the work of Lo and Wang [LW95] which showed the impact of asset return predictability on option pricing. As predictability is understood as the conditional expectation of instantaneous returns it is connected to the drift term of the asset process. The continuous-time no-arbitrage pricing framework of Black and Scholes [BS73] and Merton [M73], and in the martingale pricing approach of Cox, Ross, Harrison and Kreps [DS06] shows that option pricing formulas are functionally independent of the drift of the underlying price process. This seems to imply that predictability is irrelevant for option prices
If the unconditional variance of the true finite holding period asset return process is fixed, then as more predictability is introduced via the drift, the value of the diffusion coefficient must change to keep the unconditional variance constant. Therefore, although the option pricing formula is unaffected by changes in predictability, op-

tion prices do change. Ignoring predictability in the drift introduces an error in the volatility that can lead to incorrect prices.

The thesis is structured as follows. In Chapter 2 we review some of the known facts about stochastic processes and the pricing of European options, thereby setting the stage for the analysis of the influence of predicability in option pricing. Chapter 3 then introduces the work by Lo and Wang on the trending OU process and analyses the implications trending OU process. Chapter 4 continues with the investigation of the bivariate extension of the trending OU process. Chapter 5 presents the analysis of market data for equity indices, stocks and futures as well and estimates the potential impact of predictability on real option prices. Chapter 6 extends the trending OU process to a jump-diffusion model. Finally, Chapter 7 shows the application of the bivariate trending OU process in a simple, analytically solvable interest rate model.

Chapter 2

Theoretical Framework

2.1 Brownian Motion

The botanist Robert Brown [B28] observed in 1827 that pollen particle in water move in a random fashion, but was not able to explain the mechanism that caused this motion. In 1905 Einstein [E05] argued that the motion of the particle can be explained by the momentum and energy exchange due to collisions of the particle with the much smaller liquid molecules surrounding it. Einstein was also able to give a first mathematical description of the transition probability. The sound mathematical foundation for Brownian motion as a stochastic process was developed by Norbert Wiener in the 1920s [W23] .

The Brownian Motion process W_t serves as a basic model for the cumulative effect of pure noise. It is an adapted stochastic process on a filtered probability space $(\Omega, \mathcal{F}, \mathbb{P})$ with the following defining properties [KS87]

1. (Independence of increments) $W_t - W_s$ for $t > s$ is independent of the past, that is of W_u, $0 \leq u \leq s$ or of $\mathcal{F}_s$, the σ-field generated by W_u, $u \leq s$.

2. (Normal increments) $W_t - W_s$ has normal distribution $\mathcal{N}(0, t)$ with mean zero and variance $t - s$.

3. (Continuity of paths) W_t, $t \leq 0$ are continuous functions of t with $B_0 = 0$.

Many important continuous-time Markov processes can be defined as solutions to stochastic differential equations with drift and diffusion coefficients, that depend only on the current value of the process. The general form of such an equation (for a one-dimensional process with a one-dimensional driving Brownian motion) is

$$dX_t = \alpha(X_t)dt + \sigma(X_t)dW_t \tag{2.1}$$

where $\{W_t\}_{t\geq 0}$ is a standard Wiener process.

2.2 Stochastic Processes

2.2.1 Arithmetic Brownian Motion

The arithmetic Brownian motion (with drift) is the solution of

$$dX_t = \alpha dt + \sigma dW_t \tag{2.2}$$

with initial condition $X_0 = x_0$. It can be obtained from direct integration of the stochastic differential equation

$$X_t = x_0 + \alpha t + \sigma W_t. \tag{2.3}$$

2.2.2 Geometric Brownian Motion

The geometric Brownian motion (GBM) can be derived from the arithmetic Brownian motion by defining $Y_t = e^{X_t}$ and using Itô's lemma

$$dY_t = \left(\alpha Y_t + \frac{\sigma^2}{2} Y_t\right) dt + \sigma Y_t dW_t. \tag{2.4}$$

With $\mu = \alpha + \sigma^2/2$ the geometric Brownian motion is defined by

$$dY_t = \mu Y_t dt + \sigma Y_t dW_t \tag{2.5}$$

with initial condition $Y_0 = y_0$. The solution can then be found by using the solution of the arithmetic Brownian motion

$$Y_t = y_0 e^{\left(\mu - \frac{\sigma^2}{2}\right)t + \sigma W_t}. \tag{2.6}$$

2.2.3 Ornstein-Uhlenbeck Process

One of the main feature of the geometric Brownian motion is proportionality of the drift term to Y_t itself. Therefore the process can be interpreted to be repelled from $Y = 0$. The idea of an repelling/attracting point can be easily generalised by the Ornstein-Uhlenbeck (OU) process [OU30]. It is defined by an arbitrary equilibrium level θ and percentage drift κ

$$dU_t = \kappa \left(\theta - U_t\right) dt + \sigma dW_t. \tag{2.7}$$

The sign of κ determines if the equilibrium is attractive or repulsive. As the OU process is used to model mean reverting behaviour we have $\kappa > 0$.

The solution of the stochastic differential equation (SDE) can be found by applying Itô's lemma to $e^{\kappa t}U_t$

$$d(e^{\kappa t}U_t) = \left(\kappa e^{\kappa t}U_t + e^{\kappa t}\kappa(\theta - U_t)\right)dt + e^{\kappa t}\sigma dW_t. \tag{2.8}$$

Time integration gives then

$$e^{\kappa t}U_t - U_0 = \kappa\theta \int_0^t e^{\kappa s}ds + \sigma \int_0^t e^{\kappa s}dW_s \tag{2.9}$$

which leads to

$$U_t = e^{-\kappa t}u_0 + \theta(1 - e^{-\kappa t}) + \sigma \int_0^t e^{\kappa(s-t)}dW_s \tag{2.10}$$

for the initial condition $U_0 = u_0$.

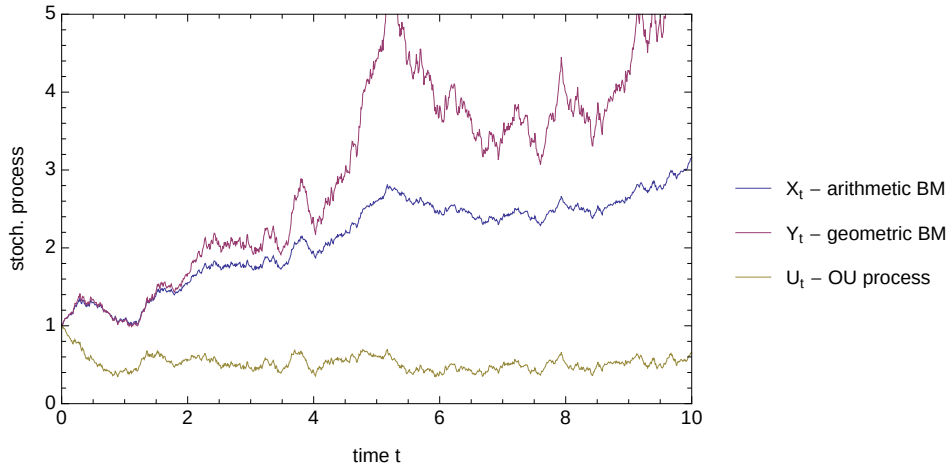

Figure 2.1: Sample paths of various stochastic processes with parameters $\mu = 0.15$, $\sigma = 0.2$, $\theta = 0.5$ and $\kappa = 5$

Mean and variance of U_t are given by

$$\mathbb{E}[U_t] = e^{-\kappa t}u_0 + \theta(1 - e^{-\kappa t}) \tag{2.11}$$

$$\begin{aligned}\text{var}[U_t] &= \sigma^2 \int_0^t e^{2\kappa(s-t)}ds \\ &= \frac{\sigma^2}{2\kappa}\left(1 - e^{-2\kappa t}\right).\end{aligned} \tag{2.12}$$

2.2.4 Trending Ornstein-Uhlenbeck Processes

In the OU process the mean reversion was towards a constant equilibrium level θ. This can in a first step be generalised to a linearly growing trend μt

$$d(V_t - \mu t) = -\kappa\left(V_t - \mu t\right)dt + \sigma dW_t. \tag{2.13}$$

This means the process when it deviates from the trend μt it is pulled back with a rate proportional to its deviation. The trending OU process is therefore called trend-stationary. The SDE can be written as

$$dV_t = (\mu - \kappa[V_t - \mu t])\, dt + \sigma dW_t. \tag{2.14}$$

The trending OU process can be integrated by using the fact that $V_t - \mu t$ is an OU process with $\theta = 0$. Therefore we obtain with the initial condition $V_0 = v_0$

$$V_t = \mu t + v_0 e^{-\kappa t} + \sigma \int_0^t e^{\kappa(u-t)} dW_u. \tag{2.15}$$

The arithmetic Brownian motion can be recovered from the trending OU process in

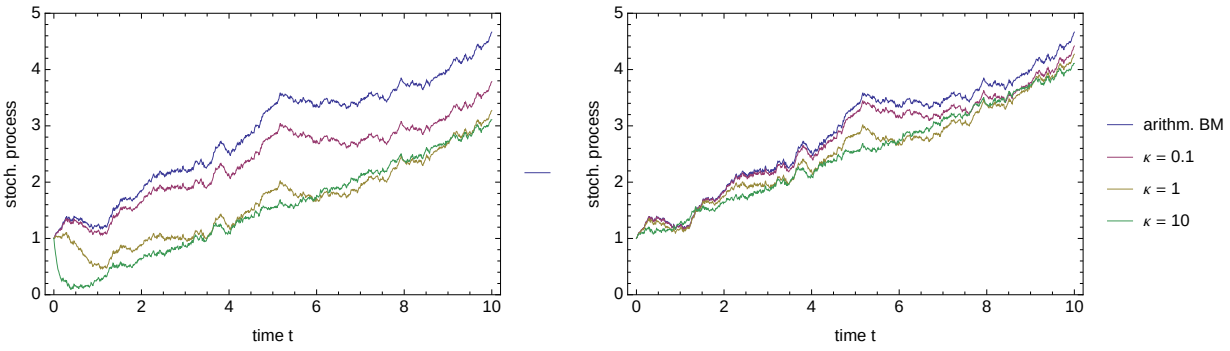

Figure 2.2: (left) Trending OU process and (right) shifted trending OU process with parameters $\mu = 0.3$, $\sigma = 0.2$ and $\kappa = 0.1, 1$ and 10. In the limit $\kappa \to 0$ the trending OU process is identical to the arithmetic Brownian motion.

the limit $\kappa \to 0$. Nevertheless a larger deviation between the arithmetic Brownian motion and the trending OU process is apparent (fig. 2.2 left). It originates from the construction as the process is mean reverting to the linear trend μt. It can be removed by making the process mean reverting to the affine trend $v_0 + \mu t$

$$dV_t = (\mu - \kappa[V_t - (V_0 + \mu t)])\, dt + \sigma dW_t \tag{2.16}$$

$$d(V_t - \mu t) = \kappa\, (V_0 - [V_t - \mu t])\, dt + \sigma dW_t. \tag{2.17}$$

The analytic solution can again be found by utilising the solution of the OU process and is given by

$$V_t = v_0 + \mu t + \sigma \int_0^t e^{\kappa(s-t)} dW_s. \tag{2.18}$$

To obtain further intuition for the behaviour of the trending OU process we calculate the unconditional moments of the process. The expectation value and the variance can be simply obtained utilising Itô's lemma

$$\mathbb{E}[V_t] = v_0 + \mu t \tag{2.19}$$

$$\begin{aligned} \text{var}[V_t] &= \mathbb{E}\left[(V_s - \mathbb{E}[V_s])^2\right] \\ &= \sigma^2 \int_0^t e^{2\kappa(u-t)} ds \\ &= \frac{\sigma^2}{2\kappa}\left(1 - e^{-2\kappa t}\right). \end{aligned} \tag{2.20}$$

The conditional transition density of V_t is given by

$$p(V_t, t; V_0, 0) = \sqrt{\frac{\kappa}{1 - e^{-2\kappa t}}} \frac{1}{\sigma\sqrt{\pi}} e^{-\frac{\kappa}{1-e^{-2\kappa t}}\left(\frac{V_t - V_0 - \mu t}{\sigma}\right)^2}. \tag{2.21}$$

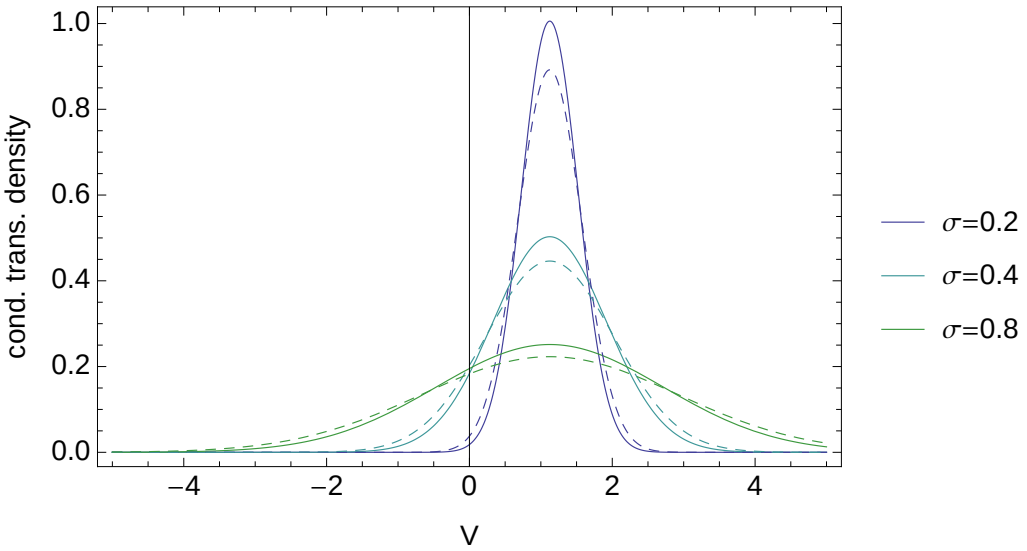

Figure 2.3: Conditional transition density for $\kappa = 0.05$ trending OU (solid) and arithmetic Brownian motion (dashed)

For the calculation of the covariance we assume $s < t$

$$\begin{aligned}
\operatorname{cov}[V_s, V_t] &= \mathbb{E}\left[(V_s - \mathbb{E}[V_s])(V_t - \mathbb{E}[V_t])\right] \\
&= \sigma^2 \mathbb{E}\left[\int_0^s e^{\kappa(u-s)} dW_u \cdot \int_0^t e^{\kappa(u-t)} dW_u\right] \\
&= \sigma^2 e^{-\kappa(s+t)} \mathbb{E}\left[\int_0^s e^{\kappa u} dW_u \cdot \int_0^t e^{\kappa u} dW_u\right] \\
&= \sigma^2 e^{-\kappa(s+t)} \mathbb{E}\left[\int_0^s e^{\kappa u} dW_u \cdot \left(\int_0^s e^{\kappa u} dW_u + \int_s^t e^{\kappa u} dW_u\right)\right] \\
&= \sigma^2 e^{-\kappa(s+t)} \mathbb{E}\left[\left(\int_0^s e^{\kappa u} dW_u\right)^2 + \left(\int_0^s e^{\kappa u} dW_u \cdot \int_s^t e^{\kappa u} dW_u\right)\right] \\
&= \sigma^2 e^{-\kappa(s+t)} \mathbb{E}\left[\left(\int_0^s e^{\kappa u} dW_u\right)^2\right] + \mathbb{E}\left[\int_0^s e^{\kappa u} dW_u \cdot \int_s^t e^{\kappa u} dW_u\right] \\
&= \sigma^2 e^{-\kappa(s+t)} \int_0^s e^{2\kappa u} du \\
&= \frac{\sigma^2}{2\kappa} e^{-\kappa(s+t)} \left(e^{2\kappa \min(s,t)} - 1\right). \qquad (2.22)
\end{aligned}$$

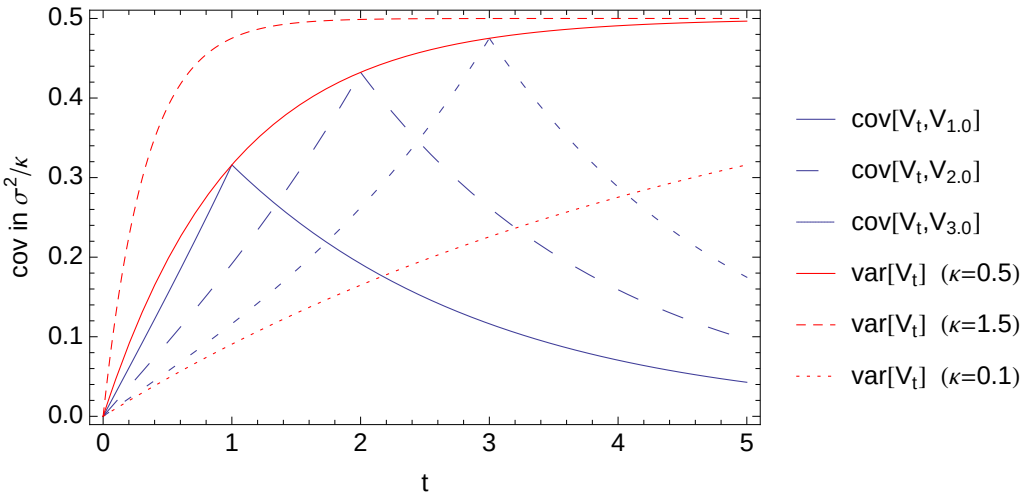

Figure 2.4: Plot of the covariance function (2.22) of the trending OU process

2.3 Black-Scholes Model

In their seminal paper Black and Scholes [BS73] developed an option pricing model which was later formalised by Merton [M73]. Due to its small number of input parameter and simplicity it enjoys great popularity among academics and practitioners.

The option value within the Black-Scholes framework is based on the concept of perfect replication of contingent claims. This means that an investor can replicate the options return by continuously rebalancing a self-financing portfolio including stocks and risk-free bonds. The price of the option is then determined by the price of the replicating portfolio.
We make the following assumptions convening the market

1. There are no market imperfections, e.g. taxes, transactions costs, short sales constraints, and trading is continuous and frictionless.

2. The stock price dynamics are given by a geometric Brownian motion.

3. There is unlimited risk-free borrowing and lending.

4. There is no arbitrage.

This can be summarised as the assumption of a perfect market.
We start by describing the price processes of two securities, a risk free bank bond and a risky asset (common stock). The first security corresponds to a money market account. The short-term interest rate r is assumed to be constant. Under continuous compounding we obtain for the price process the ordinary differential equation

$$dB_t = rB_t dt. \tag{2.23}$$

with $B_0 = 1$. The stock price process is modelled by a geometric Brownian motion S_t and is described by a linear stochastic differential equation

$$dS_t = \mu S_t dt + \sigma S_t dW_t \qquad (S_0 > 0) \tag{2.24}$$

where μ is a constant rate of return of the stock price, σ is a constant volatility and S_0 is the ignition value. As we shall see later, the restrictive condition of a constant μ can be weakened substantially.
A self-financing trading strategy is an adapted process (ϕ, ψ) consisting of a portfolio (ϕ_t, ψ_t) of risky and risk-free asset held at time t with value $V_t(\phi, \psi) = \phi_t S_t + \psi_t B_t$, and the self-financing condition

$$dV_t = \phi_t dS_t + \psi_t dB_t. \tag{2.25}$$

This means that the changes in value of the portfolio are solely due to changes in the values of the underlying assets. The concept of a self-financing trading strategy is formally based on the definition of the Itô integral. Intuitively its choice is supported

by the fact that the underlying process is integrated in a predictable way. This means that the value is taken on the left end of the infinitesimal time interval compared to the Stratonovich integral.
For the discounted value of the trading strategy and the asset price process we write

$$\tilde{V}_t = V_t/B_t \tag{2.26}$$

$$\tilde{S}_t = S_t/B_t. \tag{2.27}$$

Then Itô's lemma yields

$$\begin{aligned} d\tilde{V}_t &= \frac{1}{B_t}dV_t - \frac{V_t}{B_t^2}dB_t - \frac{1}{B_t^2}dV_t dB_t + \frac{V_t}{B_t^3}dB_t dB_t \\ &= \frac{1}{B_t}dV_t - \tilde{V}_t r dt \\ &= \frac{1}{B_t}(\phi_t dS_t + \psi_t dB_t) - \frac{1}{B_t}(\phi_t S_t + \psi_t B_t) r dt \\ &= \phi_t \left(\frac{dS_t}{B_t} - r\frac{S_t}{B_t}dt \right) \\ &= \phi_t d\tilde{S}_t \end{aligned}$$

which can directly be integrated

$$\tilde{V}_t = \tilde{V}_0 + \int_0^t \phi_s d\tilde{S}_s. \tag{2.28}$$

For the discounted price process it is found

$$\begin{aligned} d\tilde{S}_t &= \frac{dS_t}{B_t} - r\frac{S_t}{B_t}dt \\ &= (\mu - r)\tilde{S}dt + \sigma\tilde{S}_t dW_t. \end{aligned}$$

We see that the discounted stock price follows a martingale under the actual probability measure $\mathbb{P}$ if and only if $\mu = r$. A probability measure $\widetilde{\mathbb{P}}$ equivalent to $\mathbb{P}$ is called a martingale measure for $\tilde{S}$ if and only if $\tilde{S}$ is a local martingale under $\widetilde{\mathbb{P}}$. Choosing $\gamma_t = (r-\mu)/\sigma$ and utilising the Girsanov theorem (A.2), the new measure $\widetilde{\mathbb{P}}$ given by the Radon-Nykodym derivative

$$\frac{d\widetilde{\mathbb{P}}}{d\mathbb{P}} = e^{\frac{r-\mu}{\sigma}W_T - \frac{1}{2}\frac{(r-\mu)^2}{\sigma^2}T}. \tag{2.29}$$

The so called risk neutral measure with $d\widetilde{W}_t = dW_t - (r-\mu)/\sigma dt$ can be defined as the measure under which $\tilde{S}_t$ is a martingale

$$d\tilde{S}_t = \sigma\tilde{S}_t d\widetilde{W}_t. \tag{2.30}$$

The stock price at time t equals $S_t = \tilde{S}_t B_t$ and thus the dynamics of the stock price under $\widetilde{\mathbb{P}}$ is

$$dS_t = rS_t dt + \sigma S_t d\widetilde{W}_t. \tag{2.31}$$

Therefore we can express $\tilde{V}_t$ as an Itô integral

$$\tilde{V}_t = \tilde{V}_0 + \int_0^t \phi_s \sigma \tilde{S}_s d\widetilde{W}_s \tag{2.32}$$

which implies that $\tilde{V}_t$ is a martingale ($\tilde{V}_t = \widetilde{\mathbb{E}}[\tilde{V}_T|\mathcal{F}_t]$) and V_t can be written as

$$V_t = B_t \cdot \widetilde{\mathbb{E}}[{B_T}^{-1} V_T|\mathcal{F}_t].$$

The existence of the replication strategy is guaranteed by the martingale representation theorem (A.3). An European contingent claim X that settles at time T is called attainable in the Black-Scholes model if it can be replicated by means of an admissible strategy. Such a claim has a uniquely defined arbitrage price $\pi_t(X) = V_t$ at time t of any admissible trading strategy (ϕ, ψ) replicating $X = V_T(\phi, \psi)$. Using the payoff function of the call option

$$C(S_T, T) = (S_T - K)^+ \tag{2.33}$$

as boundary condition, an analytic solution of the Black-Scholes equation can be found

$$C_{\mathrm{BS}}(S, t) = e^{r(T-t)} \widetilde{\mathbb{E}} \left[(S_T - K)^+ \, | S_0 \right]. \tag{2.34}$$

Evaluating the expectation value,‘ which contains the conditional transition probability density $p(S_T, T|S_t, t)$ of the geometric Brownian motion

$$C_{\mathrm{BS}}(S_t, t) = e^{-r(T-t)} \int_{-\infty}^{\infty} (S_T - K)^+ \, p(S_T, T|S_t, t) dS_T \tag{2.35}$$

gives then by using $S_T = S_t e^{(r-\sigma^2/2)(T-t)+\sigma(W_T - W_t)}$

$$C_{\mathrm{BS}}(S_t, t; K, T, r, \sigma) = S\mathcal{N}(d_1) - Ke^{-r(T-t)}\mathcal{N}(d_2) \tag{2.36}$$

where

$$d_1 = \frac{\log \frac{Se^{-r(T-t)}}{K} + \frac{1}{2}\sigma^2(T-t)}{\sigma\sqrt{T-t}} \tag{2.37}$$

$$d_2 = d_1 - \sigma\sqrt{T-t} \tag{2.38}$$

and $\mathcal{N}(\cdot)$ is the standard normal cumulative distribution function.

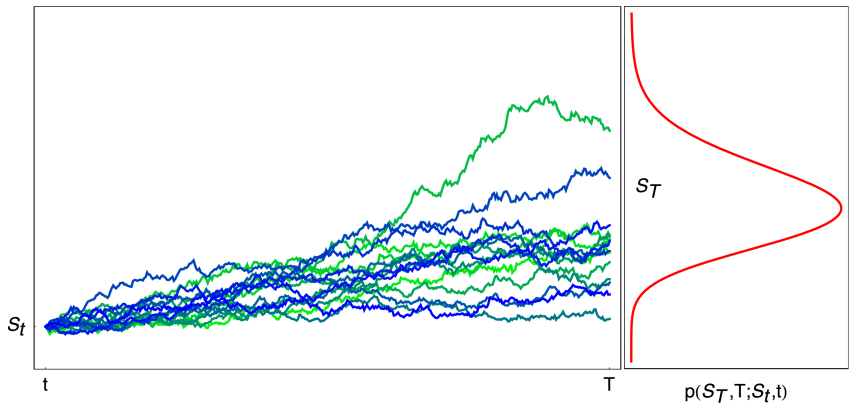

Figure 2.5: Conditional transition probability density of the geometric Brownian motion

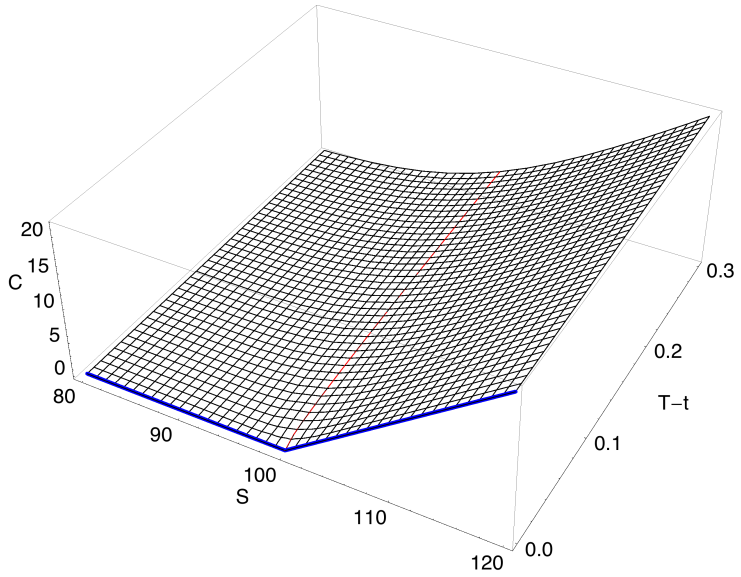

Figure 2.6: Black-Scholes call price for $r = 0.05$, $\sigma = 0.2$ and $K = 100$. The payoff function is marked in blue.

Chapter 3

The Effects of Asset Return Predictability

3.1 Definitions of Return

Although prices are the fundamental market observables most investors and empirical studies focus on returns. This can be explained by the stationarity of the prices return process. There are multiple return definitions available but here we focus on simple and log-returns.
In the derivation of the Black-Scholes equation the stock price process S_t was modelled as geometric Brownian motion

$$dS_t = \mu S_t dt + \sigma S_t dW_t. \tag{3.1}$$

A new process $s_t = \log S_t$ can now be defined which is called the log-price process. Utilising Itôs lemma yields

$$ds_t = \left(\mu - \frac{\sigma^2}{2}\right) dt + \sigma dW_t \tag{3.2}$$

which can be integrated directly

$$S_t = S_0 e^{\left(\mu - \frac{\sigma^2}{2}\right)t + \sigma W_t} \tag{3.3}$$

where S_0 is the stock price observed at time zero.

3.1.1 Simple Return

The simple return of an asset for the period dt is defined as the relative change in the asset price

$$R_{dt}(t) = \frac{S_t - S_{t-dt}}{S_{t-dt}} \tag{3.4}$$

where S_t is the price of the asset at time t and dt is the return period. If the asset is hold for k periods dt the k-period simple return is defined by

$$R_{kdt}(t) = \frac{S_t - S_{t-kdt}}{S_{t-kdt}} \tag{3.5}$$

or

$$S_t = S_{t-kdt}(1 + R_{kdt}(t)) = S_{t-kdt}(1 + R_{dt}(t - kdt + dt)) \times ... \times (1 + R_{dt}(t)). \tag{3.6}$$

Therefore the non-linear relation between the one-period and the k-period return is given by

$$1 + R_{kdt}(t) = \prod_{j=0}^{k-1}(1 + R_{dt}(t - jdt)) \tag{3.7}$$

which can be approximated by

$$R_{kdt}(t) = \sum_{j=0}^{k-1} R_{dt}(t - jdt) \tag{3.8}$$

for small returns. In the case of a geometric Brownian motion we obtain

$$\begin{aligned} R_{dt}(t) &= e^{\left(\mu - \frac{\sigma^2}{2}\right)dt + \sigma(W_t - W_{t-dt})} - 1 \\ &\simeq \left[1 + \left(\mu - \frac{\sigma^2}{2}\right)dt + \sigma(W_t - W_{t-dt}) + \frac{1}{2}\sigma^2(W_t - W_{t-dt})^2 + \cdots\right] - 1 \\ &= \mu dt + \sigma(W_t - W_{t-dt}) \end{aligned} \tag{3.9}$$

which is the same as dS_t/S_t.

3.1.2 Log-Return

For various reasons the log-return is often used instead

$$\begin{aligned} r_{dt}(t) &= \log S_t - \log S_{t-dt} \\ &= \log \frac{S_t}{S_{t-dt}}. \end{aligned} \tag{3.10}$$

which is closely related to R_{dt} by

$$\begin{aligned} r_{dt}(t) &= \log \frac{(S_t - S_{t-dt}) + S_{t-dt}}{S_{t-dt}} \\ &= \log (1 + R_{dt}(t)) \\ &= R_{dt} - \frac{1}{2}{R_{dt}}^2 + \frac{1}{3}{R_{dt}}^3 + ... \end{aligned} \tag{3.11}$$

and for small dt we have $r_{dt}(t) = R_{dt}(t)$. The major advantage of the log-return is that the k-period return is simply the sum of the one-period returns

$$\begin{aligned} r_{kdt}(t) &= \log\left(1 + R_{kdt}(t)\right) \\ &= \sum_{j=0}^{k-1} \log(1 + R(t - jdt)) \\ &= \sum_{j=1}^{k-1} r_{dt}(t - jdt). \end{aligned} \tag{3.12}$$

For the geometric Brownian motion we obtain for the log-return

$$\begin{aligned} r_{dt}(t) &= \log\left(e^{\left(\mu - \frac{\sigma^2}{2}\right)dt + \sigma(W_{t+dt} - W_t)}\right) \\ &= \left(\mu - \frac{\sigma^2}{2}\right)dt + \sigma(W_{t+dt} - W_t). \end{aligned} \tag{3.13}$$

Both returns are representations of arithmetic Brownian motions with the same volatility but different drifts. In case of the geometric Brownian motion the log-return is normally distributed with mean and variance given by

$$\mathbb{E}\left[r_{\delta t}|\mathcal{F}_t\right] = \left(\mu - \frac{\sigma^2}{2}\right)\delta t = \nu\delta t \tag{3.14}$$

$$\text{var}\left[r_{\delta t}|\mathcal{F}_t\right] = \sigma^2\delta t. \tag{3.15}$$

The best estimate of $\nu\delta t$ is given by the sample mean of the $r_{\delta t}(t_i)$, $i = 0, 1, ..., n-1$

$$\hat{\nu}\delta t = \frac{1}{n}\sum_{i=0}^{n-1} r_{\delta t}(t_i) = \bar{r}_{\delta t} \tag{3.16}$$

and the best estimate of $\sigma^2\delta t$ is given by

$$\hat{\sigma}^2\delta t = \frac{1}{n-1}\sum_{i=0}^{n-1}(r_{\delta t}(t_i) - \bar{r}_{\delta t})^2. \tag{3.17}$$

3.1.3 Distributions of Asset Returns

It is far from obvious why commodity, stock and bond prices should behave in a particular fashion. Nevertheless a number of empirical studies [BCK92, C05, CLM97] have identified a set of common features among financial days that are known as *stylised facts*. Cont [C01] in particular provides a comprehensive survey of these facts which include

- *Heavy tails*: the (unconditional) distribution of returns seems to display a power-law tail, with a finite tail index ($\xi \in [2, 5]$). In particular this excludes stable laws with infinite variance and the normal distribution. However, the precise form of the tails is difficult to determine.

- *Conditional heavy tails*: even after correcting returns for volatility clustering (e.g. via GARCH-type models) the residual time series still exhibit heavy tails. However, the tails are less heavy than in the unconditional distribution of returns.

- *Gain/loss asymmetry*: one observes large drawdowns in stock prices and stock index values but not equally large upward movements (except for exchange rates).

- *Aggregational Gaussianity*: the shape of the distribution is not the same at different time scales. In particular by increasing time scale over which returns are calculated, their distribution resemble a normal distribution.

- *Volatility clustering*: different measures of volatility display a positive autocorrelation over several days, which quantifies the fact that high-volatility events tend to cluster in time.

- *Absence of autocorrelations*: (linear) autocorrelations of asset returns are often small. Exceptions are equities and very small intraday time scales (≈ 20 minutes) for which microstructure effects come into play.

- *Slow decay of autocorrelation in absolute returns*: the autocorrelation function of absolute returns decays slowly as a function of the time lag, roughly as a power law with an exponent $\beta \in [0.2, 0.4]$. This is often interpreted as a sign of long-range dependence.

- *Leverage effect*: most measures of volatility of an asset are negatively correlated with the returns of that asset.

- *Volume/volatility correlation*: trading volume is correlated with all measures of volatility.

- *Asymmetry in time scales*: coarse-grained measures of volatility predict fine-scale volatility better than the other way round.

The properties mentioned above are model free in the sense that they do not result from a parametric hypothesis on the return process but from rather general hypotheses of qualitative nature. Therefore they should be viewed as constraints that a stochastic process has to verify in order to reproduce the statistical properties of returns accurately. Unfortunately, most currently existing models fail to reproduce all these statistical features at once, showing that they are indeed very constraining [C01].

3.2 Trending OU Return Process

Although it is well known that the Black-Scholes equation does not depend on the drift of the underlying asset μ, the drift does not need to be constant as in the case of a geometric Brownian motion. The drift can be a function of S and other model variables like σ. This implies that the Black-Scholes formula is valid for a wide range of price processes which can show complex patterns of predictability. This fact was first mentioned by Merton [M73] but is often overlooked in standard textbook.
We will now follow Lo and Wang's [LW95] work and replace the geometric Brownian motion assumption by an alternative price process. The starting point for this extension is the detrended log-price process $q_t = \log S_t - \mu t$. In the case of the geometric Brownian motion price process S_t the log-price process $s_t = \log S_t$ is the arithmetic Brownian motion and the detrended log-price process is given by

$$\begin{aligned} dq_t &= d(\log S_t - \mu t) \\ &= \sigma dW_t \end{aligned} \tag{3.18}$$

which serves as the starting point for extending the model. The idea is to make the process q_t mean reverting with a speed of reversion κ

$$dq_t = \kappa(q_0 - q_t) + \sigma dW_t \tag{3.19}$$

which is the trending OU process (2.17). Using this process seems to be an appropriate choice as it simplifies to the standard Black-Scholes model in the limit $\kappa \to 0$. The connection of the various processes is show in figure 3.1
The log-price is then given by

$$ds_t = (\mu - \kappa[s_t - s_0 - \mu t])\, dt + \sigma dW_t. \tag{3.20}$$

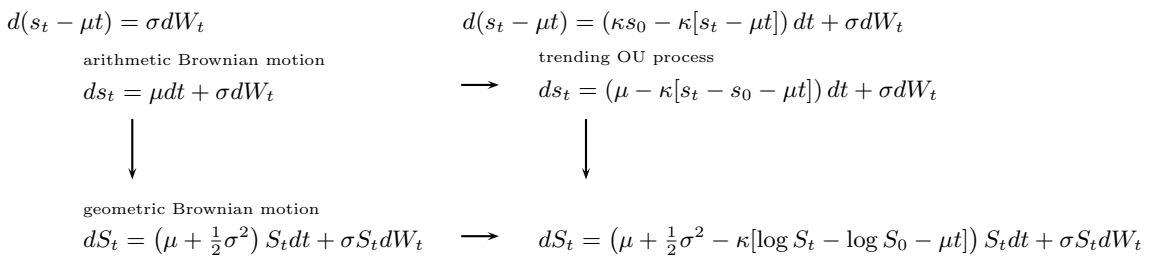

Figure 3.1: Extension of classical Black-Scholes framework by introduction of one additional parameter κ

The explicit solution is given by (2.15)

$$s_t = s_0 + \mu t + \sigma \int_0^t e^{\kappa(u-t)} dW_u \tag{3.21}$$

from which we can obtain the continuously compounded τ-period returns

$$\begin{aligned} r_\tau(t) &= s_t - s_{t-\tau} \\ &= \mu\tau + \sigma \int_0^t e^{\kappa(s-t)} dW_s - e^{\kappa\tau}\sigma \int_0^{t-\tau} e^{\kappa(s-t)} dW_s. \end{aligned} \tag{3.22}$$

Unlike the arithmetic Brownian motion which is called difference-stationary the trending OU process s_t is trend-stationary as its deviations from the trend follow a stationary process.

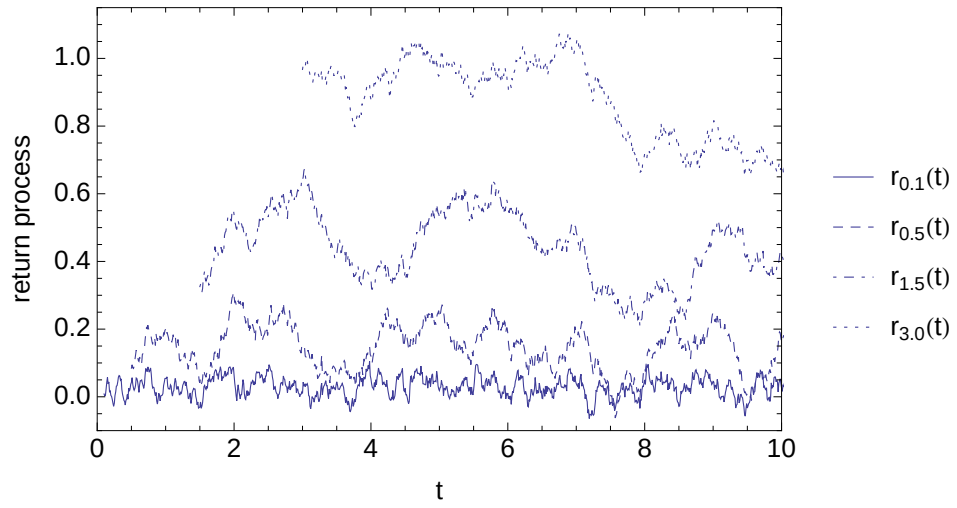

Figure 3.2: Trending OU return processes $r_\tau(t)$ for various τ ($\mu = 0.3, \sigma = 0.1, \kappa = 1$)

Figure 3.2 depicts an example of a trending OU process and the associated return. We see that expectation has a significant τ dependence but that the variance seems to have a finite limit (in contrast to the return of the arithmetic Brownian motion).

This observation can be supported by calculating the moments of $r_\tau(t)$. Indeed we obtain with the expectation

$$\mathbb{E}\left[r_\tau(t)\right] = \mu\tau \tag{3.23}$$

and the variance

$$\begin{aligned}
\operatorname{var}\left[r_\tau(t)\right] &= \mathbb{E}\left[\left(r_\tau(t) - \mathbb{E}\left[r_\tau(t)\right]\right)^2\right] \\
&= \mathbb{E}\left[\left(\sigma\int_0^t e^{\kappa(s-t)}dW_s - e^{\kappa\tau}\sigma\int_0^{t-\tau} e^{\kappa(s-t)}dW_s\right)^2\right] \\
&= \sigma^2\int_0^t e^{2\kappa(s-t)}ds - 2\sigma^2 e^{\kappa\tau}\int_0^{t-\tau} e^{2\kappa(s-t)}ds + \sigma^2 e^{2\kappa\tau}\int_0^{t-\tau} e^{2\kappa(s-t)}ds \\
&= \frac{\sigma^2}{\kappa}(1-e^{-2\kappa t}) + \frac{\sigma^2}{\kappa}e^{\kappa\tau}(e^{-2\kappa t} - e^{-2\kappa\tau}) + \frac{\sigma^2}{2\kappa}e^{2\kappa\tau}(e^{-2\kappa\tau} - e^{-2\kappa t}) \\
&= \frac{\sigma^2}{\kappa}\left[(1-e^{-\kappa\tau}) - \frac{1}{2}e^{-2\kappa t}(1-e^{\kappa\tau})^2\right].
\end{aligned} \tag{3.24}$$

Due to the existence of stationarity the unconditional moments are defined as the limit of the corresponding conditional moment as t increases without bound ($t \to \infty$). The unconditional variance is therefore given by

$$\operatorname{var}\left[r_\tau(t)\right] = \frac{\sigma^2}{\kappa}\left[1 - e^{-\kappa\tau}\right]. \tag{3.25}$$

The variance of τ period returns of the trending OU process has the finite limit σ^2/κ in contrast to the arithmetic Brownian motion in which the variance

$$\lim_{\kappa\to 0}\frac{\sigma^2}{\kappa}\left[1 - e^{-\kappa\tau}\right] = \sigma^2\tau \tag{3.26}$$

is increasing linearly with τ (see figure 3.3). This can be interpreted as an implication of the trend stationarity. For the covariance of r_τ we utilise its definition with $t-\tau \geq s$

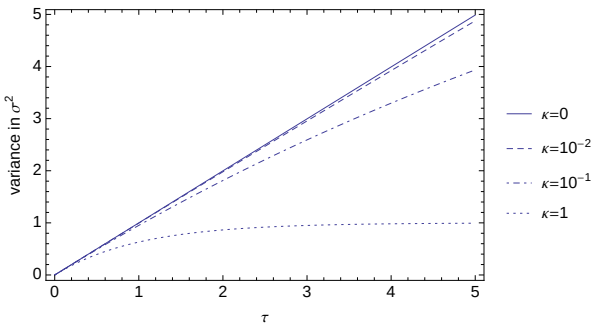

Figure 3.3: Variance of the trending OU return process for $\kappa = 0, 10^{-2}, 10^{-1}$ and 1

$$
\begin{aligned}
\operatorname{cov}(r_\tau(s), r_\tau(t)) &= \mathbb{E}[(r_\tau(s) - \mathbb{E}[r_\tau(s)])(r_\tau(t) - \mathbb{E}[r_\tau(t)])] \\
&= \sigma^2 e^{-\kappa(s+t)} \left\{ \mathbb{E}\left[\left(\int_0^s e^{\kappa u} dW_u \right)^2 \right] - e^{\kappa\tau} \mathbb{E}\left[\left(\int_0^s e^{\kappa u} dW_u \right)^2 \right] \right. \\
&\qquad - e^{\kappa\tau} \mathbb{E}\left[\left(\int_0^{s-\tau} e^{\kappa u} dW_u \right)^2 \right] \\
&\qquad \left. + e^{2\kappa\tau} \mathbb{E}\left[\left(\int_0^{s-\tau} e^{\kappa u} dW_u \right)^2 \right] \right\} \\
&= \sigma^2 e^{-\kappa(s+t)} (1 - e^{\kappa\tau}) \left\{ \mathbb{E}\left[\left(\int_0^s e^{\kappa u} dW_u \right)^2 \right] \right. \\
&\qquad \left. - e^{\kappa\tau} \mathbb{E}\left[\left(\int_0^{s-\tau} e^{\kappa u} dW_u \right)^2 \right] \right\} \\
&= \sigma^2 e^{-\kappa(s+t)} (1 - e^{\kappa\tau}) e^{-\kappa\tau} \frac{(e^{\kappa\tau} - 1)(e^{2\kappa s} + e^{\kappa\tau})}{2\kappa} \\
&= -\frac{\sigma^2}{2\kappa} e^{-\kappa(t-s-\tau)} (1 - e^{-\kappa\tau})^2 (1 + e^{\kappa(\tau - 2s)}).
\end{aligned} \tag{3.27}
$$

The correlation function is then given by

$$
\begin{aligned}
&\operatorname{corr}(r_\tau(t - k\tau), r_\tau(t)) \\
&= \frac{-\frac{\sigma^2}{2\kappa} e^{-\kappa(t-(t-k\tau)-\tau)} (1 - e^{-\kappa\tau})^2 (1 + e^{\kappa(\tau - 2(t-k\tau))})}{\sqrt{\frac{\sigma^2}{\kappa}\left[1 - e^{-\kappa\tau} - \frac{1}{2} e^{-2\kappa t} \left(1 - e^{\kappa\tau}\right)^2\right]} \sqrt{\frac{\sigma^2}{\kappa}\left[1 - e^{-\kappa\tau} - \frac{1}{2} e^{-2\kappa(t-k\tau)} \left(1 - e^{\kappa\tau}\right)^2\right]}} \\
&= \frac{-\frac{\sigma^2}{2\kappa} e^{-\kappa(k-1)\tau} (1 - e^{-\kappa\tau})^2 (1 + e^{-2\kappa t + \kappa(2k+1)\tau})}{\sqrt{\frac{\sigma^2}{\kappa}\left[1 - e^{-\kappa\tau} - \frac{1}{2} e^{-2\kappa t} \left(1 - e^{\kappa\tau}\right)^2\right]} \sqrt{\frac{\sigma^2}{\kappa}\left[1 - e^{-\kappa\tau} - \frac{1}{2} e^{-2\kappa(t-k\tau)} \left(1 - e^{\kappa\tau}\right)^2\right]}}
\end{aligned} \tag{3.28}
$$

Therefore we obtain for the unconditional ($t \to \infty$) first-order autocorrelation function

$$
\begin{aligned}
\rho_{\tau,k} &\equiv \lim_{t\to\infty} \operatorname{corr}(r_\tau(t - k\tau), r_\tau(t)) \\
&= -\frac{1}{2} e^{-\kappa(k-1)\tau} \left(1 - e^{-\kappa\tau}\right).
\end{aligned} \tag{3.29}
$$

We see that $\rho_{\tau,k}$ is always negative and bound from below by $-\frac{1}{2}$ for $k \to \infty$ with $k > 1$ (figure 3.4). In the special case $k = 1$ we have the first order autocorrelation function

$$
\rho_{\tau,1} = -\frac{1}{2} \left(1 - e^{-\kappa\tau}\right). \tag{3.30}
$$

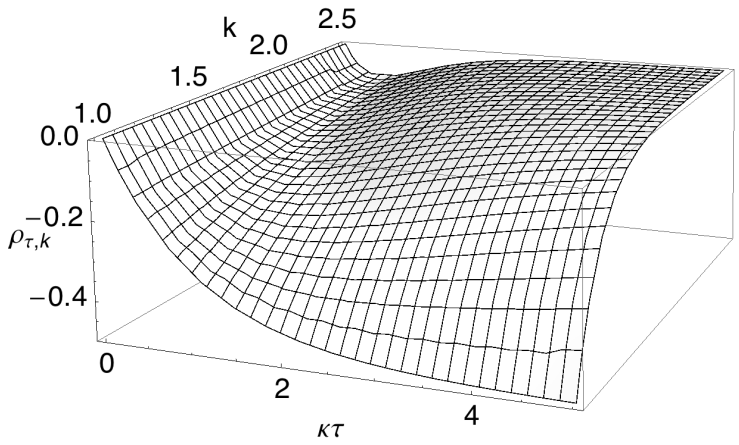

Figure 3.4: Autocorrelation function $\rho_{\tau,k}$ of the log return process $r_\tau(t)$

The comparison with empirical data shows that this might actually be a serious drawback of the trending OU process and motivates the introduction of alternative processes which have more flexible autocorrelation functions. However, to study the impact of serial correlation on option prices the trending OU process seems ideal.

3.3 Parameterisation of Unconditional Moments

The differences between the arithmetic Brownian motion $d\hat{s}_t$ and the OU process ds_t for the log-price process $s_t = \log S_t$

$$d\hat{s}_t = \hat{\mu}dt + \hat{\sigma}dW_t \tag{3.31}$$

$$ds_t = (\mu - \kappa[s_t - s_0 - \mu t])\,dt + \sigma dW_t \tag{3.32}$$

lead to two different price processes

$$d\hat{S}_t = \left(\hat{\mu} + \frac{\hat{\sigma}^2}{2}\right)\hat{S}_t dt + \hat{\sigma}\hat{S}_t dW_t \tag{3.33}$$

$$dS_t = \left(\mu + \frac{\sigma^2}{2} - \kappa[\log S_t - \log S_0 - \mu t]\right) S_t dt + \sigma S_t dW_t. \tag{3.34}$$

The conditional transition density of S_t is given by

$$p(S_t, t; S_0, 0) = \sqrt{\frac{\kappa}{\sigma^2(1-e^{-2\kappa t})}}\frac{1}{\sqrt{\pi}S_t}e^{-\frac{\kappa}{\sigma^2(1-e^{-2\kappa t})}(\log(S_t/S_0)-\mu t)^2}. \tag{3.35}$$

The unconditional mean $\bar{r}_\tau$, variance $\bar{v}_\tau^2$ and autocorrelation $\rho_{\tau,1}$ of the log-return process can be defined without specifying a particular model for the log-price process.

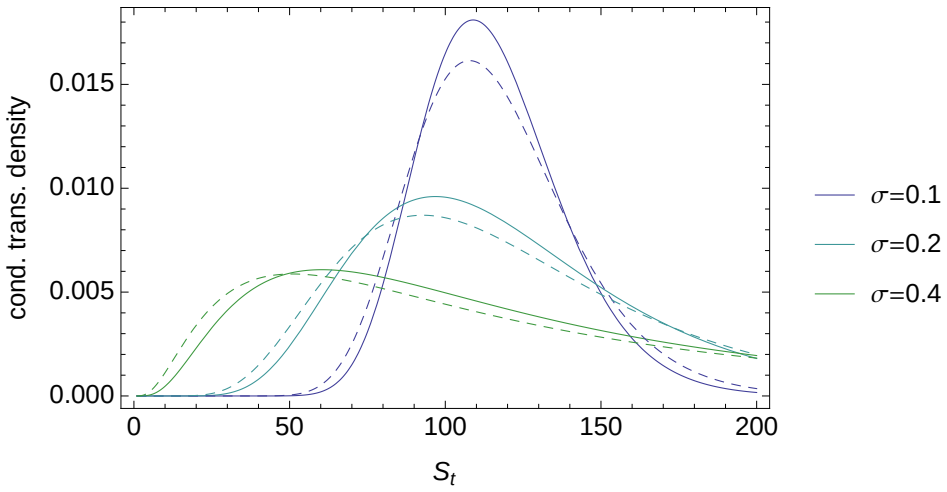

Figure 3.5: Conditional transition density of S_t for trending OU (solid) and geometric Brownian motion (dashed) for $\mu = 0.025$, $S_0 = 100$ and $\kappa = 0.05$ at $t = 5$

A good model of the process should match empirical log-return distribution. For this it is necessary that all three quantities fit reasonably well. This means that it should be possible to find one set of model parameters to reproduce all three quantities. In case of the arithmetic Brownian motion (3.31) with the two parameters $\hat{\mu}$ and $\hat{\sigma}$ we find

$$\begin{aligned} \bar{r}_\tau &= \hat{\mu}\tau \\ \bar{v}_\tau^2 &= \hat{\sigma}^2\tau \\ \rho_{\tau,1} &= 0 \end{aligned} \tag{3.36}$$

where the second equation gives the well known Black-Scholes result $\hat{\sigma}^2 = \bar{v}_\tau^2/\tau$ (3.15). As the all three equations are decoupled both parameter can be found easily. For the trending OU process (3.32) the model parameters μ, σ and κ must satisfy

$$\begin{aligned} \bar{r}_\tau &= \mu\tau \\ \bar{v}_\tau^2 &= \frac{\sigma^2}{\kappa}(1 - e^{-\kappa\tau}) \\ \rho_{\tau,1} &= -\frac{1}{2}\left(1 - e^{-\kappa\tau}\right) \end{aligned} \tag{3.37}$$

with respect to the observed quantities $\bar{r}_\tau$, $\bar{v}_\tau^2$ and $\rho_{\tau,1}$. The third equation gives

$$\kappa = -\frac{1}{\tau}\ln(1 + 2\rho_{\tau,1}). \tag{3.38}$$

The second equation yields

$$\begin{aligned}\sigma^2 &= \frac{\kappa \bar{v}_\tau^2}{1 - e^{-\kappa\tau}} \\ &= \frac{\bar{v}_\tau^2}{\tau} \cdot \frac{\kappa\tau}{1 - e^{-\kappa\tau}}\end{aligned} \tag{3.39}$$

which shows explicitly the dependence of σ on κ. σ^2 can be written as a product of the Black-Scholes estimate $\hat{\sigma}^2$ (under assumption of an arithmetic Brownian motion for the log-price process) and an adjustment factor for the trending OU process

$$\sigma^2 = \hat{\sigma}^2 \cdot \frac{\kappa\tau}{1 - e^{-\kappa\tau}}. \tag{3.40}$$

As the adjustment factor is strictly larger than one and increases with κ, an increase in the negative autocorrelation in the returns results in a larger σ and therefore in higher option prices.
Substituting κ into (3.39) gives an equation for σ^2 which only depends on the two observed parameters $\bar{v}_\tau$ and $\rho_{\tau,1}$

$$\sigma^2 = \frac{\bar{v}_\tau^2}{\tau} \cdot \frac{\ln(1 + 2\rho_{\tau,1})}{2\rho_{\tau,1}} \tag{3.41}$$

where the restriction $\rho_{\tau,1} \in (-1/2, 0]$ corresponds to the restriction $\kappa \geq 0$.
In general the return periods in the definitions of $\bar{v}_{\tau_1}$ and ρ_{τ_2} can be different

$$\bar{v}_{\tau_1}^2 = \frac{\sigma^2}{\kappa}(1 - e^{-\kappa\tau_1}) \tag{3.42}$$

$$\rho_{\tau_2,1} = -\frac{1}{2}\left(1 - e^{-\kappa\tau_2}\right). \tag{3.43}$$

As the log-price process is defined in continuous time we obtain with $\kappa = -\frac{1}{\tau_2}\ln(1 + 2\rho_{\tau_2})$

$$\begin{aligned}\sigma^2 &= \frac{\kappa \bar{v}_{\tau_1}^2}{1 - e^{-\kappa\tau_1}} \\ &= \frac{\bar{v}_{\tau_1}^2}{\tau_1} \cdot \frac{\tau_1}{\tau_2} \frac{\ln(1 + 2\rho_{\tau_2,1})}{(1 + 2\rho_{\tau_2,1})^{\frac{\tau_1}{\tau_2}} - 1} \\ &= \sigma_{\text{GBM}}^2 \cdot \frac{\tau_1}{\tau_2} \frac{\ln(1 + 2\rho_{\tau_2,1})}{(1 + 2\rho_{\tau_2,1})^{\frac{\tau_1}{\tau_2}} - 1}.\end{aligned} \tag{3.44}$$

This expression gives a simple adjustment for the Black-Scholes input σ^2.

3.4 Impact on Option Pricing

To see the impact of the introduction of the trending OU log-price process on the option price $V_t = V(S_t, t)$ we need to find an appropriate pricing equation. To do so we use the standard Black-Scholes assumptions but replace the geometric Brownian motion by the process

$$dS_t = \left(\mu + \frac{\sigma^2}{2} - \kappa[\log S_t - \log S_0 - \mu t]\right) S_t dt + \sigma S_t dW_t. \tag{3.45}$$

The derivation of the Black-Scholes equation is straightforward. The replicating portfolio is set up by an option and -Δ underlying assets

$$\Pi_t = V_t - \Delta S_t. \tag{3.46}$$

The infinitesimal change in the portfolio value is given by

$$\begin{aligned} d\Pi_t &= dV_t - \Delta_t dS_t \\ &= \frac{\partial V}{\partial t} dt + \frac{\partial V}{\partial S} dS_t + \frac{1}{2}\frac{\partial^2 V}{\partial S^2} dS_t^2 - \Delta dS_t. \end{aligned} \tag{3.47}$$

The valuation of the dS_t^2 is the only time we use the explicit form of the price process (3.45). We see that the form of the drift term does not matter and only the volatility term $dS_t^2 = \sigma^2 S_t^2 dt$ is necessary

$$d\Pi_t = \left(\frac{\partial V}{\partial t} + \frac{1}{2}\sigma^2 S^2 \frac{\partial^2 V}{\partial S^2}\right) dt + \left(\frac{\partial V}{\partial S} - \Delta\right) dS_t \tag{3.48}$$

which can be made instantaneously risk free by choosing $\Delta = \partial V / \partial S$. Since the change in the portfolio value is risk-free, it must be equal to the change in the portfolio's market value were that value is to be invested at the risk-free rate

$$\begin{aligned} d\Pi_t &= r\Pi_t dt \\ &= r\left(V_t - \frac{\partial V}{\partial S} S_t\right) dt. \end{aligned} \tag{3.49}$$

This gives the differential equation

$$\frac{\partial V}{\partial t} + r\frac{\partial V}{\partial S} S + \frac{1}{2}\sigma^2 S^2 \frac{\partial^2 V}{\partial S^2} - rV = 0 \tag{3.50}$$

for the price function $V(S, t)$, for all $S > 0$ and $t < T$. This is obviously the standard Black-Scholes equation which is due to the fact that only the drift term of the price process was changed.

$\rho_{\tau,1}$	$\Delta(1\text{d}, 1\text{d}, \rho_{\tau,1})$	$\Delta(1\text{d}, 7\text{d}, \rho_{\tau,1})$	$\Delta(1\text{d}, 31\text{d}, \rho_{\tau,1})$
0.0000	1.000	1.000	1.000
-0.1000	1.056	1.008	1.002
-0.2000	1.130	1.018	1.004
-0.3500	1.311	1.043	1.009
-0.4500	1.599	1.083	1.019
-0.4900	1.998	1.143	1.032
-0.4990	2.495	1.228	1.051
-0.4999	2.918	1.312	1.069

Table 3.1: Ratio $\Delta(\tau_1, \tau_2, \rho_{\tau_1,1}) = \sigma/\sigma_{\text{GBM}}$ for the trending OU process for various holding values of first-order autocorrelation $\rho_{\tau,1}$ and periods τ

For pricing options under the trending OU dynamics we use (3.44) as volatility input for the Black Scholes equation. With the unconditional variance of daily returns $\bar{v}_1$ and the first order autocorrelation of the τ-period returns ρ_τ, the price of a call option is given by (2.36)

$$C_{\text{OU}}(S(t), t) = C_{\text{BS}}\left(S(t), T-t, K, r, \sigma\right) \tag{3.51}$$

with the adjusted volatility σ

$$\begin{aligned}\sigma &= \sigma_{\text{GBM}} \cdot \sqrt{\frac{1}{\tau}\frac{\ln(1+2\rho_{\tau,1})}{(1+2\rho_{\tau,1})^{\frac{1}{\tau}}-1}} \\ &= \sigma_{\text{GBM}} \cdot \Delta(1\text{d}, \tau, \rho_{\tau,1}).\end{aligned} \tag{3.52}$$

This is just the Black-Scholes price with an adjusted volatility to account for the negative autocorrelation of the trending OU process. The adjustment factor $\Delta(1\text{d}, \tau, \rho_{\tau,1})$ (see table 3.1) is for all values of $\rho_{\tau,1} \in (-1/2, 0]$ greater equal one and increasing with decreasing autocorrelation.

Therefore the option price is always greater or equal to the standard Black-Scholes prices (fig. 3.6) and a decreasing function of the first order autocorrelation. To estimate the impact of the autocorrelation adjustment, figures 3.7, 3.8 and 3.9 show the absolute differences of the Black-Scholes prices under geometric Brownian motion and the OU process for various times-to-maturity $T-t$, strikes K, autocorrelations ρ and an underlying spot price of $S_t = 40$. The unconditional standard deviation of the daily returns is set to 2% per day. Figure 3.7 depicts the option price difference for values of daily ($\tau = 1\text{d}$) autocorrelations from -0.05 to -0.45 and figures 3.8 and 3.9 for weekly ($\tau = 7\text{d}$) and monthly ($\tau = 31\text{d}$) autocorrelations for the same values of ρ.

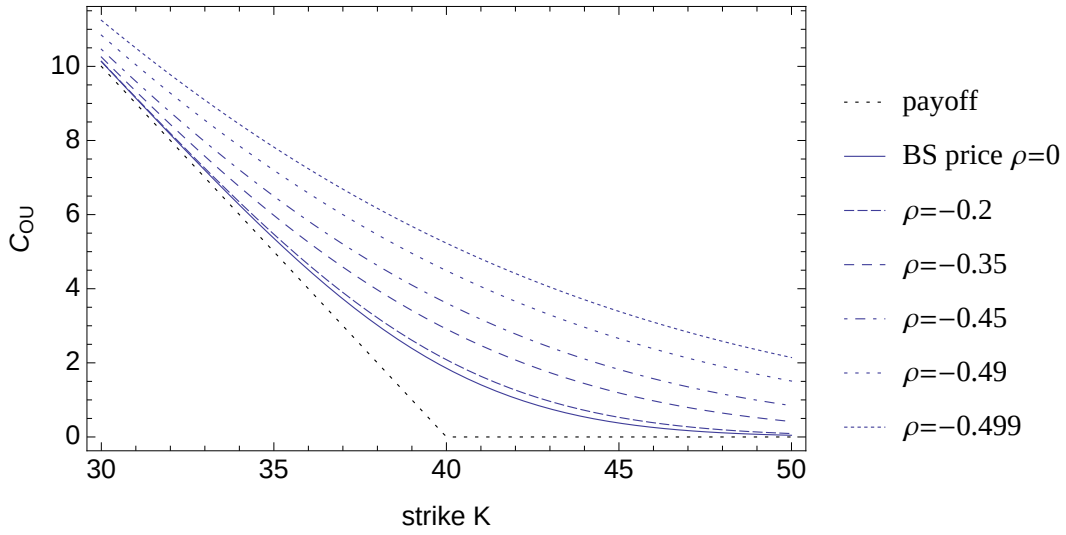

Figure 3.6: Call prices for $S_t = 40$, $r = 0.05$, $\hat{\sigma} = 0.38$ and $\tau = 7/364$ for various values of autocorrelation

Figure 3.7 (top left graph) shows that in-the money options with short maturities ($K = 30$, $T = 7$d) experience no significant change in price ($2.48 \cdot 10^{-4}$) even for the extreme autocorrelation of -0.45. For at-the-money options the impact becomes more pronounced. However even in the case of such a short maturity the autocorrelation of -0.05 increases the price of a $K = 40$ call by 0.022 which is 2.6% and for $\rho = -0.15$ the increase is already at 8.6%.

The other graphs in figure 3.7 show that an increase in the time-to-maturity also also increases the effect of the autocorrelation. For example the 12-month call with a strike of $K = 50$ and a Black-Scholes price of 3.49 increases its price to 4.03 for a daily autocorrelation of -0.15 and to 7.12 for $\rho = -0.45$. This constitutes an increase of 15.5% and 103.9% respectively. This particular behaviour can be explained by the fact that the negative autocorrelation of the return induces a price oscillation which subsequently implies an increased volatility which becomes more important with longer times-to-maturity.

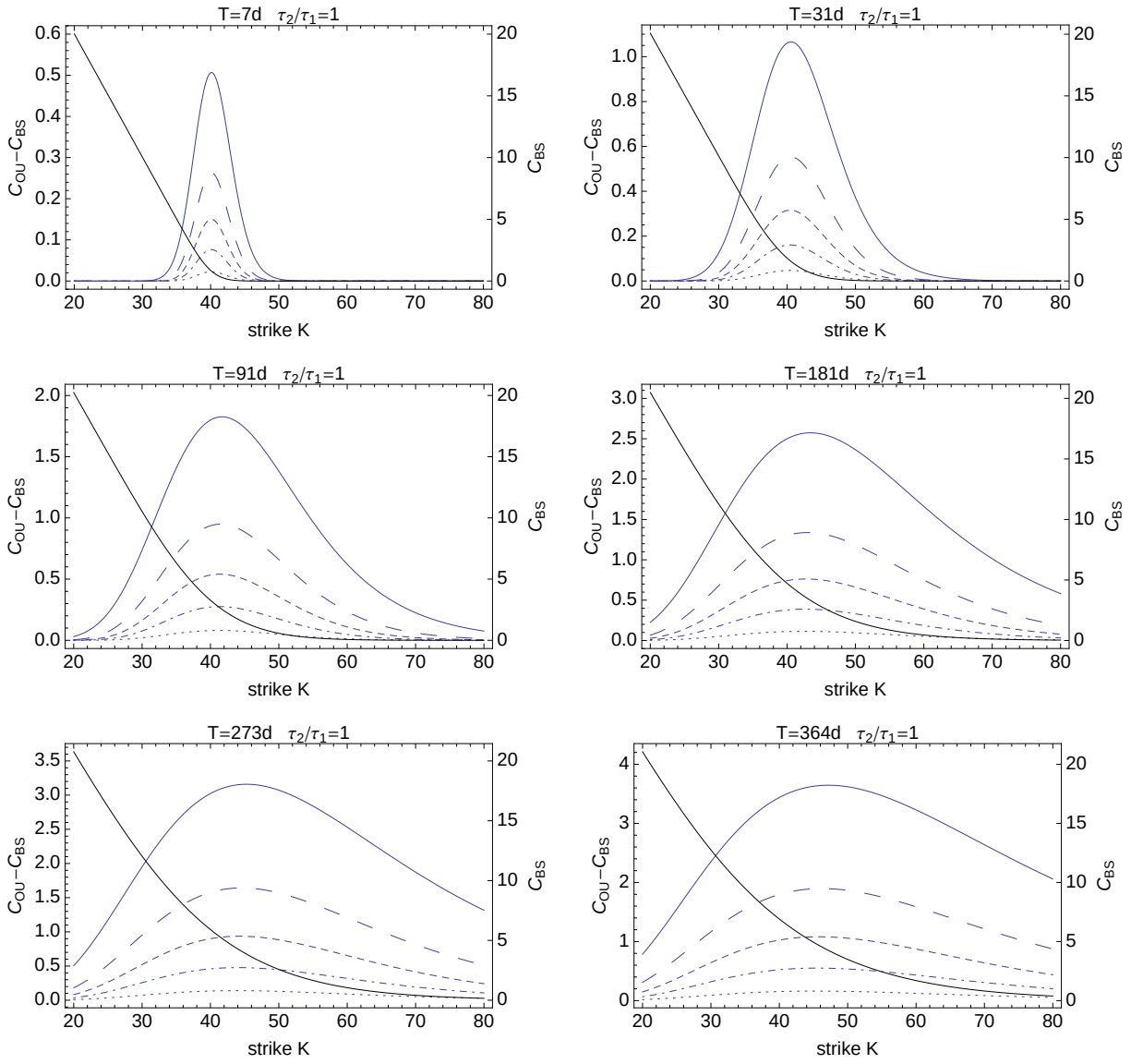

Figure 3.7: Total impact $C_{\mathrm{OU}} - C_{\mathrm{BS}}$ of the autocorrelation on the price of a European call ($S_t = 40, r = 0.05$ and $\hat{\sigma} = 0.02\sqrt{364}$) for various maturities T and daily ($\tau = 1\mathrm{d}$) autocorrelations $\rho_{\tau,1}$. The price of the Black-Scholes option C_{BS} is depicted in black. —— -0.45, – – -0.35, - - -0.25, -·-· -0.15, ····· -0.05. The price of the Black-Scholes option C_{BS} is depicted in black.

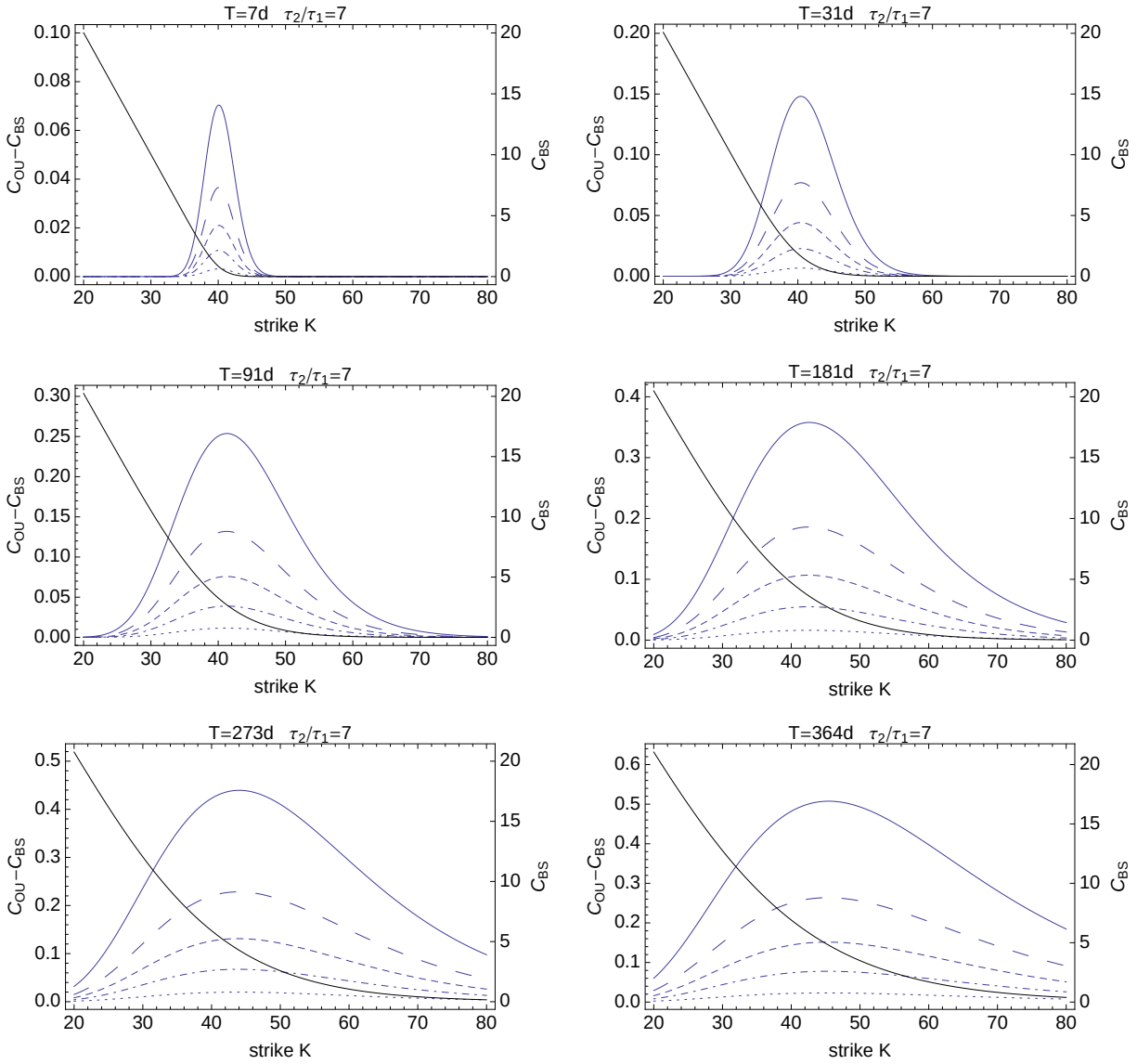

Figure 3.8: Total impact $C_{\mathrm{OU}} - C_{\mathrm{BS}}$ of the autocorrelation on the price of a European call ($S_t = 40, r = 0.05$ and $\hat{\sigma} = 0.02\sqrt{364}$) for various maturities T and weekly ($\tau = 7\mathrm{d}$) autocorrelations $\rho_{\tau,1}$. The price of the Black-Scholes option C_{BS} is depicted in black. —— -0.45, – – -0.35, - - - -0.25, -·- -0.15, ····· -0.05. The price of the Black-Scholes option C_{BS} is depicted in black.

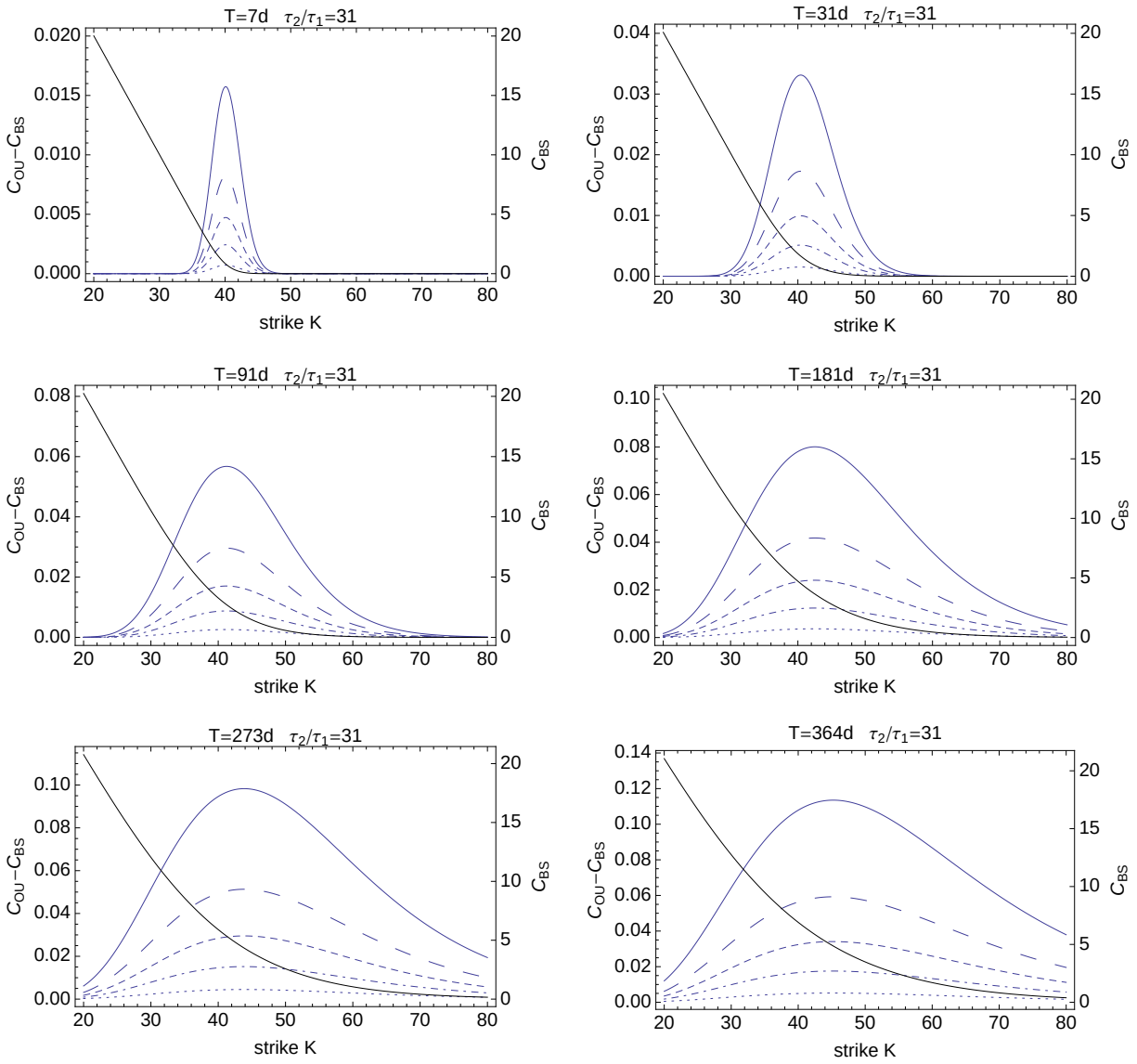

Figure 3.9: Total impact $C_{\mathrm{OU}} - C_{\mathrm{BS}}$ of the autocorrelation on the price of a European call ($S_t = 40, r = 0.05$ and $\hat{\sigma} = 0.02\sqrt{364}$) for various maturities T and monthly ($\tau = 31$d) autocorrelations $\rho_{\tau,1}$ —— -0.45, – – -0.35, - - - -0.25, -·-· -0.15, ····· -0.05. The price of the Black-Scholes option C_{BS} is depicted in black.

There is also a more quantitative explanation. As the OU process only rescales the σ-input of the Black Scholes equation the ρ sensitivity is easily calculated and is with $\varrho = 1 + 2\rho$ given by

$$\begin{aligned}\frac{\partial C}{\partial \rho} &= \frac{\partial C}{\partial \sigma}\frac{\partial \sigma}{\partial \rho} \\ &= S\hat{\sigma}\sqrt{T-t}\,\mathcal{N}'(d_1)\cdot\frac{\varrho^{\frac{1}{\tau}}(1-\frac{1}{\tau}\log\varrho)-1}{\left(\varrho^{\frac{1}{\tau}}-1\right)^{3/2}\varrho\sqrt{\tau\log\varrho}}\end{aligned} \tag{3.53}$$

and shown in figure 3.10.

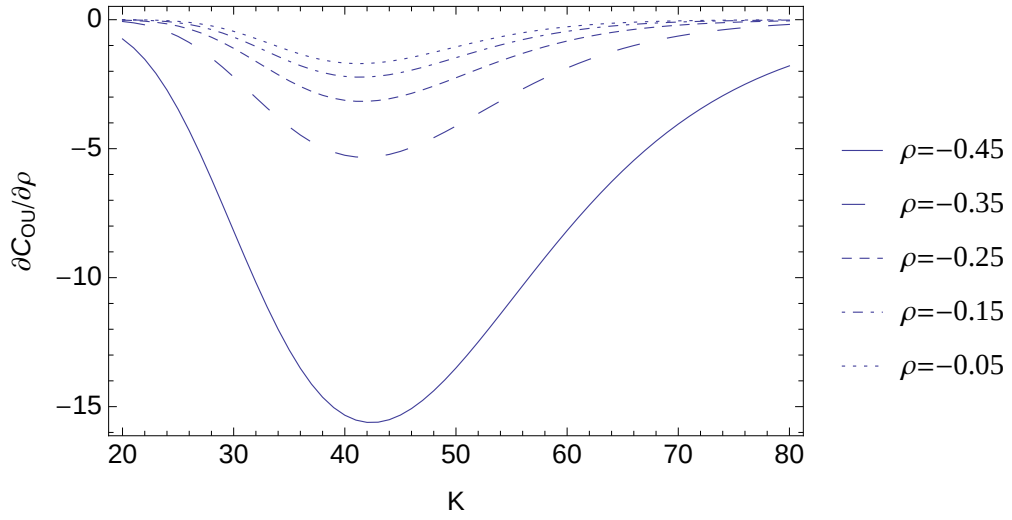

Figure 3.10: Autocorrelation sensitivity $\partial C_{\mathrm{OU}}/\partial\rho$ of the price of a European call ($S_t = 40, r = 0.05$ and $\hat{\sigma} = 0.02\sqrt{364}$) for maturities $T = 91/364$ and various autocorrelations $\rho_{\tau,1}$.

The square root $\sqrt{T-t}$ in (3.53) is the reason for the increasing autocorrelation sensitivity of longer-maturity options.
All results can also be found in figures 3.8 and 3.9 with the only difference that the overall impact of the autocorrelation becomes significantly smaller for weekly and monthly correlation periods τ.

Chapter 4

The Bivariate Trending OU Process

4.1 General Model

The trending OU process shows (compared to the geometric Brownian motion) a non-vanishing autocorrelation of the price returns. Unfortunately, the autocorrelation is negative for all lags (figure 3.4) which is inconsistent with empirical findings [LM88, L90, FF88a, FF88b]. The studies of the empirical correlations of the returns

$$\mathrm{corr}[r_\tau(t - k\tau), r_\tau(t)] \tag{4.1}$$

is typically positive for short horizons τ and negative for larger τ (see chapter 5). In addition the trending OU drift can not accommodate other economic variables as it only depends on the detrended log-price $q_t = s_t - \mu t$.
This situation can be improved by extending the trending OU process (3.19) by an additional degree of freedom $dW_t^{(x)}$. The so called bivariate trending OU process is then given by

$$dq_t = (\kappa[q_0 - q_t] + \lambda X_t)\, dt + \sigma dW_t^{(s)} \tag{4.2}$$

$$dX_t = -\delta X_t dt + \sigma_x dW_t^{(x)} \tag{4.3}$$

with $\kappa, \delta \geq 0$ $q(0) = q_0$, $X(0) = X_0$. $W^{(s)}$ and $W^{(x)}$ are two standard Wiener processes with $dW_t^{(x)} dW_t^{(s)} = \eta dt$. The added process X_t only serves to enrich the model and is not observable. For $\lambda = 0$ the model reduces to the known trending OU process. In the case $\kappa \neq 0$ the process q_t can be written as

$$dq_t = \kappa \left(\left[q_0 + \frac{\lambda}{\kappa} X_t \right] - q_t \right) dt + \sigma dW_t^{(s)} \tag{4.4}$$

which shows that q_t is reverting to a stochastic mean $q_0 + (\lambda/\kappa)X_t$ instead of the deterministic mean q_0 in the trending OU case. Utilising Itô's lemma we can derive the associated log-price process s_t

$$\begin{aligned} ds_t &= d(q_t + \mu t) \\ &= (\mu - \kappa[s_t - s_0 - \mu t] + \lambda X_t)\, dt + \sigma dW_t^{(s)} \end{aligned} \tag{4.5}$$

and the price process

$$\begin{aligned} dS_t &= de^{s_t} \\ &= \left(e^{s_t} \left(\mu - \kappa[s_t - s_0 - \mu t] + \lambda X_t\right) + \frac{1}{2}\sigma^2 e^{s_t} \right) dt + \sigma e^{s_t} dW_t^{(s)} \\ &= \left(\mu + \frac{\sigma^2}{2} - \kappa[\log S_t - \log S_0 - \mu t] + \lambda X_t \right) S_t dt + \sigma S_t dW_t^{(s)}. \end{aligned} \tag{4.6}$$

The relation between the various stochastic processes is depicted in diagram 4.1.

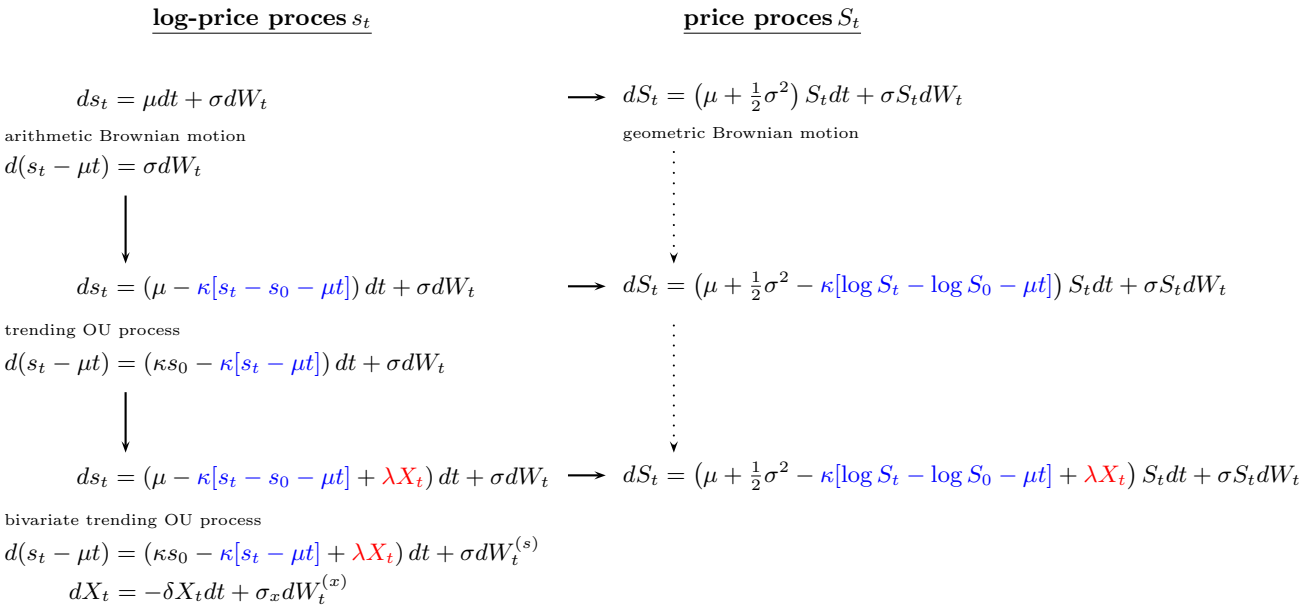

To find a solution of the system (4.2-4.3) we start with the equation for X_t. Applying Itô's lemma to the ansatz $e^{\delta t} X_t$ we obtain

$$d(e^{\delta t} X_t) = \left(\delta e^{\delta t} X_t - \delta X_t e^{\delta t}\right) dt + \sigma_x e^{\delta t} dW_t^{(x)} \tag{4.7}$$

which can be integrated

$$e^{\delta t} X_t - X_0 = \sigma_x \int_0^t e^{\delta s} dW_s^{(x)}. \tag{4.8}$$

The solution of (4.3) is then given by

$$X_t = X_0 e^{-\delta t} + e^{-\delta t}\sigma_x \int_0^t e^{\delta s} dW_s^{(x)}. \tag{4.9}$$

Using this result we are in a position to solve (4.2). Applying Itô's lemma to the similar ansatz $e^{\delta t} q_t$ yields

$$\begin{aligned} d\left(e^{\kappa t} q_t\right) &= \left(\kappa e^{\kappa t} q_t + \kappa \left[\left(q_0 + \frac{\lambda}{\kappa} X_t\right) - q_t\right] e^{\kappa t}\right) dt + \sigma e^{\kappa t} dW_t^{(s)} \\ &= \left(\kappa q_0 e^{\kappa t} + \lambda X_t e^{\kappa t}\right) dt + \sigma e^{\kappa t} dW_t^{(s)} \end{aligned} \tag{4.10}$$

which can be formally integrated

$$e^{\kappa t} q_t - q_0 = q_0\left(e^{\kappa t} - 1\right) + \lambda \int_0^t e^{\kappa s} X_s ds + \sigma \int_0^t e^{\kappa s} dW_s^{(s)}. \tag{4.11}$$

Substituting (4.9) gives

$$q_t = q_0 + \lambda \int_0^t e^{-\kappa(t-s)} \left(X_0 e^{-\delta s} + e^{-\delta s}\sigma_x \int_0^s e^{\delta u} dW_u^{(x)}\right) ds + \sigma \int_0^t e^{-\kappa(t-s)} dW_s^{(s)}. \tag{4.12}$$

Now we can split the integrals

$$\begin{aligned} q_t = q_0 &+ \lambda e^{-\kappa t} \int_0^t e^{(\kappa-\delta)s} ds \cdot X_0 \\ &+ \sigma \int_0^t e^{-\kappa(t-s)} dW_s^{(s)} + \lambda e^{-\kappa t} \int_0^t e^{(\kappa-\delta)s} \sigma_x \int_0^s e^{\delta u} dW_u^{(x)} ds \end{aligned} \tag{4.13}$$

and perform simple integration

$$\begin{aligned} q_t = q_0 &+ \frac{\lambda}{\kappa - \delta} e^{-\kappa t}\left(e^{(\kappa-\delta)t} - 1\right) \cdot X_0 \\ &+ \sigma \int_0^t e^{-\kappa(t-s)} dW_s^{(s)} + \lambda e^{-\kappa t} \int_0^t \int_0^s e^{\delta u} e^{(\kappa-\delta)s} \sigma_x dW_u^{(x)} ds. \end{aligned} \tag{4.14}$$

By changing the order of integration in the last term we obtain

$$\begin{aligned} q_t = q_0 &+ \frac{\lambda}{\kappa - \delta}\left(e^{-\delta t} - e^{-\kappa t}\right) \cdot X_0 \\ &+ \sigma \int_0^t e^{-\kappa(t-s)} dW_s^{(s)} + \lambda e^{-\kappa t} \int_0^t e^{\delta u} \sigma_x \int_u^t e^{(\kappa-\delta)s} ds dW_u^{(x)} \end{aligned} \tag{4.15}$$

which allows us to calculated the deterministic integral

$$\begin{aligned} q_t = q_0 &+ \frac{\lambda}{\kappa - \delta}\left(e^{-\delta t} - e^{-\kappa t}\right) \cdot X_0 \\ &+ \sigma \int_0^t e^{-\kappa(t-s)} dW_s^{(s)} + \frac{\lambda}{\kappa - \delta} e^{-\kappa t} \int_0^t e^{\delta u} \sigma_x \left(e^{(\kappa-\delta)t} - e^{(\kappa-\delta)u}\right) dW_u^{(x)}. \end{aligned} \tag{4.16}$$

The explicit solution of (4.2-4.3) is therefore given by

$$q_t = q_0 + \frac{\lambda}{\kappa-\delta}\left(e^{-\delta t} - e^{-\kappa t}\right)\cdot X_0 + \sigma\int_0^t e^{-\kappa(t-s)}dW_s^{(s)} + \frac{\lambda}{\kappa-\delta}\int_0^t \sigma_x\left(e^{-\delta(t-s)} - e^{-\kappa(t-s)}\right)dW_s^{(x)} \tag{4.17}$$

$$X_t = X_0 e^{-\delta t} + e^{-\delta t}\sigma_x\int_0^t e^{\delta s}dW_s^{(x)}. \tag{4.18}$$

where $t \geq 0$ and (q_t, X_t) are jointly normal distributed. From this the joint moments of (q_t, X_t) can be obtained. The expectations can be directly read off from (4.17, 4.18)

$$\mathbb{E}[X_t] = X_0 e^{-\delta t} \tag{4.19}$$

$$\mathbb{E}[q_t] = q_0 + \frac{\lambda}{\kappa-\delta}\left(e^{-\delta t} - e^{-\kappa t}\right)\cdot X_0. \tag{4.20}$$

For the variances we utilise Itôs isometry

$$\begin{aligned}\mathrm{var}[X_t] &= e^{-2\delta t}\sigma_x^2\int_0^t e^{2\delta s}ds \\ &= \frac{\sigma_x^2}{2\delta}e^{-2\delta t}\left(e^{2\delta t}-1\right) \\ &= \frac{\sigma_x^2}{2\delta}\left(1-e^{-2\delta t}\right).\end{aligned} \tag{4.21}$$

For $\mathrm{var}[q_t]$ the calculation is a more complex

$$\begin{aligned}\mathrm{var}[q_t] &= \sigma^2\mathbb{E}\left[\left(\int_0^t e^{-\kappa(t-u)}dW_u^{(s)}\right)^2\right] + \left(\frac{\lambda\sigma_x}{\kappa-\delta}\right)^2\mathbb{E}\left[\left(\int_0^t\left(e^{-\delta(t-u)}-e^{-\kappa(t-u)}\right)dW_u^{(x)}\right)^2\right] \\ &\quad + 2\frac{\lambda\sigma\sigma_x}{\kappa-\delta}\mathbb{E}\left[\int_0^t e^{-\kappa(t-u)}dW_u^{(s)}\int_0^t\left(e^{-\delta(t-u)}-e^{-\kappa(t-u)}\right)dW_u^{(x)}\right] \\ &= \sigma^2\int_0^t e^{-2\kappa(t-u)}du + \left(\frac{\lambda\sigma_x}{\kappa-\delta}\right)^2\int_0^t\left(e^{-\delta(t-u)}-e^{-\kappa(t-u)}\right)^2du \\ &\quad + 2\frac{\lambda\eta\sigma\sigma_x}{\kappa-\delta}\int_0^t e^{-\kappa(t-u)}\left(e^{-\delta(t-u)}-e^{-\kappa(t-u)}\right)du \\ &= \frac{\sigma^2}{2\kappa}\left(1-e^{-2\kappa t}\right) + \left(\frac{\lambda\sigma_x}{\kappa-\delta}\right)^2\left(\frac{1-e^{-\delta t}}{2\delta} + \frac{2(e^{-(\kappa+\delta)t}-1)}{\kappa+\delta} + \frac{1-e^{-\kappa t}}{2\kappa}\right) \\ &\quad + 2\frac{\lambda\eta\sigma\sigma_x}{\kappa-\delta}\left(\frac{1-e^{-(\kappa+\delta)t}}{\kappa+\delta} + \frac{e^{-2\kappa t}-1}{2\kappa}\right) \\ &= \frac{\sigma^2}{2\kappa}\left(1-e^{-2\kappa t}\right) + \frac{\lambda\eta\sigma\sigma_x}{\kappa(\kappa+\delta)}\left(\frac{\kappa(1-2e^{-(\kappa+\delta)t}+e^{-2\kappa t})+\delta(e^{-2\kappa t}-1)}{\kappa-\delta}\right) \\ &\quad + \frac{\lambda^2\sigma_x^2}{2\kappa\delta(\kappa+\delta)}\left(\frac{\kappa^2(1-e^{-\delta t})+\kappa\delta[-2-e^{-\delta t}-e^{-\kappa t}+4e^{-(\kappa+\delta)t}]+\delta^2(1-e^{-\kappa t})}{(\kappa-\delta)^2}\right).\end{aligned} \tag{4.22}$$

The covariances are given by

$$\begin{aligned}
\operatorname{cov}[q_t, X_t] &= \sigma\sigma_x e^{-\delta t}\mathbb{E}\left[\int_0^t e^{-\kappa(t-u)}dW_u^{(s)}\int_0^t e^{\delta u}dW_u^{(x)}\right] \\
&\quad + \frac{\lambda\sigma_x^2}{\kappa-\delta}e^{-\delta t}\mathbb{E}\left[\int_0^t (e^{-\delta(t-u)}-e^{-\kappa(t-u)})dW_u^{(x)}\int_0^t e^{\delta u}dW_u^{(x)}\right] \\
&= \eta\sigma\sigma_x e^{-\delta t}\int_0^t e^{-\kappa(t-u)}e^{\delta u}du + \frac{\lambda\sigma_x^2}{\kappa-\delta}e^{-\delta t}\int_0^t (e^{-\delta(t-u)}-e^{-\kappa(t-u)})e^{\delta u}du \\
&= \frac{\eta\sigma\sigma_x}{\kappa+\delta}(1-e^{-(\kappa+\delta)t}) + \frac{\lambda\sigma_x^2}{2\delta(\kappa+\delta)}\left(\frac{\kappa(1-e^{-2\delta t})-\delta(1-2e^{-(\kappa+\delta)t}+e^{-2\delta t})}{\kappa-\delta}\right)
\end{aligned} \tag{4.23}$$

$$\begin{aligned}
\operatorname{cov}[q_s, q_t]_{s\le t} &= \sigma^2\mathbb{E}\left[\int_0^s e^{-\kappa(s-u)}dW_u^{(s)}\int_0^t e^{-\kappa(t-u)}dW_u^{(s)}\right] \\
&\quad + \frac{\lambda\sigma\sigma_x}{\kappa-\delta}\mathbb{E}\left[\int_0^s e^{-\kappa(s-u)}dW_u^{(s)}\int_0^t \left(e^{-\delta(t-u)}-e^{-\kappa(t-u)}\right)dW_u^{(x)}\right] \\
&\quad + \frac{\lambda\sigma\sigma_x}{\kappa-\delta}\mathbb{E}\left[\int_0^s \left(e^{-\delta(s-u)}-e^{-\kappa(s-u)}\right)dW_u^{(x)}\int_0^t e^{-\kappa(t-u)}dW_u^{(s)}\right] \\
&\quad + \left(\frac{\lambda\sigma_x}{\kappa-\delta}\right)^2\mathbb{E}\left[\int_0^s \left(e^{-\delta(s-u)}-e^{-\kappa(s-u)}\right)dW_u^{(x)}\int_0^t \left(e^{-\delta(t-u)}-e^{-\kappa(t-u)}\right)dW_u^{(x)}\right] \\
&= \sigma^2\int_0^s e^{-\kappa(s-u)}e^{-\kappa(t-u)}du \\
&\quad + \frac{\lambda\sigma\sigma_x}{\kappa-\delta}\int_0^s e^{-\kappa(s-u)}\left(e^{-\delta(t-u)}-e^{-\kappa(t-u)}\right)du \\
&\quad + \frac{\lambda\sigma\sigma_x}{\kappa-\delta}\int_0^s \left(e^{-\delta(s-u)}-e^{-\kappa(s-u)}\right)e^{-\kappa(t-u)}du \\
&\quad + \left(\frac{\lambda\sigma_x}{\kappa-\delta}\right)^2\int_0^s \left(e^{-\delta(s-u)}-e^{-\kappa(s-u)}\right)\left(e^{-\delta(t-u)}-e^{-\kappa(t-u)}\right)du \\
&= e^{-\kappa(s+t)}\left(\frac{\delta\eta\lambda\sigma\sigma_x}{2\kappa\left(\kappa^2-\delta^2\right)}+\frac{\eta\lambda\sigma\sigma_x}{2\kappa(\kappa-\delta)}+\frac{\eta\lambda\sigma\sigma_x}{2(\kappa-\delta)(\delta+\kappa)}-\frac{\lambda^2\sigma_x^2}{2\kappa(\delta-\kappa)^2}-\frac{\sigma^2}{2\kappa}\right) \\
&\quad + e^{\kappa(s-t)}\left(\frac{\eta\lambda\sigma\sigma_x}{2\left(\kappa^2-\delta^2\right)}+\frac{\lambda^2\sigma_x^2}{2\kappa(\delta-\kappa)^2}-\frac{\lambda^2\sigma_x^2}{(\delta-\kappa)^2(\delta+\kappa)}+\frac{\sigma^2}{2\kappa}\right) \\
&\quad + e^{\delta(s-t)}\left(-\frac{\eta\lambda\sigma\sigma_x}{\delta^2-\kappa^2}-\frac{\lambda^2\sigma_x^2}{(\delta-\kappa)^2(\delta+\kappa)}+\frac{\lambda^2\sigma_x^2}{2\delta(\delta-\kappa)^2}\right) \\
&\quad + e^{-\delta t-\kappa s}\left(\frac{\eta\lambda\sigma\sigma_x}{\delta^2-\kappa^2}+\frac{\lambda^2\sigma_x^2}{(\delta-\kappa)^2(\delta+\kappa)}\right)+e^{-\delta s-\kappa t}\left(\frac{\eta\lambda\sigma\sigma_x}{\delta^2-\kappa^2}+\frac{\lambda^2\sigma_x^2}{(\delta-\kappa)^2(\delta+\kappa)}\right) \\
&\quad + e^{\kappa(s-t)}\left(\frac{\delta\eta\lambda\sigma\sigma_x}{2\kappa(\delta^2-\kappa^2)}+\frac{\eta\lambda\sigma\sigma_x}{2\delta\kappa-2\kappa^2}\right)-e^{-\delta(s+t)}\frac{\lambda^2\sigma_x^2}{2\delta(\delta-\kappa)^2}
\end{aligned} \tag{4.24}$$

The expressions simplify for $t \to \infty$ to

$$\mathbb{E}[X_t]_\infty = 0 \tag{4.25}$$

$$\mathbb{E}[q_t]_\infty = q_0 \tag{4.26}$$

$$\mathrm{var}[X_t]_\infty = \frac{\sigma_x^2}{2\delta} \tag{4.27}$$

$$\mathrm{var}[q_t]_\infty = \frac{\sigma^2}{2\kappa} + \frac{\lambda\eta\sigma\sigma_x}{\kappa(\kappa+\delta)} + \frac{\lambda^2\sigma_x^2}{2\kappa\delta(\kappa+\delta)} \tag{4.28}$$

$$\mathrm{cov}[q_t, X_t] = \frac{\eta\sigma\sigma_x}{\kappa+\delta} + \frac{\lambda\sigma_x^2}{2\delta(\kappa+\delta)} \tag{4.29}$$

$$\begin{aligned}\mathrm{cov}[q_t, q_{t-\tau}]_\infty = {} & \frac{e^{-\kappa\tau}}{2\kappa(\delta^2-\kappa^2)}\left(2\delta\eta\lambda\sigma\sigma_x + \lambda^2\sigma_x^2 + \sigma^2(\delta^2-\kappa^2)\right) \\ & - \frac{e^{-\delta\tau}}{2\delta(\delta^2-\kappa^2)}\left(2\delta\eta\lambda\sigma\sigma_x + \lambda^2\sigma_x^2\right).\end{aligned} \tag{4.30}$$

For the τ-period returns we obtain then

$$\begin{aligned} r_\tau(t) &= s_t - s_{t-\tau} \\ &= q_t - q_{t-\tau} + \mu\tau \\ &= \mu\tau + \frac{\lambda}{\kappa-\delta}\left(e^{-\delta\tau} - e^{-\kappa\tau}\right)\cdot X_{t-\tau} \\ &\quad + \sigma\int_{t-\tau}^{t} e^{-\kappa(t-s)} dW_s^{(s)} + \frac{\lambda}{\kappa-\delta}\int_{t-\tau}^{t}\sigma_x\left(e^{-\delta(t-s)} - e^{-\kappa(t-s)}\right) dW_s^{(x)} \end{aligned}$$

$$\mathbb{E}[r_\tau(t)]_\infty = \mu\tau + X_0\frac{\lambda}{\kappa-\delta}\left(e^{-\delta t}(1-e^{\delta\tau}) - e^{-\kappa t}(1-e^{\kappa\tau})\right) \tag{4.31}$$

$$\begin{aligned}\mathrm{var}[r_\tau(t)]_\infty &= 2\mathrm{var}[q_t]_\infty - 2\mathrm{cov}[q_t, q_{t-\tau}]_\infty \\ &= \left(\frac{2\eta\lambda\sigma\sigma_x}{\kappa(\delta+\kappa)} + \frac{\lambda^2\sigma_x^2}{\delta\kappa(\delta+\kappa)} + \frac{\sigma^2}{\kappa}\right) + 2e^{-\delta\tau}\frac{\lambda}{\delta^2-\kappa^2}\left(\eta\sigma\sigma_x + \frac{\lambda\sigma_x^2}{2\delta}\right) \\ &\quad - e^{-\kappa\tau}\frac{\delta}{\delta-\kappa}\left(\frac{2\eta\lambda\sigma\sigma_x}{\kappa(\delta+\kappa)} + \frac{\lambda^2\sigma_x^2}{\delta\kappa(\delta+\kappa)} + \frac{\sigma^2}{\kappa} - \frac{\sigma^2}{\delta}\right).\end{aligned} \tag{4.32}$$

The covariance can then be calculated using (4.30)

$$\begin{aligned}\mathrm{cov}[r_\tau(t-k\tau), r_\tau(t)]_\infty &= \mathrm{cov}[q_{t-k\tau}, q_t]_\infty + \mathrm{cov}[q_{t-k\tau-\tau}, q_t]_\infty + \mathrm{cov}[q_{t-k\tau}, q_{t-\tau}]_\infty \\ &\quad + \mathrm{cov}[q_{t-k\tau-\tau}, q_{t-\tau}]_\infty \\ &= \left(e^{\delta\tau}-1\right)^2 e^{-\delta(k+1)\tau}\frac{1}{2\delta(\delta^2-\kappa^2)}\left(2\delta\eta\lambda\sigma\sigma_x + \lambda^2\sigma_x^2\right) \\ &\quad - \left(e^{\kappa\tau}-1\right)^2 e^{-\kappa(k+1)\tau}\frac{1}{2\kappa(\delta^2-\kappa^2)}\left(2\delta\eta\lambda\sigma\sigma_x + \lambda^2\sigma_x^2 + (\delta^2-\kappa^2)\sigma^2\right).\end{aligned} \tag{4.33}$$

The autocorrelation is given by

$$\begin{aligned}\operatorname{corr}[r_\tau(t-k\tau), r_\tau(t)]_\infty &= \frac{\operatorname{cov}[r_\tau(t-k\tau), r_\tau(t)]_\infty}{\operatorname{var}[r_\tau(t)]_\infty} \\ &= \frac{\alpha\left(e^{\delta\tau}-1\right)^2 e^{-\delta(k+1)\tau} - \frac{\delta}{2(\delta-\kappa)}\left(\beta-\frac{\sigma^2}{\delta}\right)\left(e^{\kappa\tau}-1\right)^2 e^{-\kappa(k+1)\tau}}{2\alpha e^{-\delta\tau}+\beta-\frac{\delta}{\delta-\kappa}\left(\beta-\frac{\sigma^2}{\delta}\right)e^{-\kappa\tau}}\end{aligned} \tag{4.34}$$

with

$$\alpha = \frac{\lambda}{\delta^2-\kappa^2}\left(\eta\sigma\sigma_x + \frac{\lambda\sigma_x^2}{2\delta}\right) \tag{4.35}$$

$$\beta = \frac{2\eta\lambda\sigma\sigma_x}{\kappa(\delta+\kappa)} + \frac{\lambda^2\sigma_x^2}{\delta\kappa(\delta+\kappa)} + \frac{\sigma^2}{\kappa}. \tag{4.36}$$

The first order autocorrelation function $\operatorname{corr}[r_\tau(t-\tau), r_\tau(t)]_\infty$ is then

$$\rho_{\tau,1} = \frac{\alpha\left(e^{\delta\tau}-1\right)^2 e^{-2\delta\tau} - \frac{\delta}{2(\delta-\kappa)}\left(\beta-\frac{\sigma^2}{\delta}\right)\left(e^{\kappa\tau}-1\right)^2 e^{-2\kappa\tau}}{2\alpha e^{-\delta\tau}+\beta-\frac{\delta}{\delta-\kappa}\left(\beta-\frac{\sigma^2}{\delta}\right)e^{-\kappa\tau}}. \tag{4.37}$$

An illustration of the autocorrelation and variance patterns for various parameter is shown in figures 4.1 and 4.2. It can be seen that the bivariate trending OU model allows for a wider variety of correlation variance patterns than its univariate counterpart.

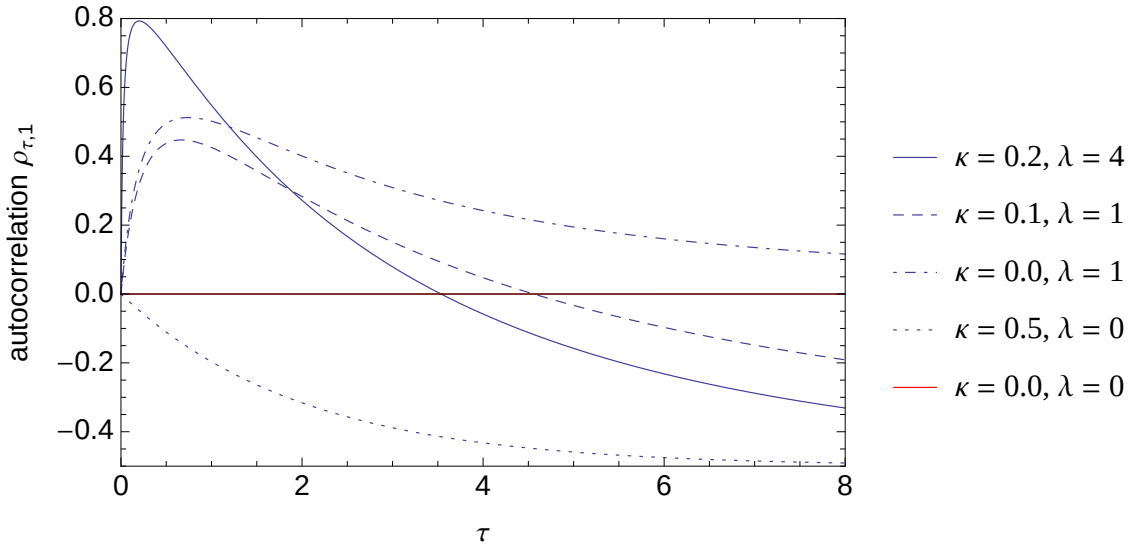

Figure 4.1: First order autocorrelation patterns $\rho_{\tau,1}$ of the bivariate trending OU process for $\sigma^2 = 0.5$, $\delta = 0.6$, $\sigma_x^2 = 2$, $\eta = 0$

As reference the autocorrelation $\rho_{\tau,1} = 0$ and variance $\operatorname{var}[r_\tau] = \sigma^2\tau$ of the geometric Brownian motion are shown (red) as well.

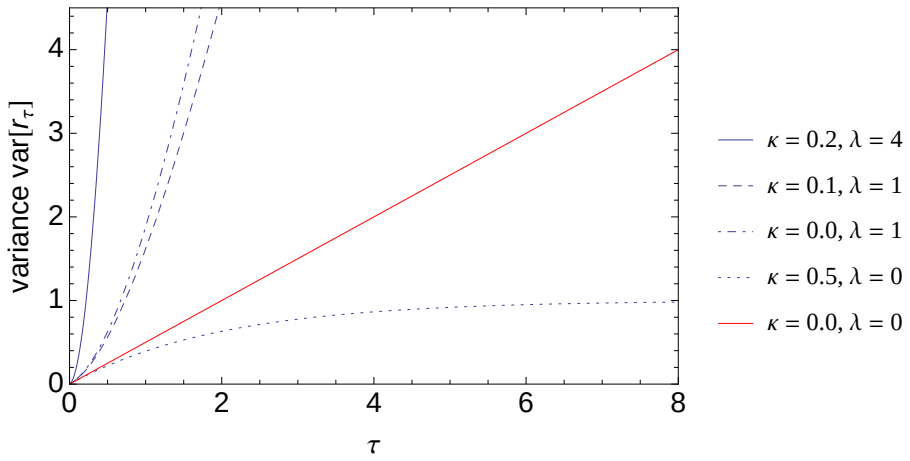

Figure 4.2: Variance patterns $\rho_{\tau,1}$ of the bivariate trending OU process for $\sigma^2 = 0.5$, $\delta = 0.6$, $\sigma_x^2 = 2$, $\eta = 0$

A more systematic overview of the first order autocorrelation and the variance is given in figures 4.3 and 4.4. For a better comparability the τ-axis is log-scaled.

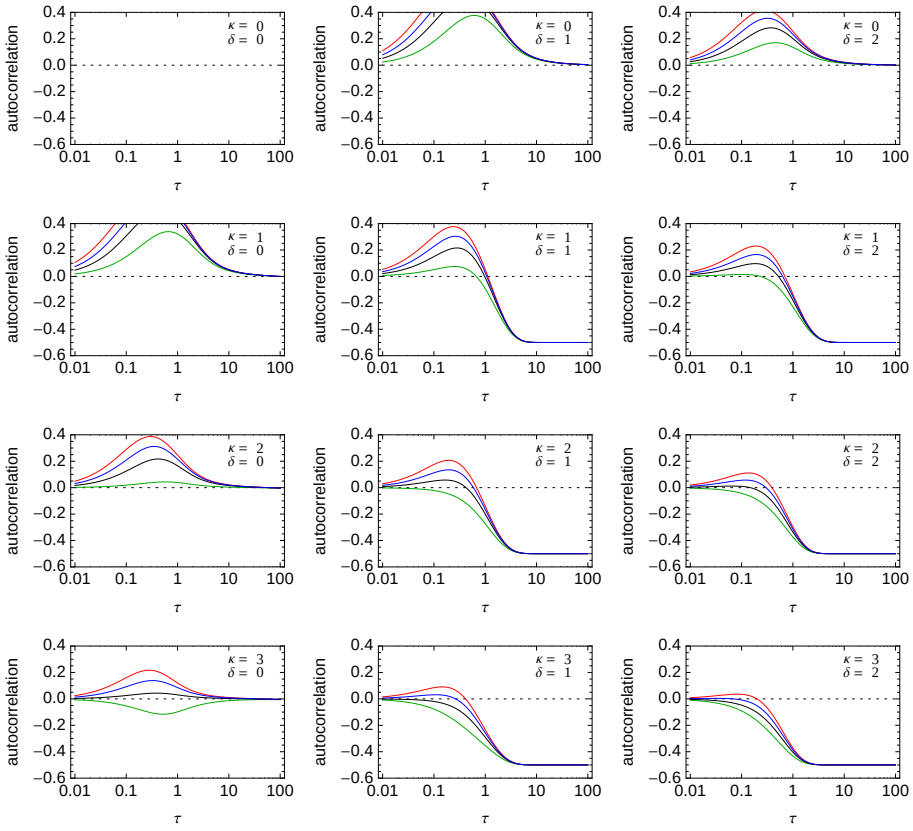

Figure 4.3: First order autocorrelation for $\sigma = 0.3$, $\sigma_x = 1.0$, $\lambda = 1.0$, $\kappa = 0$ (black), increase in σ to 0.45 (green), increase in σ_x to 1.5 (red), increase in λ to 1.25 (blue)

As in the trending OU model for $\kappa, \delta \neq 0$ the autocorrelation $\rho_{\tau,1}$ approaches $-1/2$ for large τ. When τ decreases to 0 the autocorrelation also approaches zero but the first derivative at $\tau = 0$ can now possess both signs

$$\rho_{\tau,1} \simeq \frac{\sigma_x^2 - (\kappa+\delta)\kappa\sigma^2 + 2\eta\delta\lambda\sigma_x}{2(\kappa+\delta)\sigma^2}\tau + \mathcal{O}(\tau^2). \tag{4.38}$$

Therefore it matches the empirical findings of both Lo and MacKinlay [LM88] and Fama and French [FF88a, FF88b] simultaneously. We can also see that increasing σ has qualitatively the opposite effect as increasing σ_x or λ.

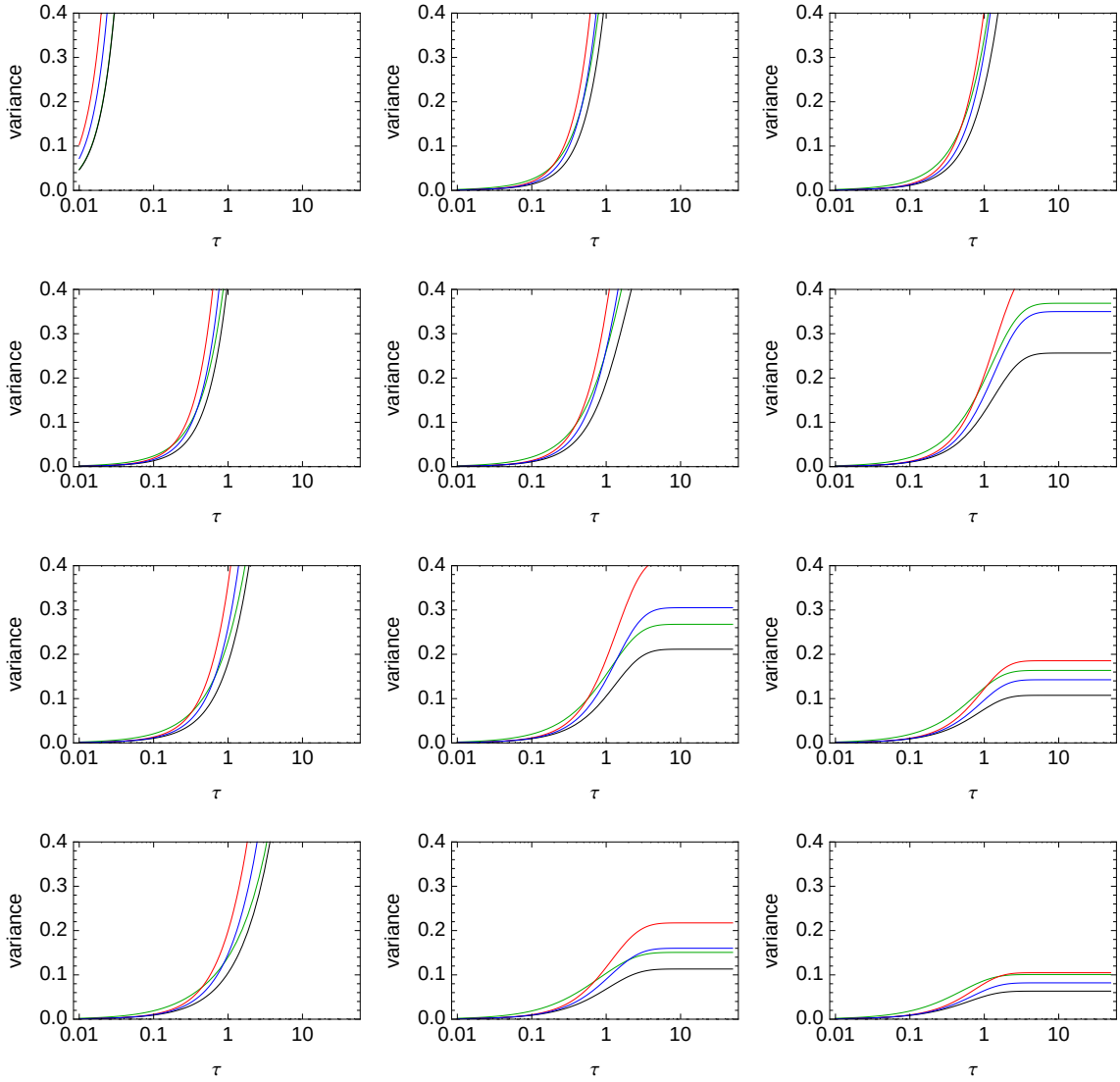

Figure 4.4: Variance for $\sigma = 0.3$, $\sigma_x = 1.0$, $\lambda = 1.0$, $\kappa = 0$ (black), increase in σ to 0.45 (green), increase in σ_x to 1.5 (red), increase in λ to 1.25 (blue)

In case of the variance we see that an increase of σ, σ_x or λ leads to an increase in variance.
The bivariate trending OU model can be simplified to

$$dq_t = \lambda X_t dt + \sigma dW_t^{(s)} \tag{4.39}$$

$$dX_t = -\delta X_t dt + \sigma_x dW_t^{(x)} \tag{4.40}$$

by setting $\eta = 0$ and $\kappa = 0$. So dW_t^s and dW_t^X are independent and the returns are positively autocorrelated for all τ (fig. 4.1).
The autocorrelation (4.37) is then given by

$$\rho_{\tau,1} = \frac{(e^{-\delta\tau} - 1)^2 \sigma_x^2 \lambda^2}{2\delta\tau e^{2\delta\tau}\delta^2\sigma^2 + 2\sigma_x^2\lambda^2 e^{\delta\tau}(1 + e^{\delta\tau}(\delta\tau - 1))} \tag{4.41}$$

which is an increasing function of λ. The variance (4.32) simplifies to

$$\text{var}[r_\tau(t)]_\infty = \sigma^2\tau + \frac{\lambda^2\sigma_x^2}{\delta^3}\left(e^{-\delta\tau} - (1 - \delta\tau)\right) \tag{4.42}$$

which can be rearranged to

$$\sigma^2 = \frac{\bar{v}_\tau^2}{\tau} - \frac{\lambda^2\sigma_x^2}{\delta^3}\frac{(e^{-\delta\tau} - (1 - \delta\tau)}{\tau}. \tag{4.43}$$

This equation shows that an increase in autocorrelation (via an increase in λ) is accompanied by a decrease in σ (the Black-Scholes input) which results in a decrease in option price.

4.2 Option Pricing

4.2.1 Theoretical Considerations

We now consider an European call option with strike K and expiry T with the goal to derive a rigorous fair price $C(S,t)$ for the underlying process (4.6). Following [DS06, R14, RY99] we show the existence of an admissible self-financing strategy to duplicate the call option. We use the standard Black-Scholes trading strategy

$$\phi_t = \frac{\partial C_{\text{BS}}(S,t)}{\partial S} \tag{4.44}$$

$$\psi_t = e^{-rt}\left(C_{\text{BS}}(S,t) - S_t\frac{\partial C_{\text{BS}}(S,t)}{\partial S}\right) \tag{4.45}$$

of ϕ_t shares S and ψ_t bonds $B_t = e^{et}$. The wealth process is then

$$\begin{aligned} V(S_t,t) &= \phi_t S_t + \psi_t B_t \\ &= C_{\text{BS}}(S_t,t) \end{aligned} \tag{4.46}$$

which implies that the trading strategy has a.s. the same final value as the considered call option. Applying Itôs lemma

$$\begin{aligned} dV(S_t,t) &= \frac{\partial C_{\mathrm{BS}}}{\partial t}dt + \frac{\partial C_{\mathrm{BS}}}{\partial S}dS + \frac{1}{2}\frac{\partial^2 C_{\mathrm{BS}}}{\partial S^2}dS^2 \\ &= \frac{\partial C_{\mathrm{BS}}}{\partial t}dt + \frac{\partial C_{\mathrm{BS}}}{\partial S}dS + \frac{1}{2}\frac{\partial^2 C_{\mathrm{BS}}}{\partial S^2}\sigma^2 S^2 dt \end{aligned} \tag{4.47}$$

and expressing the second derivative of C_{BS} by the Black-Scholes equation

$$\frac{\partial^2 C_{\mathrm{BS}}}{\partial S^2} = \frac{2}{\sigma^2 S^2}\left(rC_{\mathrm{BS}} - rS\frac{\partial C_{\mathrm{BC}}}{\partial S} - \frac{\partial C_{\mathrm{BS}}}{\partial t}\right) \tag{4.48}$$

we see that

$$\begin{aligned} dV(S_t,t) &= \frac{\partial C_{\mathrm{BS}}}{\partial S}dS + \left(rC_{\mathrm{BS}} - rS\frac{\partial C_{\mathrm{BC}}}{\partial S}\right)dt \\ &= \phi_t dS + \psi_t dB_t \end{aligned} \tag{4.49}$$

which proves that the trading strategy (ϕ, ψ) is indeed self-financing. By finding an appropriate hedging strategy it is usually concluded that the fair option price is found.

Nevertheless even in the Black-Scholes model there exist pathological suicide strategies [DS06] which are admissible and self-financing with $V(0,S) > 0$ and $V(T, S_T) \equiv 0$.

Therefore the fair option price of an attainable claim is defined by

$$\begin{aligned} c_0 = \inf\{y \geq 0 : &\text{ there exist an admissible self-financing} \\ &\text{strategy } (\tilde{\phi}_t, \tilde{\psi}_t) \text{ with } y = \tilde{\phi}_0 S_0 + \tilde{\psi}_0 B_0\}. \end{aligned} \tag{4.50}$$

To prove that the strategy (ϕ_t, ψ_t) implies the proposed option price $c_0 = C_{\mathrm{BS}}(S_0, 0)$ it is sufficient to show that the discounted wealth process is a martingale under an equivalent martingale measure $\mathbb{Q}$. The discounted wealth process is a supermartingale

$$\begin{aligned} c_0 \equiv \tilde{\phi}_0 S_0 + \tilde{\psi}_0 B_0 &\geq e^{-rT}\mathbb{E}^{\mathbb{Q}}\left[\tilde{\phi}_T S_T + \tilde{\psi}_T B_T\right] \\ &= e^{-rT}\mathbb{E}^{\mathbb{Q}}\left[C(T, S_T)\right] \\ &= e^{-rT}\mathbb{E}^{\mathbb{Q}}\left[\phi_T S_T + \psi_T B_T\right] \\ &= \phi_0 S_0 + \psi_0 B_0 \end{aligned} \tag{4.51}$$

for any admissible self-financing strategies $(\tilde{\phi}_t, \tilde{\psi}_t)$. With the infimum condition $c_0 \leq \phi_0 S_0 + \psi_0 B_0$ this gives

$$c_0 = \phi_0 S_0 + \psi_0 B_0. \tag{4.52}$$

Now we have to prove the existence of the equivalent martingale measure. Therefore we define the stochastic process

$$L_t = \left.\frac{d\widetilde{\mathbb{P}}}{d\mathbb{P}}\right|_{\mathcal{F}_t} = e^{\int_0^t \gamma_s dW_s - \frac{1}{2}\int_0^t \gamma_s^2 ds}$$

with

$$\gamma_t = \frac{\mu + \frac{\sigma^2}{2} - \kappa[\log S_t - \log S_0 - \mu t] + \lambda X_t - r}{\sigma} \tag{4.53}$$

obtained form the bivariate trending OU process

$$dS_t = \left(\mu + \frac{\sigma^2}{2} - \kappa[\log S_t - \log S_0 - \mu t] + \lambda X_t\right) S_t dt + \sigma S_t dW_t^{(s)}. \tag{4.54}$$

If γ_t is a martingale measure the Girsanov theorem (A.2) ensures that

$$d\widetilde{W}_t^{(s)} = dW_t^{(s)} + \gamma_t dt \tag{4.55}$$

$$d\widetilde{W}_t^{(x)} = dW_t^{(x)} \tag{4.56}$$

form a two dimensional Wiener process under the measure $\mathbb{Q}$ defined by $\mathbb{Q}(A) = \mathbb{E}[L_T \mathbb{I}_A]$ for all $A \in \mathcal{F}_t$ [AP10]. As the conditions

$$\sup_{t \le T} \mathbb{E}[|\gamma_t|] < \infty \tag{4.57}$$

$$\sup_{t \le T} \mathrm{var}[\gamma_t] < \infty \tag{4.58}$$

are fulfilled for the process γ_t this imply that

$$\sup_{t \le T} \mathbb{E}[e^{\varepsilon \gamma_t^2}] < \infty \tag{4.59}$$

for some $\varepsilon > 0$ [LS01] which implies subsequently that the process L_t is a martingale. Thus the asset price dynamics under the measure $\mathbb{Q}$ is given by

$$d(e^{-rt} S_t) = e^{-rt} \sigma S_t d\widetilde{W}_t^{(s)}. \tag{4.60}$$

which shows that it is a martingale measure. For the wealth process we obtain then

$$\begin{aligned} d(e^{-rt} V_t) &= \phi_t \left(-r e^{-rt} S_t dt + e^{-rt} dS_t\right) \\ &= \phi_t e^{-rt} \sigma S_t d\widetilde{W}_t^{(s)} \end{aligned} \tag{4.61}$$

which proves that the fair option price in indeed given by the Black-Scholes formula $c_0 = C_{\mathrm{BS}}(S_0, 0)$.

4.2.2 Practical Considerations

The necessary steps to calculate the option price are

1. obtain historical (closing) prices S_t of the underlying asset
2. calculate τ-returns $r_\tau(t)$
3. calculate τ-return autocorrelation $\rho_{\tau,1}$ and variance $\mathrm{var}[r_\tau]$
4. obtain parameters κ, λ, δ, σ, σ_x and η from fit of (4.37) and (4.32)
5. use the obtained σ in the Black-Scholes formula

To see the impact on the option price we need to use a real market example. The analysis is only exemplary as a thorough analysis of market data is given in the following chapter. For now we select the Deutsche Bank stock (Bloomberg ticker: `DBK GR Equity`) and use the closing prices of the period 01/11/2004 to 31/10/2014. In figure 4.5 historical prices are displayed as well as the calculated daily returns and the historical volatility.

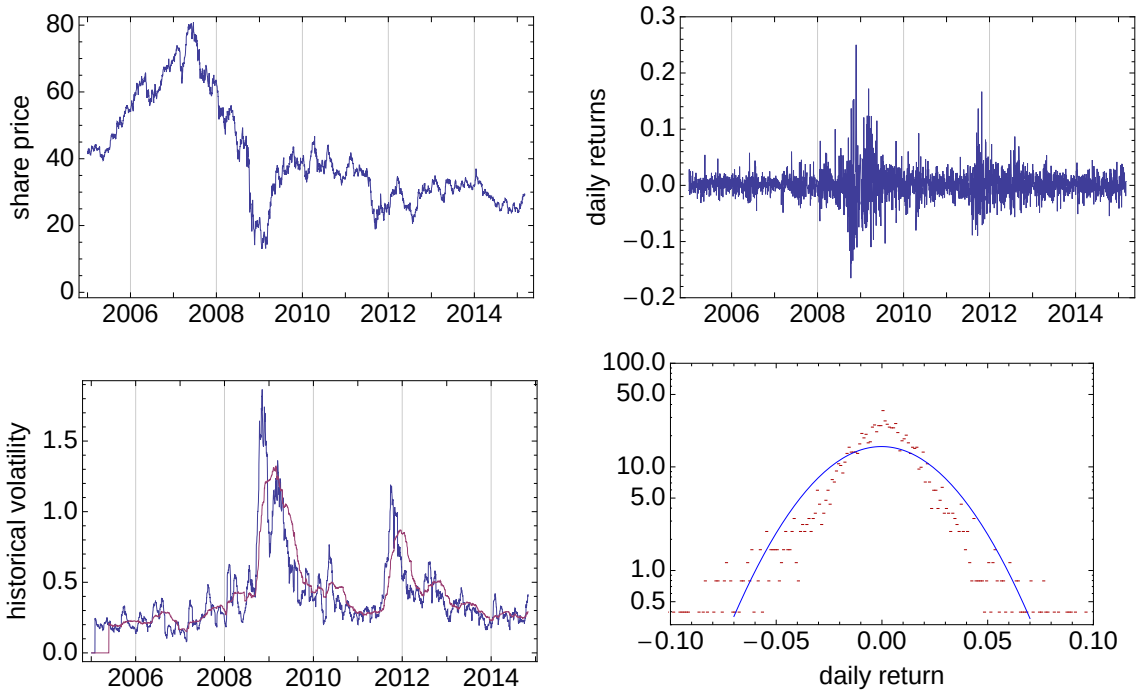

Figure 4.5: (top) Share price and daily returns of Deutsche Bank stock, (bottom) historical volatility from 20d (blue) and 100d (red) moving variance of the daily returns and a histogram of the daily returns

The periods of volatility clustering around 2009 and 2012 with historical volatilities above 100 vols are clearly visible. In times of less distressed markets the volatility is moving between 23 and 35 vols. The existence of this different market/volatility regimes shows already that a 10 year sample period might be too large to find appropriate model parameters as they obviously change over time. Therefor a fit will return only an averaged picture.
The fits of the model parameters to the historical τ-return autocorrelations and variances are shown in the following graphs

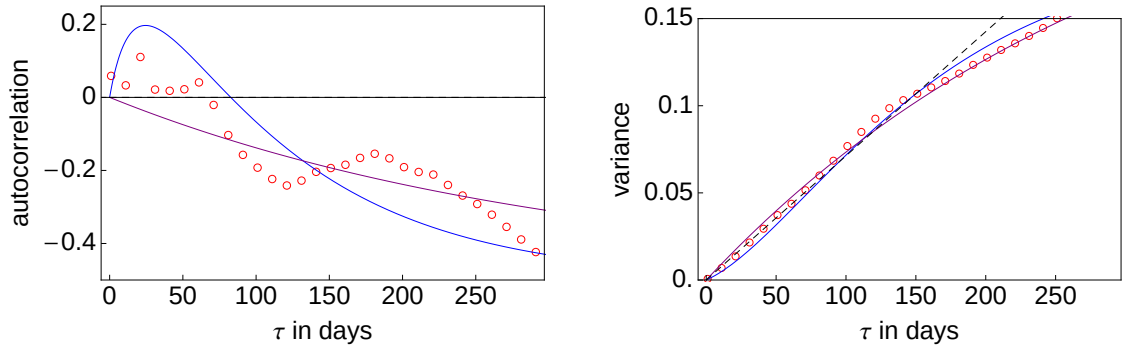

Figure 4.6: First order autocorrelation and variance of the Deutsche Bank stock τ-returns (red circles) with parameter fits for different models: geometric Brownian motion (black dotted), trending OU (purple), bivariate trending OU (blue)

The geometric Brownian motion, the trending OU process and the bivariate trending OU process return quite different σ values. A σ value of 0.51 for the GMB seems rather high compared to common market standards but is plausible due to including the two high volatility periods into the time series. The value of $\sigma = 0.56$ for the trending OU process is as predicted (chap. 3.4) even larger.

model parameter	GBM	trend. OU	bivariate trend. OU
σ	0.51 ± 0.03	0.56 ± 0.04	0.36 ± 0.07
κ	-	1.18 ± 0.15	3.68 ± 0.98
λ	-	-	1.00
δ	-	-	4.77 ± 0.72
σ_x	-	-	4.79 ± 1.02
η	-	-	0.00

Table 4.1: model parameters fitted to the historical τ-return autocorrelations and variances

options	market	GBM	trend. OU	bivariate trend. OU
DBK Dec2014 Call 23	2.19	2.914	3.074	2.455
DBK Dec2014 Call 25	0.96	1.825	2.007	1.279
DBK Dec2014 Call 27	0.32	1.072	1.246	0.573

Table 4.2: Impact of the selected model on call option price on 31/10/2014 with a share closing price of 24.942 and an interest rate of 0.87%

Using the bivariate trending OU process to model the dynamics of the underlying asset reduces volatility significantly to $\sigma = 0.36$. To calculate the option price the various σ values are inserted into the Black-Scholes equation. As example we use Dec2014 European calls on the DBK stock with six weeks to maturity and strikes of 23, 25 and 27. With a share price of 24.942 they can be considered as liquid in, at and out of the money calls.
The model impact on the option price is summarised in table 4.2. As the bivariate trending OU process had the smallest σ it also implies the lowest call price with deviation from the market price between 12% and 78% which is not good but much more reasonable than the deviations of 33% and 235% of the geometric Brownian motion.

Chapter 5

Analysis of Market Data

In this chapter we will compare the previously discussed price processes with real market data. We will focus on equity instruments such as indices, stocks and futures.

5.1 Simulated Price Processes

In oder to test the implementation of the code and to benchmark the parameter estimation process we start with three synthetic assets. The price processes of synthetic assets I - III are modelled by a geometric Brownian motion, a trending OU process and a bivariate OU process respectively. The used parameters are summarised in table 5.1. The sample paths are generated by a Monte Carlo simulation utilising Mathematica.

asset	μ	κ	δ	λ	σ	σ_x	η
synthetic asset I *(geometric BM)*	0.025	-	-	-	0.200	-	-
synthetic asset II *(trending OU)*	0.025	5.00	-	-	0.200	-	-
synthetic asset III *(bivariate OU)*	0.025	5.00	3.00	1.00	0.200	2.0	0.0

Table 5.1: Parameters used for Monte Carlo simulation of synthetic assets I - III.

If not mentioned otherwise we used an initial asset value of $S_0 = 100$, a time horizon of 10 years and time steps of $\Delta t = 1/365$. For synthetic asset III we set $\eta = 0$ as this additional degree of freedom did not imply a significant advantage to the model.

5.1.1 Synthetic Asset I - Geometric Brownian Motion

For the simulation we used for the drift and the volatility the typical values of $\mu = 0.025$ and $\sigma = 0.20$. Figure 5.1 shows a typical price process of synthetic asset I. The parameters allow for larger price variations in a period of 10 years which resembles typical market observations.

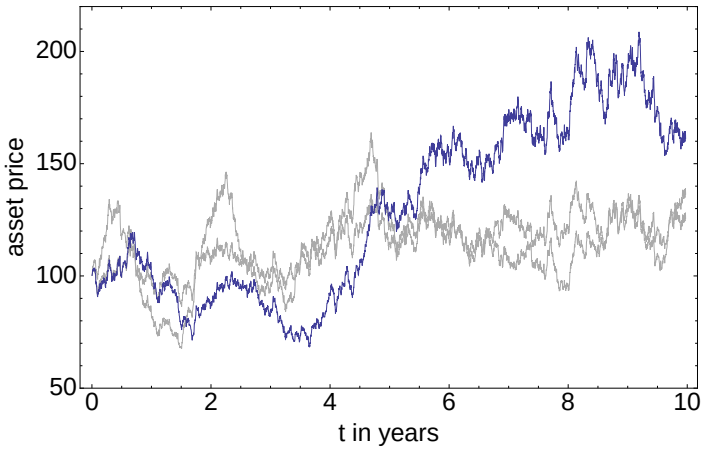

Figure 5.1: Sample path of synthetic asset I (blue), asset II and III are shown in grey

The Monte Carlo time step $\Delta t = 1/365$ emulates daily closing prices and gives in a 10 year period 3650 τ-returns for the statistical analysis. The empirical daily, weekly and monthly return distributions of one process are shown in the histogram in figure 5.2 (left). Due to the construction of the price process as a geometric Brownian motion they are normal distributed

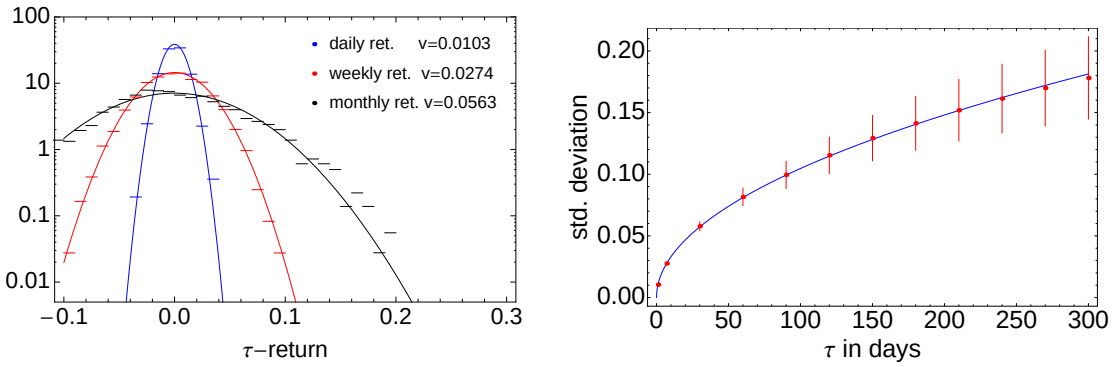

Figure 5.2: Histogram of the daily, weekly and monthly returns (synthetic asset I) of one simulated process (left), estimated τ-return variances from $N = 50$ simulations (right)

The standard deviation of the τ-return distributions can be fitted to the histogram

data (fig. 5.2). The averaged results over $N = 50$ simulations are shown on the right hand side which match the theoretical prediction of $\sigma\sqrt{\tau}$ from (3.36) quite well.
Later on we will use τ-return time series data to estimate model parameters. Therefore we will have to deal with the problem arising from small sample sizes which may lead to spurious trends and subsequently to wrong parameter fits.
This can be observed in the variance and the autocorrelation plot of the τ-returns for a simulated 10 year and a 100 year time series. The variances in figure 5.3 fit quite well with the theoretical prediction of $\sigma^2\tau$ (3.36). Nevertheless the autocorrelation data from the 10 year time series deviates significantly from the prediction $\rho_1 = 0$. The situation improves clearly for the 100 year data.

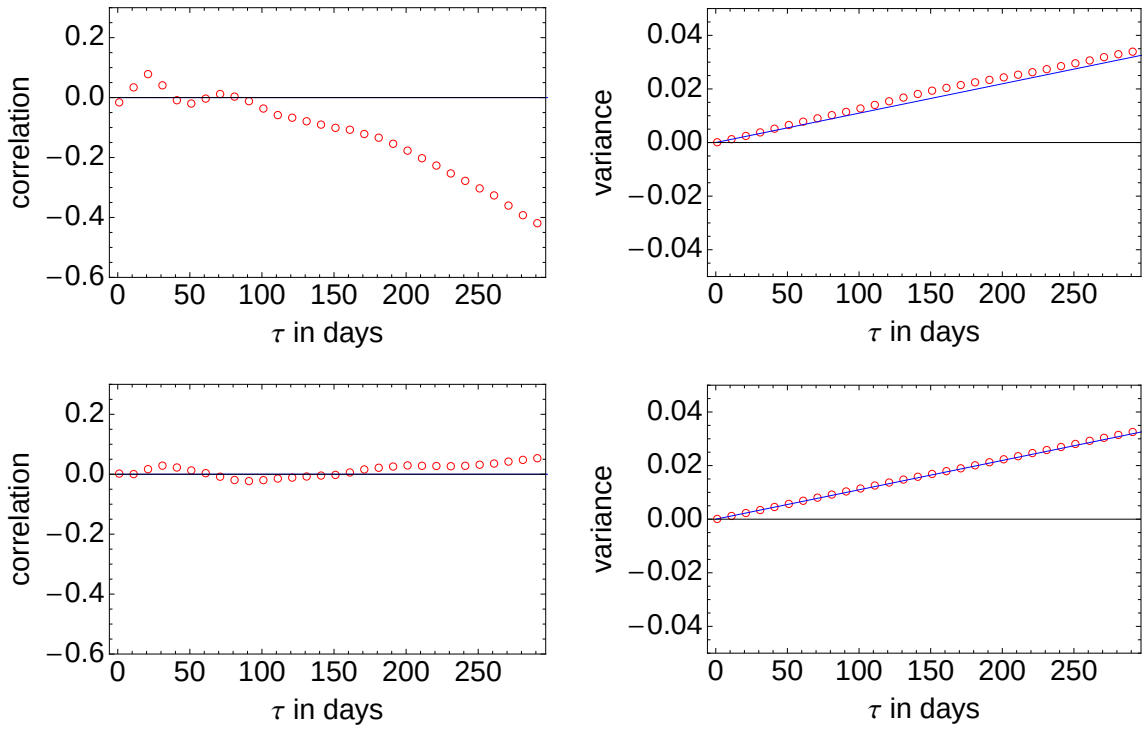

Figure 5.3: Autocorrelation variance of τ-returns for one simulated time series for a 10 year period (top) and a 100 year period (bottom). The data obtained from the simulation is shown in red. The blue graphs show the theoretical prediction.

The fitting of the model parameter is rather simple in this case. The single parameter σ can be obtained from a least square fit of the variance data.

5.1.2 Synthetic Asset II - Trending OU Process

For comparability we used for the drift and the volatility the same values ($\mu = 0.025$ and $\sigma = 0.20$) as before and set $\kappa = 5.0$. Figure 5.4 shows a typical price process of

synthetic asset II. Partly due to a relatively strong trending parameter κ the sample time series looks rather uniform (compared to the geometric Brownian motion of synthetic asset I) and too superficial to resemble 10 year market data.

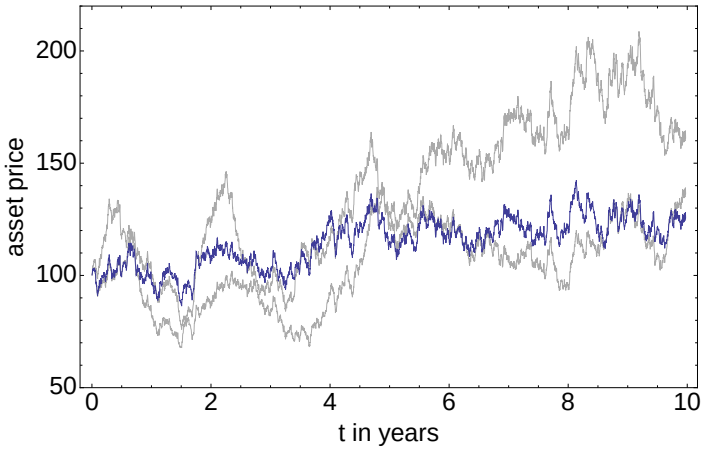

Figure 5.4: Sample path of synthetic asset II (blue), asset I and III are shown in grey

The τ-returns are again normal distributed with a standard deviation of $\sigma\sqrt{(1-e^{-\kappa\tau})/\kappa}$ which also can be observed empirically (fig. 5.5 right).

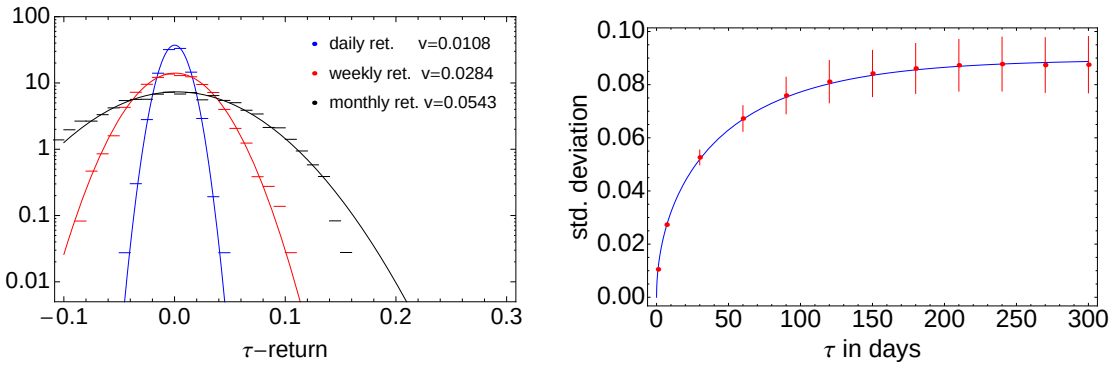

Figure 5.5: Histogram of the daily, weekly and monthly returns (synthetic asset II) of one simulated process (left), estimated τ-return variances from $N = 50$ simulations (right)

The τ-return variance and autocorrelation from the 10 year and 100 year data are shown in figure 5.6. While the variances of the 10 year fits reasonable well with the theoretical prediction (blue) the autocorrelation functions shows larger deviations beyond 200 days. For the 100 year data the situation improves significantly especially for the autocorrelation. To obtain the two model parameters κ and σ we perform a

series expansion in τ of (3.37). For the variance we obtain

$$\bar{v}_\tau^2 = \frac{\sigma^2}{\kappa}(1 - e^{-\kappa\tau}) \tag{5.1}$$

$$\simeq \sigma^2\tau - \frac{1}{2}\kappa\sigma^2\tau^2 + \mathcal{O}(\tau^3) \tag{5.2}$$

and for the autocorrelation

$$\rho_{\tau,1} = -\frac{1}{2}\left(1 - e^{-\kappa\tau}\right)$$

$$\simeq -\frac{1}{2}\kappa\tau + \frac{1}{2}\kappa^2\tau^2 + \mathcal{O}(\tau^3)\,. \tag{5.3}$$

As the first order approximations are decoupled, σ and κ can be obtained independently. The slopes of the linear fits of the variance and the autocorrelation (dashed lines in fig. 5.6) can be used to estimate the parameters

$$\sigma = \sqrt{b_{\bar{v}^2}} \tag{5.4}$$

$$\kappa = -2b_{\rho_{\tau,1}}. \tag{5.5}$$

Another estimator is the limit of the variance for $\tau \to \infty$ which is given by

$$\bar{v}_\infty^2 = \frac{\sigma^2}{\kappa}. \tag{5.6}$$

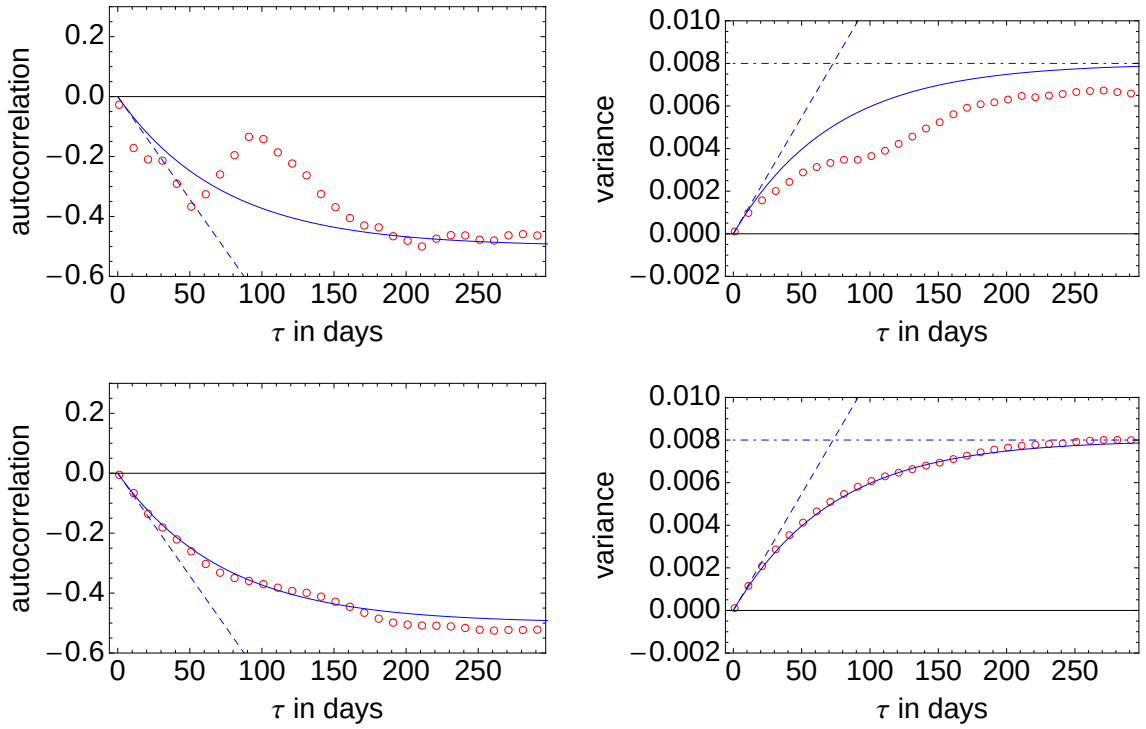

Figure 5.6: Autocorrelation and Variance of τ-returns from one simulated process with a 10 year period (top) and a 100 year period (bottom)

5.1.3 Synthetic Asset III - Bivariate OU Process

We used for the drift and the volatility the same values ($\mu = 0.025$ and $\sigma = 0.20$) as before and chose $\kappa = 5.0$, $\delta = 3$, $\sigma_x = 2$, $\lambda = 1.0$ and $\eta = 0$ for the other parameters of the bivariate OU process. Figure 5.7 shows a typical price process of synthetic asset III.

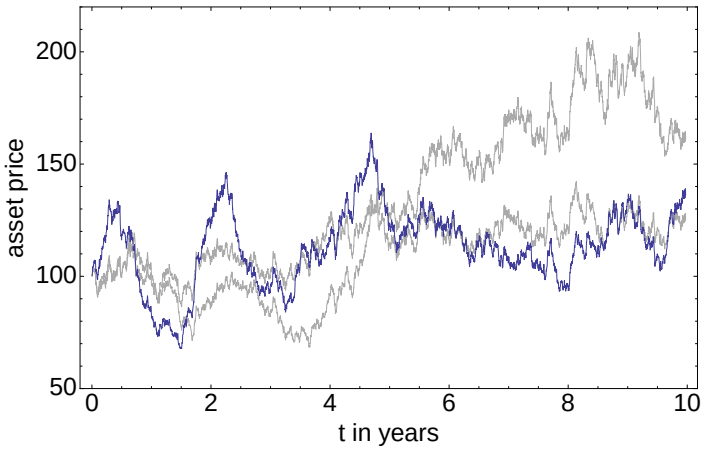

Figure 5.7: Sample path of synthetic asset III (blue), asset I and II are shown in grey

The sample path of asset III shows more features then asset II and seems more realistic compared with real market data. The daily, weekly and monthly returns from 10 year data are shown in the histogram in figure 5.8. The τ-returns are normal distributed with a standard deviation

$$\sqrt{\frac{\sigma^2}{\kappa}(1-e^{-\kappa\tau}) + \left(\frac{\lambda^2\sigma_x^2}{\delta\kappa(\delta+\kappa)} + \frac{2\lambda\eta\sigma\sigma_x}{\delta+\kappa}\right)\left((1-e^{-\kappa\tau}) - \frac{\kappa\left(e^{-\delta\tau}-e^{-\kappa\tau}\right)}{\kappa-\delta}\right)} \qquad (5.7)$$

which fits quite well with the results from the Monte Carlo simulations.

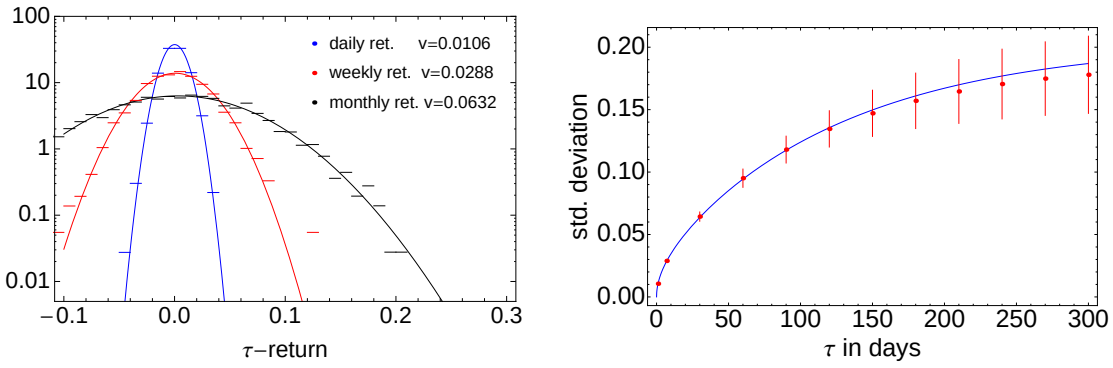

Figure 5.8: Histogram of the daily, weekly and monthly returns (synthetic asset III) of one simulated process (left), estimated τ-return variances from $N = 50$ simulations (right)

The autocorrelation and variance of the τ-return data from a 10 year and a 100 year simulation is shown in figure 5.9. We see that the theoretical predictions (blue line) using the simulation parameters fit reasonably well for the 10 year data and the situation improves for the 100 year data. The deviation in 10 year autocorrelation data is particularly large. In addition the first (dotted) and second (dashed) order Taylor expansion of the theoretical curves at $\tau = 0$ are shown. They fit reasonably well with the data so they could be used to fit the model parameters.

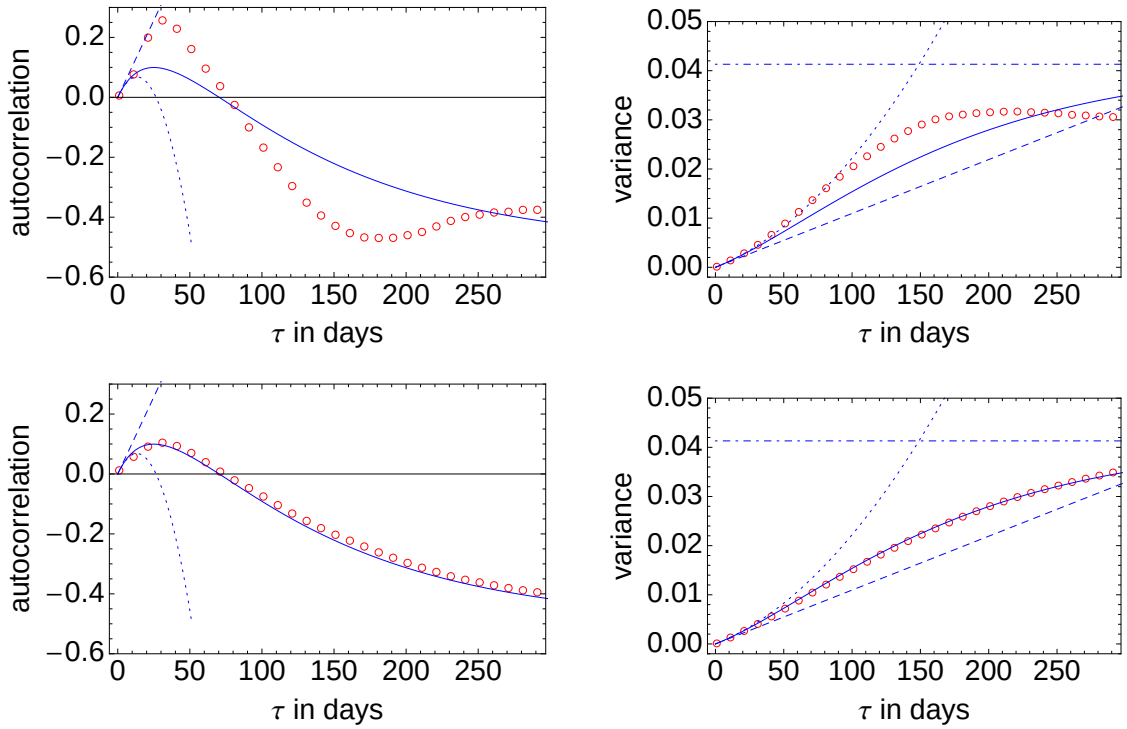

Figure 5.9: Variance and autocorrelation of τ-returns from one simulated process with a 10 year period (top) and a 100 year period (bottom)

Quantities which are suitable for the parameter estimations are the limit $\bar{v}_\infty^2$ and first and second derivative of the variance and the autocorrelation at $\tau = 0$

$$\bar{v}_\infty^2 \simeq \frac{\sigma^2}{\kappa} + \frac{\sigma_x^2}{\delta\kappa(\delta+\kappa)} \tag{5.8}$$

$$\bar{v}_\tau^2 \simeq \sigma^2\tau + \frac{\sigma_x^2 - (\kappa+\delta)\kappa\sigma^2}{2(\kappa+\delta)}\tau^2 + \mathcal{O}(\tau^3) \tag{5.9}$$

$$\begin{aligned}\rho_{\tau,1} \simeq{}& \frac{\sigma_x^2 - (\kappa+\delta)\kappa\sigma^2}{2(\kappa+\delta)\sigma^2}\tau \\ &+ \frac{(\kappa^2\sigma^4(\kappa+\delta)^2 - 2\delta\sigma^2\sigma_x^2(\kappa+\delta) - \sigma_x^4)}{4\sigma^4(\kappa+\delta)^2}\tau^2 + \mathcal{O}(\tau^3).\end{aligned} \tag{5.10}$$

As the second derivative of the variance and the first derivative of the autocorrelation have the same values this results in four equations for the parameters κ, δ, σ and σ_x which can be solved numerically. From equation (5.10) we see that for the parameter combination

$$\kappa^2 + \delta\kappa - \frac{\sigma_x^2}{\sigma^2} > 0 \tag{5.11}$$

a positive autocorrelation can be achieved for small τ.

5.1.4 Parameter Estimation

We test now the parameter estimation before we analyse the real market data to evaluate its reliability. The data generated for the synthetic assets I - III in figures 5.3, 5.6 and 5.9 is used for this propose. An overview of the results are shown in table 5.2 where the bold values were used as parameters in the simulations.
For synthetic asset I - the geometric Brownian motion - σ is the only parameter. It is obtained from a least square fit of the variance data. With 0.200 ± 0.01 and 0.198 ± 0.03 it gives very accurate results for the 100 year and even for the 10 year data mainly due to the fact that the autocorrelation data is not used.
For the trending OU process used in synthetic asset II the situation is a bit more complicated. The results from the 100 year data fit quite well with the parameters. In contrast for the 10 year data the slope of the variance at $\tau = 0$ is difficult to estimate which increases the error in the σ estimate to 0.186 ± 0.08. The estimation of the slope of the autocorrelation at $\tau = 0$ and the variance limit $\bar{v}_\infty^2$ is very inaccurate which results in a large error for κ.
Synthetic asset III is the most demanding case as for the bivariate OU process four parameters κ, δ, σ and σ_x have to be estimated. In addition to the parameter estimation process described in section 5.1.3 (denoted as method i) we use a non-linear parameter least square optimiser from a previous work [T08] (denoted as method ii). The reason for this is the large error introduced by the estimation of the second derivatives. For the 100 year data both methods yield in general comparable values with smaller errors for the second method. For the 10 year data an accurate estimation of the second derivatives is almost impossible resulting in a high deviation of the results and larger errors. The least square optimiser delivers more reliable results and therefore seems to be the optimal choice for the analysis of the market data.
However for real market data it makes no sense to analyse 100 year time series as on this time scale model parameters tend to have a significant time dependence. We chose this particular time span solely to generate large enough data samples to be

asset	κ	δ	σ	σ_x
synthetic asset I	-	-	**0.200**	-
estimate from 10y data	-	-	0.198 ± 0.03	-
estimate from 100y data	-	-	0.200 ± 0.01	-
synthetic asset II	**5.00**	-	**0.200**	-
estimate from 10y data	5.12 ± 0.29	-	0.166 ± 0.08	-
estimate from 100y data	4.98 ± 0.03	-	0.202 ± 0.02	-
synthetic asset III	**5.00**	**3.00**	**0.200**	**2.0**
i) estimate from 10y data	5.72 ± 1.41	4.3 ± 1.2	0.241 ± 0.09	2.7 ± 1.2
ii) estimate from 10y data	5.57 ± 1.28	3.9 ± 0.9	0.232 ± 0.08	2.6 ± 1.2
i) estimate from 100y data	5.24 ± 0.36	2.7 ± 0.4	0.188 ± 0.03	2.2 ± 0.8
ii) estimate from 100y data	5.16 ± 0.33	3.2 ± 0.3	0.194 ± 0.02	1.9 ± 0.6

Table 5.2: Overview of parameter estimations for synthetic assets I - III. The bold values were used as parameter inputs in the simulations

able to test our implementation under optimal conditions. Shorter time periods of course are more desirable for the analysis of real market data. In addition to the 10y data we tried also 5, 2 and 1 year data but especially for the bivariate OU process the statistics failed and a reliable parameter estimation was not feasible. As an example figure 5.10 shows the analysis of the Deutsche Bank stock analysis (analog to fig. 4.6) but using 1 year data instead of 10 years.

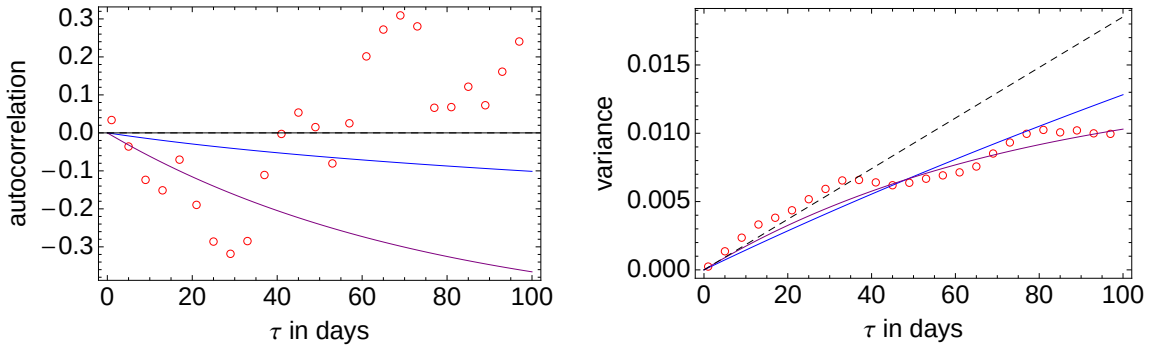

Figure 5.10: First order autocorrelation and variance of the Deutsche Bank stock τ-returns (red circles) with parameter fits for different models: geometric Brownian motion (black dotted), trending OU (purple), bivariate trending OU (blue)

Using 10 year data was a compromise as this was short enough to allow for reasonably constant model parameters as well as useful parameter estimations. Nevertheless, the fitting allows only a σ estimate with an error of around 20%. As this parameter is

subsequently used in the Black-Scholes equation to calculate the option price, we can conclude already that the usability of the bivariate OU process to model asset returns is clearly limited.

5.2 Equity Indices

As a first asset class we chose equity indices which are underlyings to various liquid put and call options available in the market. We restrict ourselves to a small subset of six indices distributed on different continents namely the American SP500, the British FTSE, the German DAX, the Chinese HSI the Japanese Nikkei and the Korean KS11. The indices are baskets of stocks of listed companies in their counties and are non-tradable themselves. Nevertheless, futures contracts on the indices with monthly expiries are traded almost 24/7 and therefore the agreed market standard is that the index prices are implied by the futures contract which is closest to deliver.
For our analysis we use the daily closing prices from 01/01/1993-31/10/2014 published by Bloomberg (BBG ticker: SPX Index, UKX Index, DAX Index, HSI Index, NKY Index). In figure 5.11 the daily returns for four indices are shown. Various economic events like collapse of LTCM (1998), Worldcom/Enron (2002) and the credit crisis (2008) are visible as clusters with a higher variance in the daily returns.

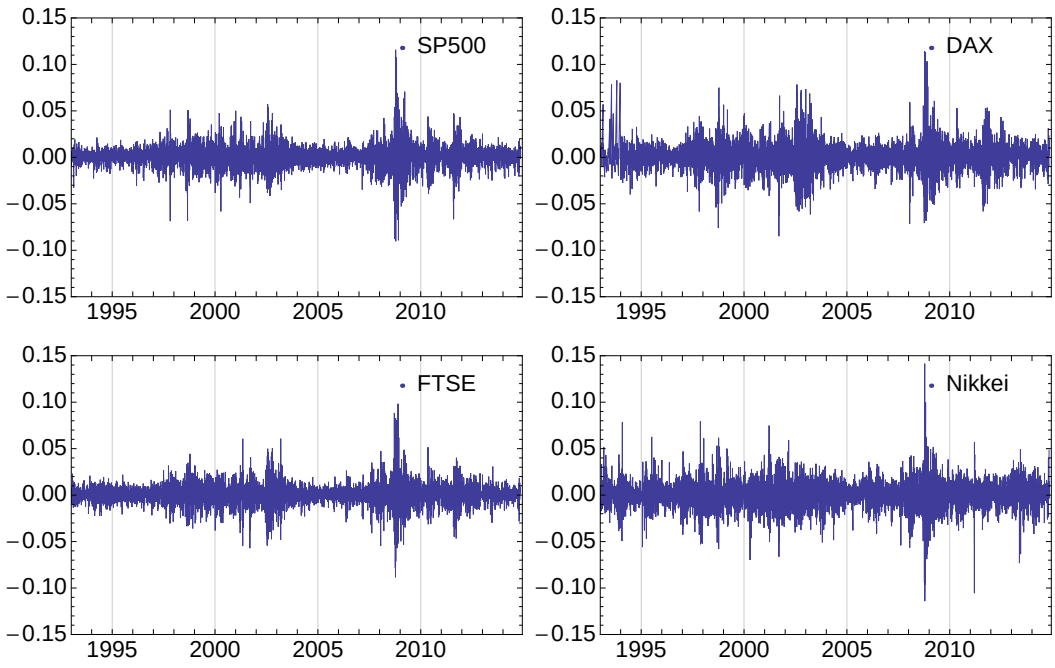

Figure 5.11: Daily log-returns for major indices for the time period 1993-2014

In figure 5.12 histograms of the daily returns of major equity indices are shown together with a fitted normal distribution. It is apparent that the return distribution can be approximated by a normal distributed only to a certain extend as the occurrence of extreme returns do not decrease exponentially.

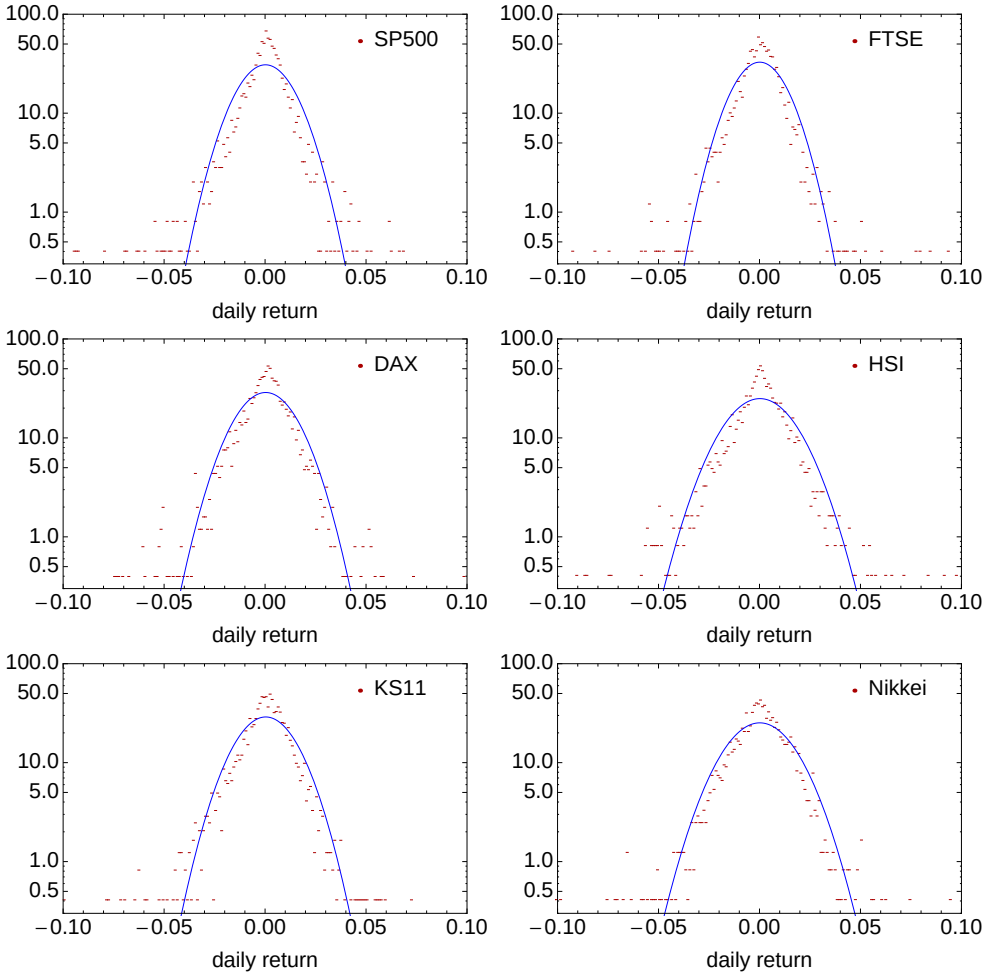

Figure 5.12: Histograms of daily log-returns of major equity indices

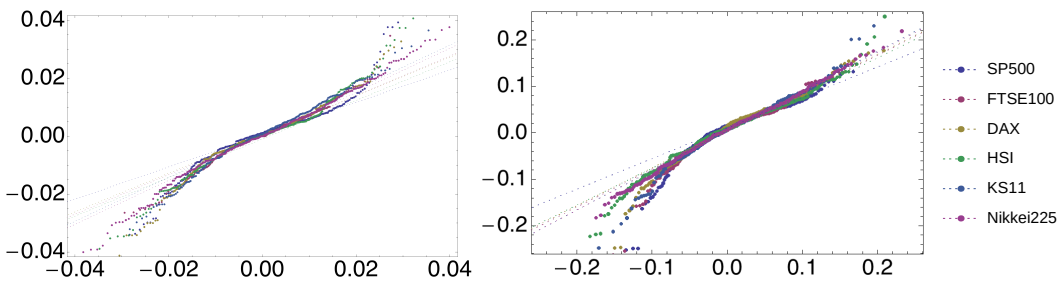

Figure 5.13: Quantile-quantile plot of daily (left) and monthly (right) log-returns of major equity indices

If the returns periods is extended from a day to a month the returns become slightly more normal distributed which is visible in the QQ plot (fig. 5.13). Table 5.3 presents a summary statistics of four stock market returns measured at different frequencies.

	SP500	FTSE100	DAX	Nikkei225
daily				
mean	0.037	0.035	0.036	0.009
std. dev	1.047	0.987	1.432	1.213
skewness	-1.611	-0.876	-0.614	-0.174
kurtosis	47.847	11.532	10.871	13.873
weekly				
mean	0.175	0.165	0.179	0.039
std. dev	2.419	3.912	3.533	3.328
skewness	-1.899	-0.776	-0.572	-0.155
kurtosis	27.818	13.142	8.698	7.143
monthly				
mean	0.851	0.716	0.701	0.145
std. dev	4.627	5.542	6.554	4.387
skewness	-0.846	-1.471	-0.883	-0.431
kurtosis	7.162	9.655	5.922	3.195
yearly				
mean	10.164	9.001	8.751	1.761
std. dev	13.966	16.659	23.223	19.121
skewness	-0.776	-1.328	-0.871	-0.394
kurtosis	3.612	4.517	3.010	2.531

Table 5.3: Statistics of log-returns for four major stock markets and various frequencies

Annualised mean and variances, derived from daily, weekly and monthly data is similar to the annual data. In conclusion we can say that the assumption of normal distributed returns is reasonable and therefore the return can be modelled by a Gaussian process like the geometric Brownian motion or the trending OU process.
As described in the previous section we need to use 10 year of data to obtain a decent sample size such that the calculated autocorrelations and variances are stable. Therefore we used the period $01/11/2004 - 31/10/2014$. The empirical τ-return autocorrelations and variances are shown in figure 5.14. We find positively correlated τ-returns at smaller times predominantly between 50 and 100 days. For larger τ the autocorrelation function becomes negative and seems to approach -0.5.

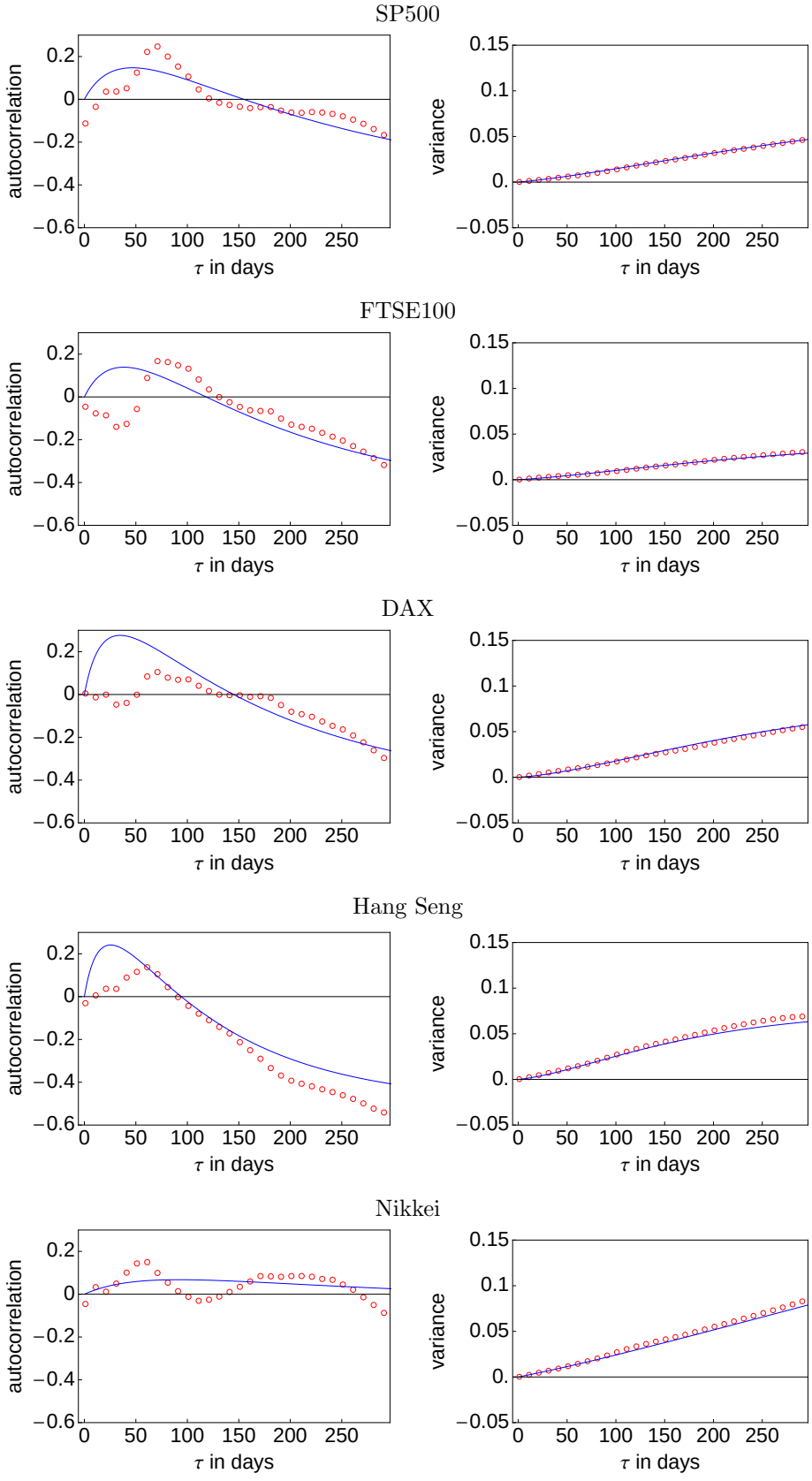

Figure 5.14: Autocorrelation and variance of returns for selected equity indices

Although the parameter fitting of the variance function is very good the found shapes of autocorrelation function can only be roughly resembled by the model. The fit parameters are summarised in table 5.4. For all indices the parameter σ is smaller than σ_{GBM} which was fitted under the assumption of the geometrical Brownian motion price process. The largest deviation $\Delta\sigma$ is found for the DAX and the HSI with almost 10 vols. These two indices show also the highest κ value.

index	κ	δ	λ	σ	σ_x	η	σ_{GBM}	$\Delta\sigma = \sigma - \sigma_{\text{GBM}}$
S&P500	3.93	1.02	1.00	0.188	1.42	0.00	0.245	-0.057
FTSE100	3.75	1.81	1.00	0.154	1.20	0.00	0.183	-0.029
DAX30	4.52	1.56	1.00	0.162	1.92	0.00	0.259	-0.097
Hang Seng	4.99	3.05	1.00	0.195	2.89	0.00	0.287	-0.092
Nikkei225	3.67	0.06	1.00	0.275	1.24	0.00	0.301	-0.026

Table 5.4: parameter for equity indicies

5.3 Common Stocks

The second asset class we want to investigate are common stocks which are underlyings to various liquid ATM put and call options. We restrict ourselves to a small set of six stocks from three different market sectors. The two technology titles are Apple and IBM (ticker: APPL US Equity, IBM US Equity). From the automotive sector we selected Daimler and Ford (ticker: DAI GR Equity, F US Equity) and from banking HSBC and Deutsche Bank (ticker: HSBA LN Equity, DBK GR Equity)
The daily log-return distributions for the period 01/01/1994-31/10/2014 are shown in figure 5.12. The results look rather similar to the return distributions of the equity indices (fig. 5.12) although skewness and kurtosis are found to be larger for the single stocks. The reason for this is the reduction of larger returns for equity indices which is caused by the diversification of the basket.

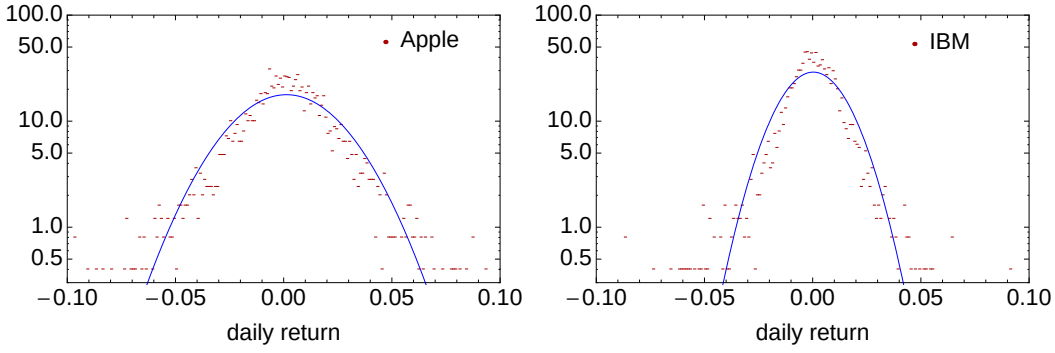

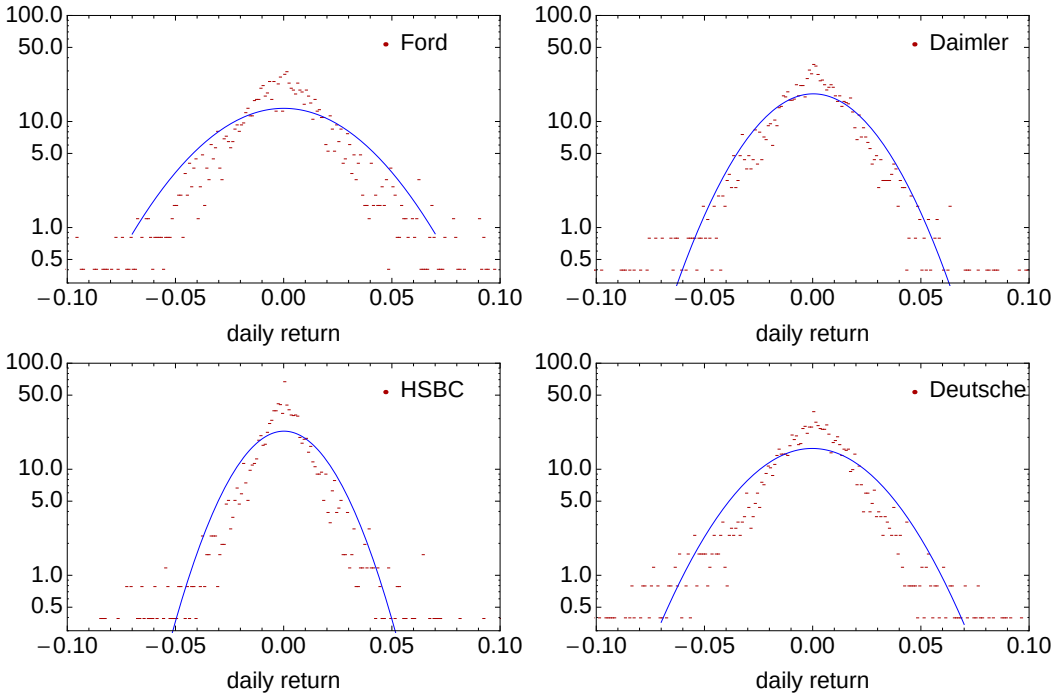

Figure 5.15: Histograms of daily log-returns of selected stocks

The τ-return autocorrelation and variance for the 10 year data (01/11/2004-31/11/2014) are displayed in figure 5.16. We find positively correlated τ-returns at smaller times predominantly between 0 and 100 days (except of the Daimler stock). For larger τ the autocorrelation function is negative for all stocks and seems to approach -0.5.

Apple Inc

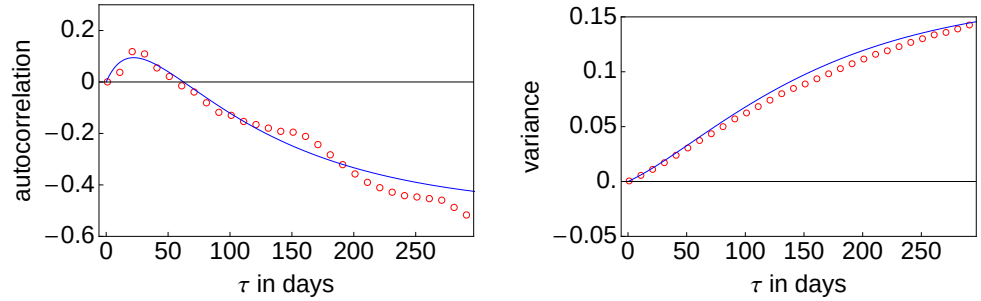

IBM

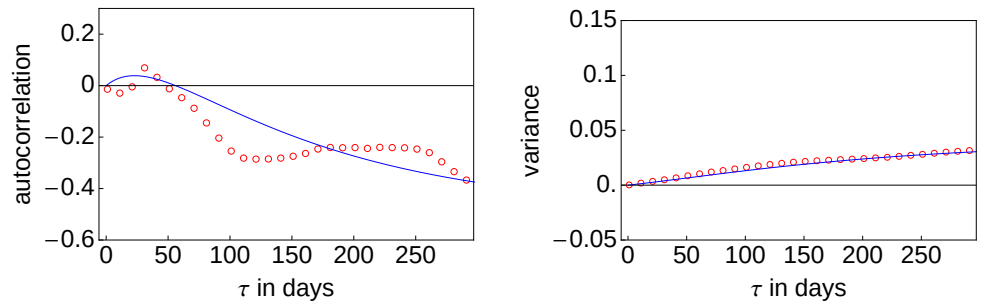

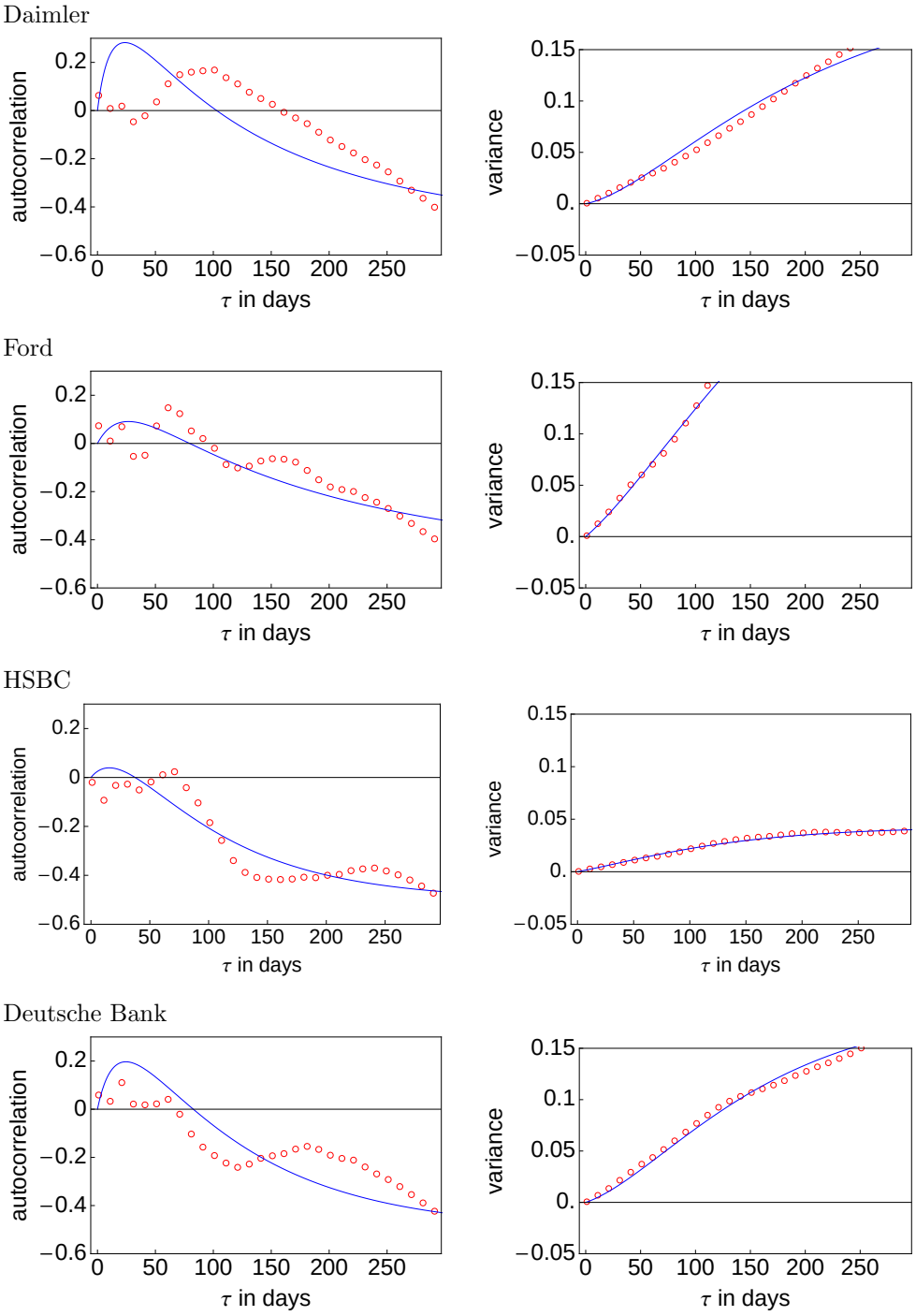

Figure 5.16: Autocorrelation and variance of returns for selected stocks

The variance shows a predominantly linear dependence on τ with a decreasing slope for $\tau > 100$. As for the equity indices the variance function looks rather smooth while the autocorrelation function shows a large variety of oscillations especially on

the short end.
The parameters estimated from fitting the empirical data are summarised in table 5.5. We note that the κ and δ parameters are similar for the stocks from the same sector. For all indices the parameter σ is smaller than σ_{GBM} which was fitted under the assumption of the geometrical Brownian motion price process at $\tau = 100$. The largest deviation $\Delta\sigma$ is found for the Daimler and the Deutsche Bank stocks with around 15 vols.

stock	κ	δ	λ	σ	σ_x	η	σ_{GBM}	$\Delta\sigma = \sigma - \sigma_{\text{GBM}}$
technology								
Apple Inc.	6.24	2.91	1.00	0.424	4.84	0.00	0.458	-0.034
Int. Bus. Mach. Corp	5.01	2.14	1.00	0.206	1.55	0.00	0.232	-0.026
automotive								
Daimler AG	1.91	7.07	1.00	0.281	4.66	0.00	0.431	-0.150
Ford Motor Co	1.47	7.15	1.00	0.576	4.80	0.00	0.657	-0.081
banking								
HSCB Holdings PLC	4.58	5.35	1.00	0.271	2.55	0.00	0.308	-0.037
Deutsche Bank AG	3.68	4.77	1.00	0.362	4.79	0.00	0.511	-0.149

Table 5.5: parameters for stocks

5.4 Futures

As the last asset class we want to analyse are futures. Options on futures began trading in 1983 and currently, puts and calls on agricultural, metal, and financial (foreign currency, interest-rate and stock index) futures are traded by open outcry in designated pits.
We restrict ourselves to a small set of seven futures split into the five agricultural titles cotton (CT), cocoa (CC), corn (KC), wheat (W), soya bean (SB), index futures on the SP500 (ES) and energy futures on WTI crude oil (CL).
As futures contracts usually expire at the end of the quarter (Mar, Jun, Sep, Dec) there are four contracts available in a year at CBOY and CMB. As only the futures closest to expiry are liquid we only used their prices in our time series. The daily log-return distributions for the period 01/01/1994 -31/10/2014 are shown in figure 5.17. The returns from agricultural and crude oil futures the look much more normal distributed than the returns of the stocks and equity indicies.
The reason for this might be that commodities are a completely separate asset class because they cannot be priced by arguments of net present value. A bond, whether

a Treasury or a defaultable corporate bond, is priced as the discounted expectation (under the risk-neutral measure) of future coupon and principal payments. The same type of reasoning may apply to the pricing of a stock, with dividend payments as future cash flows. Therefore commodities are priced by supply, demand and inventory which makes the geometric Brownian motion assumption more reasonable [G05].

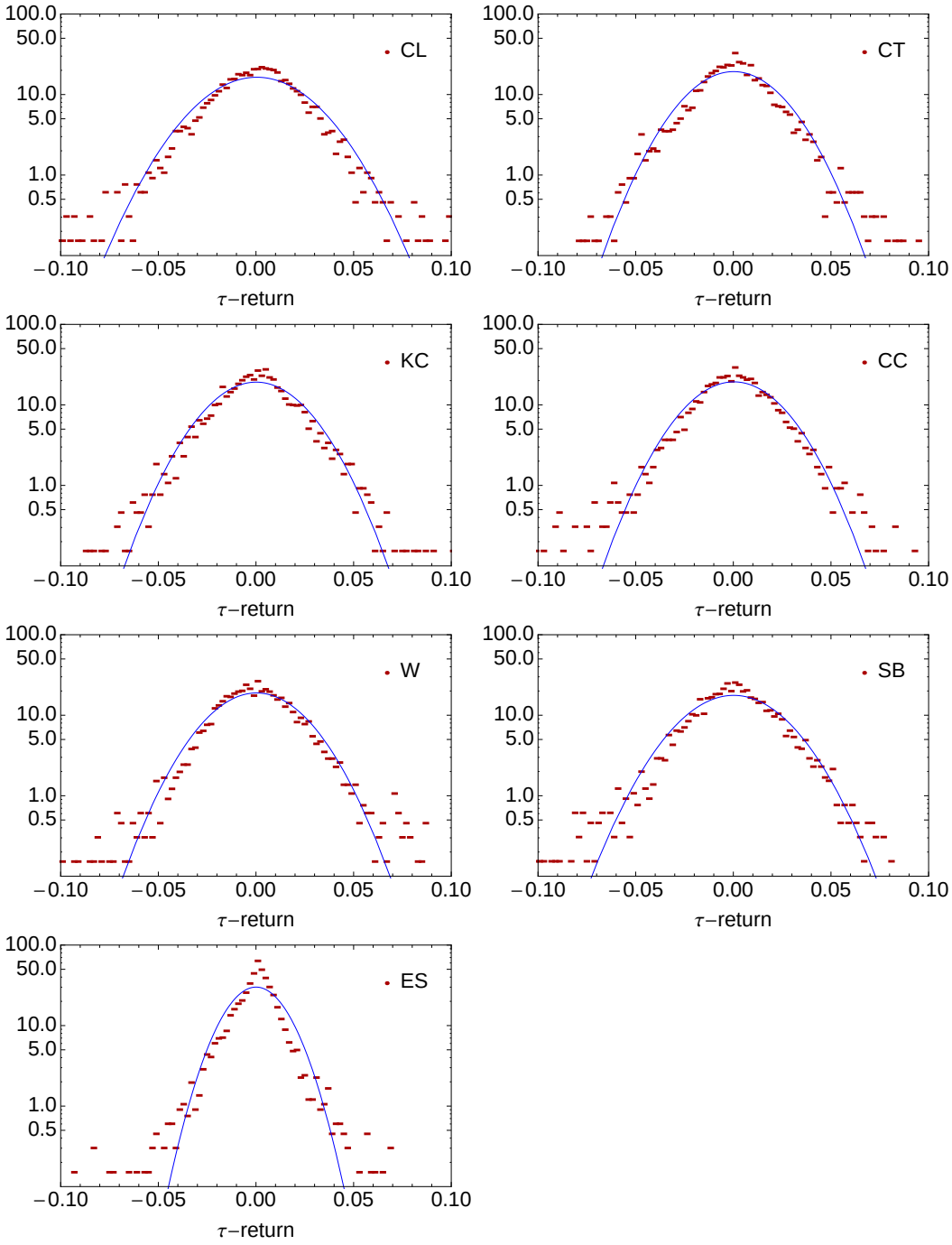

Figure 5.17: Histograms of daily log-returns of selected futures

The τ-return autocorrelation and variance for the 10 year data (01/11/2004-31/11/2014) are displayed in figure 5.18. We find positively correlated τ-returns at smaller times up to 100 days for most futures but purely negative correlations for cocoa and wheat. For larger τ the autocorrelation function is negative and seems to approach -0.5 for all assets but cocoa.

Crude oil

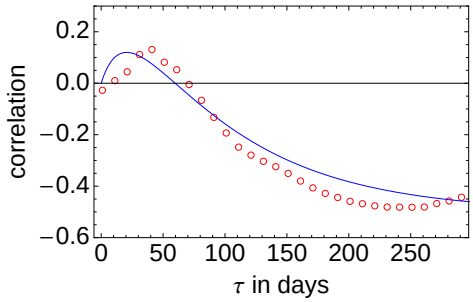

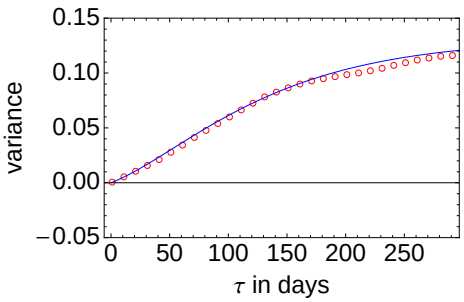

Cotton

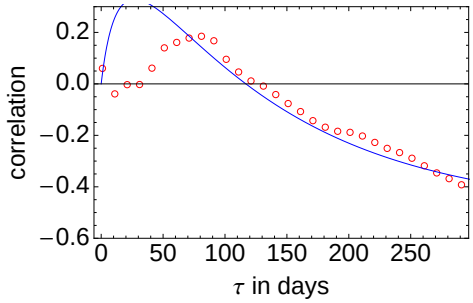

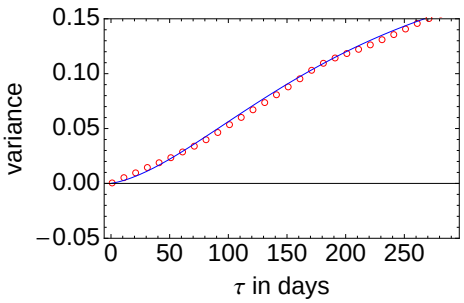

Cocoa

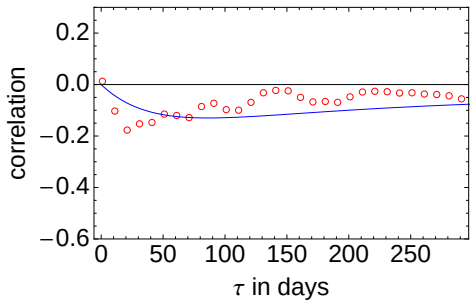

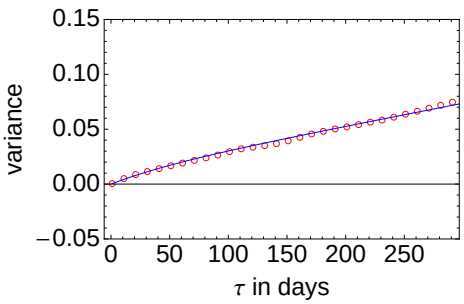

Corn

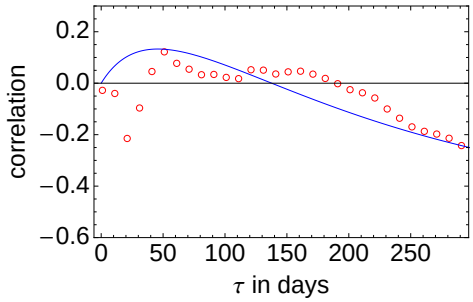

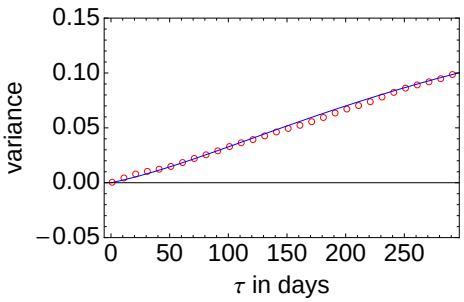

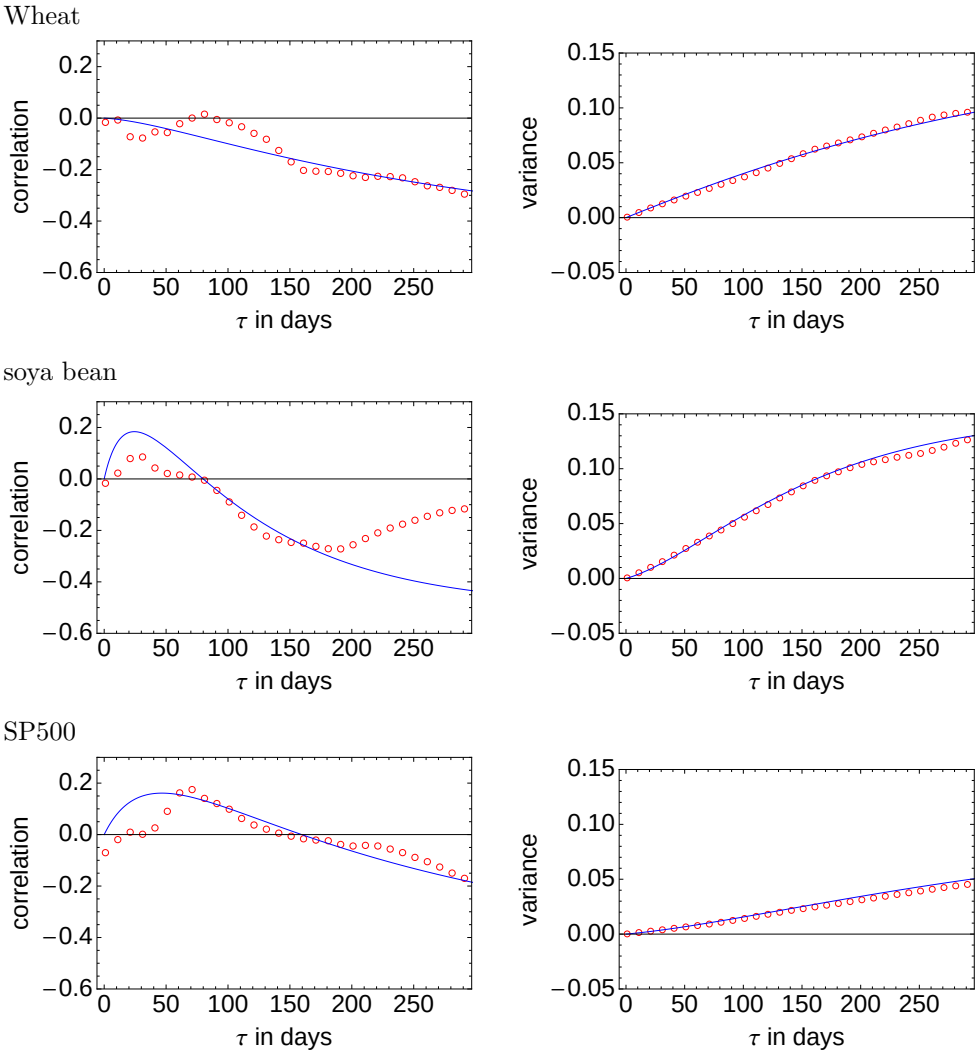

Figure 5.18: Autocorrelation and variance of returns for selected futures

The parameters estimated from fitting the empirical data are summarised in table 5.6. We note that the κ and δ parameters are widely spread without any obvious patterns. For all futures (except cocoa and wheat) the parameter σ is smaller than σ_{GBM} which was fitted under the assumption of the geometrical Brownian motion price process at $\tau = 100$. The largest deviation $\Delta\sigma$ is found for cotton with 18.3 vols.

futures underlyings	κ	δ	λ	σ	σ_x	η	σ_{GBM}	$\Delta\sigma = \sigma - \sigma_{\text{GBM}}$
crude oil	5.10	4.70	1.00	0.386	4.88	0.00	0.471	-0.085
cotton	4.15	2.80	1.00	0.254	3.94	0.00	0.438	-0.183
cocoa	6.85	0.01	1.00	0.388	1.90	0.00	0.328	0.059
corn	1.70	2.85	1.00	0.284	1.65	0.00	0.377	-0.093
wheat	5.25	1.10	1.00	0.396	2.24	0.00	0.371	0.024
soya bean	4.00	4.50	1.00	0.332	4.30	0.00	0.458	-0.126
S&P500	3.95	1.01	1.00	0.188	1.40	0.00	0.232	-0.044

Table 5.6: parameters for futures

5.5 Summary and Impact on Option Prices

The fitting of the bivariate OU τ-return autocorrelation and variances to real market data was a quite difficult undertaking. To obtain a sufficient sample size 10 year closing prices had to be used. Nevertheless, the remaining fitting errors can be quite substantial which can be seen in the large deviations between market data and the fit of the τ-return autocorrelation.

For all assets (except cocoa and wheat) the σ parameter was usually smaller than σ_{GBM}. The same is observed for implied volatilities. As the historical volatility σ_{GBM} measures the past volatility (as it look back in time) and the implied volatility looks into the future the bivariate OU model can be located somewhere in the middle as it also look into the past but uses the autocorrelation to include some future influence.

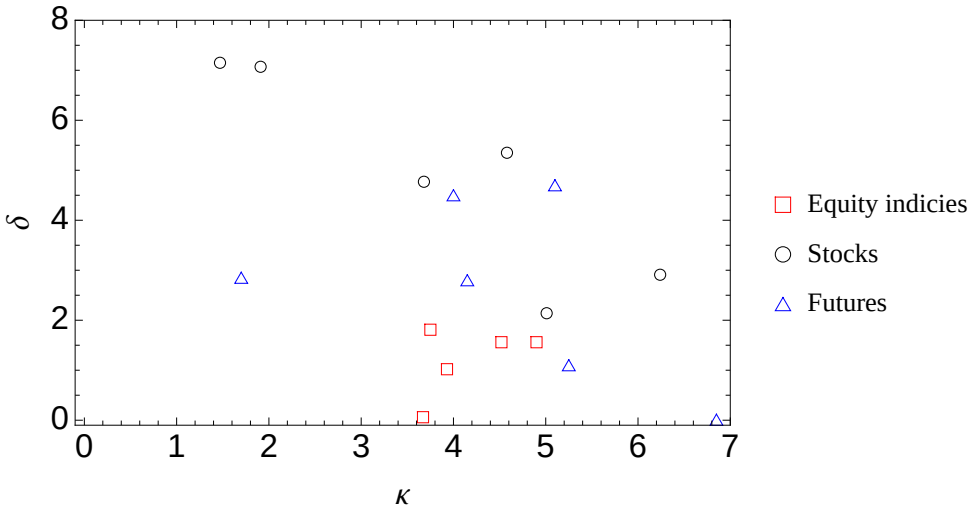

Figure 5.19: Scatter plot of the found fit parameters κ and δ

Scatter plot (fig. 5.19) of the found fit parameters κ and δ we can see that all equity indices can be found in a rather confined region. For stocks this region is harder to see and for futures no particular region can be found. Nevertheless, a larger sample size of assets are necessary to come to a conclusive answer.

call price/strike	σ =0.15	0.20	0.25	0.30	0.35
indicies, stocks					
OTM (95%)	0.0113	0.0196	0.0284	0.0375	0.0467
ATM	0.0311	0.0411	0.0510	0.0610	0.0709
ITM (105%)	0.0638	0.0723	0.0815	0.0910	0.1006
futures					
OTM (95%)	0.0107	0.0188	0.0275	0.0365	0.0457
ATM	0.0298	0.0398	0.0497	0.0596	0.0695
ITM (105%)	0.0618	0.0705	0.0797	0.0892	0.0989

Table 5.7: Relative call prices C_{BS}/K for option with a 3-month expiry and $r = 0.01$

Finally we want to analyse the impact on option prices. Therefore we selected European call options with a three month expiry which is typical for liquid single name calls. The results are shown in figure 5.7. Assuming an ATM call (strike 100 and $\sigma_{\mathrm{GBM}} = 0.30$) the option price drops from 6.10 to 5.10 if we replace the σ_{GBM} by a bivariate OU parameter $\sigma = 0.20$.

Chapter 6

Trending OU Jump-Diffusion

The jump-diffusion process proposed by Merton [M76] to model stock returns as a mix of both continuous diffusion and and discontinuous jumps can be written as

$$ds_t = \mu dt + \sigma dW_t + \log J_t dN_t. \tag{6.1}$$

where $s_t = \log S_t$ and N_t is a Poisson process with amplitude λ. Our goal is now to model predictability within a jump-diffusion framework to see if this extension allows for a change in the τ-return autocorrelation function in the same way the extension to the bivariate OU process did.
There are several possibilities for the extension

1. predictable diffusion

$$ds_t = (\mu - \kappa[s_t - s_0 - \mu t])\, dt + \sigma dW_t + \log J_t dN_t \tag{6.2}$$

2. predictable jumps

$$ds_t = \mu dt + \sigma dW_t + \log J_t dN_t \tag{6.3}$$
$$d \log J_t = -\delta \log J_t dt + \sigma_J dW_t^{(J)} \tag{6.4}$$

3. predictable diffusion and jumps

$$ds_t = (\mu - \kappa[s_t - s_0 - \mu t])\, dt + \sigma dW_t + \log J_t dN_t \tag{6.5}$$
$$d \log J_t = -\delta \log J_t dt + \sigma_J dW_t^{(J)} \tag{6.6}$$

Unfortunately only the predictable diffusion seems to have an analytic solution and is therefore presented here. The detrending OU process (with $q_t = s_t - \mu t$) and with

jump term (we assume a jump amplitude with $\log J_t \sim \mathcal{N}(\mu_J, \sigma_J^2)$ can then be written as

$$dq_t = \kappa \left(q_0 - q_{t^-}\right) dt + \sigma dW_t + \log J_t dN_t \tag{6.7}$$

Then we can use the ansatz $e^{\kappa t} q_t$ and write

$$d(e^{\kappa t} q_t) = \kappa e^{\kappa t} q_t dt + e^{\kappa t} dq_t + \kappa^2 e^{\kappa t} q_t dt^2 + ... \tag{6.8}$$

With Itôs lemma and $dN_t^2 = dN_t$ we have

$$d(e^{\kappa t} q_t) = \kappa e^{\kappa t} q_t dt + \sigma e^{\kappa t} dW_t + e^{\kappa t} \log J_t dN_t \tag{6.9}$$

and therefore

$$q_t = q_0 + \sigma \int_0^t e^{-\kappa(t-u)} dW_u + \int_0^t e^{-\kappa(t-u)} \log J_u dN_u. \tag{6.10}$$

Since

$$\int_t^T e^{-\kappa(T-u)} \log J_u dN_u = \sum_{i=N_t}^{N_T} e^{-\kappa(T-t_i)} \log J_i = \sum_{i=1}^{N_{T-t}} e^{-\kappa(T-t-t_i)} \log J_i \tag{6.11}$$

where J_i is the random jump size occurring at time t_i and $N_{T-t} = N_T - N_t$ is the total number of jumps in the interval $(t, T]$ we can write subsequently

$$q_t = q_0 + \sigma \int_0^t e^{-\kappa(t-u)} dW_u + \sum_{i=1}^{N_t} e^{-\kappa(t-t_i)} \log J_i. \tag{6.12}$$

Using the moment generating function

$$\phi_J(\xi) = \mathbb{E}\left[e^{\xi J}\right] \tag{6.13}$$

we can the moment generating function of $Y_t = \sum_{i=1}^{N_t} e^{-\kappa(t-t_t)} J_i$ is given by

$$\phi_Y(\xi, t) = e^{\lambda \int_0^t [\phi_J(\xi e^{-\kappa s}) - 1] ds}. \tag{6.14}$$

The mean and the variance of Y_t are then given by $\frac{\partial^2 \phi_Y(0,t)}{\partial \xi^n}$ with $n = 1, 2$

$$\mathbb{E}\left[\sum_{i=1}^{N_{T-t}} e^{-\kappa(T-t-t_i)} \log J_i\right] = \frac{\lambda \mu_J}{\kappa} \left[1 - e^{-\kappa(T-t)}\right] \tag{6.15}$$

$$\text{var}\left[\sum_{i=1}^{N_{T-t}} e^{-\kappa(T-t-t_i)} \log J_i\right] = \frac{\lambda}{2\kappa} (\mu_J^2 + \sigma_J^2) \left[1 - e^{-2\kappa(T-t)}\right] \tag{6.16}$$

which leads to

$$\mathbb{E}\left[q_t\right] = q_0 + \frac{\lambda\mu_J}{\kappa}\left[1 - e^{-\kappa t}\right] \tag{6.17}$$

$$\text{var}\left[q_t\right] = \frac{\sigma^2}{2\kappa}[1 - e^{-2\kappa t}] + \frac{\lambda}{2\kappa}(\mu_J^2 + \sigma_J^2)\left[1 - e^{-2\kappa t}\right]. \tag{6.18}$$

Now we can calculate the τ-return (and restricting ourselves to $\mu_J = 0$)

$$\begin{aligned} r_\tau(t) &= s_t - s_{t-\tau} \\ &= q_t - q_{t-\tau} + \mu\tau \\ &= \mu\tau + \sigma\int_0^t e^{-\kappa(t-u)}dW_u - \sigma\int_0^{t-\tau} e^{-\kappa(t-u)}dW_u \\ &\quad + \sum_{i=1}^{N_t} e^{-\kappa(t-t_i)}\log J_i - \sum_{i=1}^{N_{t-\tau}} e^{-\kappa(t-\tau-t_i)}\log J_i \end{aligned} \tag{6.19}$$

and the moments can be obtain from a straightforward calculation

$$\mathbb{E}\left[r_\tau(t)\right] = \mu\tau \tag{6.20}$$

$$\text{var}\left[r_\tau(t)\right] = \frac{\sigma^2 + \lambda\sigma_J^2}{\kappa}\left[1 - e^{-\kappa\tau}\right]. \tag{6.21}$$

$$\text{cov}[r_\tau(t - k\tau), r_\tau(t)] = -\frac{\sigma^2 + \lambda\sigma_J^2}{2\kappa}e^{-\kappa(k-1)\tau}(1 - e^{-\kappa\tau})^2 \tag{6.22}$$

$$\begin{aligned} \text{corr}[r_\tau(t - k\tau), r_\tau(t)] &= \frac{-\frac{\sigma^2+\lambda\sigma_J^2}{2\kappa}e^{-\kappa(k-1)\tau}(1 - e^{-\kappa\tau})^2}{\sqrt{\frac{\sigma^2+\lambda\sigma_J^2}{\kappa}\left[1 - e^{-\kappa\tau}\right]}\sqrt{\frac{\sigma^2+\lambda\sigma_J^2}{\kappa}\left[1 - e^{-\kappa\tau}\right]}} \\ &= -\frac{1}{2}e^{-\kappa(k-1)\tau}(1 - e^{-\kappa\tau}) \end{aligned} \tag{6.23}$$

The τ-return autocorrelation function is exactly the same as case of the trending OU model without jump diffusion (bound between $(-\frac{1}{2}, 0]$). Therefore the addition of jumps leads to no new behaviour in the autocorrelation modelling.

For completeness and future reverence we note that the call price for the trending OU jump diffusion model is given by the standard Merton equation

$$C_M(S(t), T - t, K, r, \sigma^2) = \sum_{n=0}^{\infty}\frac{e^{-\lambda'(T-t)}[\lambda'(T-t)]^n}{n!}C_{BS}(S(t), T - t, K, r_n, \sigma_n^2) \tag{6.24}$$

with

$$\begin{aligned} \lambda' &= \lambda e^{\frac{\sigma_J^2}{2}} \\ r_n &= r - \lambda\left(e^{\frac{\sigma_J^2}{2}} - 1\right) + \frac{n}{T-t}\frac{\sigma_J^2}{2} \\ \sigma_n^2 &= \sigma^2 + \frac{n}{T-t}\sigma_J^2. \end{aligned} \tag{6.25}$$

For $\lambda \to 0$ only the first term ($n = 0$) in series expansion is non-vanishing and the Merton price is equal to the Black-Scholes price.

Chapter 7

Application for Interest Rates

7.1 Model Description

In chapter 4 we used the bivariate OU process (4.2) to model equity log-returns. The mean reversion property build into the model makes it interesting to investigate if it is also applicable to model interest rates.
A simple substitution of the log-return by the instantaneous short-rate leads to a two-factor short-rate model as shown in figure 7.1

$$dr_t = (\theta(t) - \kappa r_t + X_t)\, dt + \sigma dW_t \tag{7.1}$$

$$dX_t = -\delta X_t dt + \sigma_x dW_t^{(x)}. \tag{7.2}$$

This model could not be found in the available textbook literature [B09, F09, R03, S00, S03, T02, T12] as the known two-factor interest rate models (generalised Vasicek and Longstaff-Schwartz model) model the short rate as a sum of correlated Gaussian or CIR processes which is quite different from our approach. For an overview of existing models see figure 7.1.

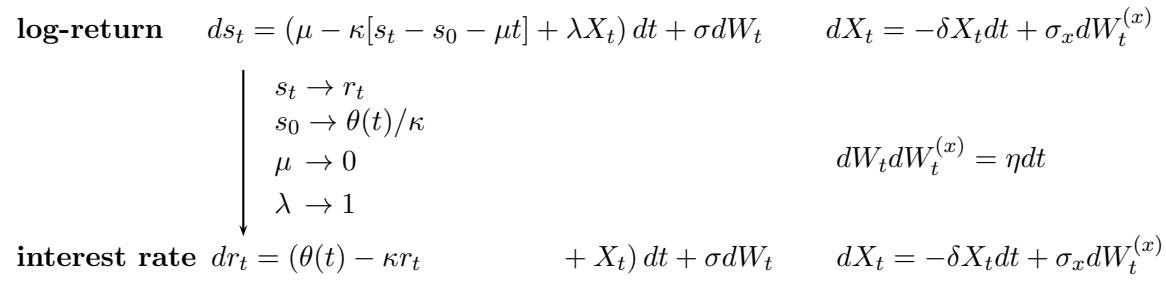

Figure 7.1: Transformation of the bivariate trending OU model to an interest rate model

model	*short rate dynamics*
one-factor	
Vasicek	$dr_t = \kappa(\theta - r_t)dt + \sigma dW_t$
Cox-Ingersoll-Ross	$dr_t = \kappa(\theta - r_t)dt + \sigma\sqrt{r_t}dW_t$
Ho-Lee	$dr_t = \theta(t)dt + \sigma dW_t$
Hull-White	$dr_t = \kappa(\theta(t) - r_t)dt + \sigma dW_t$
Black-Karasinski	$d(\log r_t) = \kappa(t)(\theta(t) - \log r_t)dt + \sigma(t)dW_t$
Black-Derman-Toy	$d(\log r_t) = -\frac{\sigma'(t)}{\sigma(t)}(\theta(t) - \log r_t)dt + \sigma(t)dW_t$
two-factor	
Generalized Vasicek	$dr_t = dx_t^1 + dx_t^2 + \theta(t)dt$
	$dx_t = -\theta_i(t)x_t^i dt + \sigma_i dW_t^{(i)}, \qquad dW^{(1)}dW^{(2)} = \rho dt$
Longstaff-Schwartz	$dr_t = dx_t^1 + dx_t^2$
	$dx_t = a_i(b_i - x_t^i)dt + \sigma_i\sqrt{x_t^i}dW_t^{(i)}$, $dW^{(1)}dW^{(2)} = \rho dt$

Table 7.1: Overview of interest rate models

Nevertheless, we believe that the simplicity of the model makes it likely that it might has been considered elsewhere before but the rather involved analytical solution prevented publication in the standard literature.
Writing the short rate process in the slightly different from

$$dr_t = \left(\kappa\left[\frac{\theta(t) - X_t}{\kappa} - r_t\right]\right)dt + \sigma dW_t \tag{7.3}$$

we can see that the short rate is reverting to a fluctuating reversion level with constant reversion speed κ where the reversion level itself is a scaled sum of deterministic function $\theta(t)$ and and a stochastic process X_t which is itself mean reverting to zero with speed δ.

7.2 Analytic Solution

Application of Itôs lemma gives for a T-bond price $P(t,T)$ gives

$$\begin{aligned} dP(t,T) &= \frac{\partial P}{\partial t}dt + \frac{\partial P}{\partial r}dr + \frac{\partial P}{\partial X}dX + \frac{1}{2}\frac{\partial^2 P}{\partial X \partial r}dXdr + \frac{1}{2}\frac{\partial^2 P}{\partial r^2}dr^2 + \frac{1}{2}\frac{\partial^2 P}{\partial X^2}dX^2 \\ &= \frac{\partial P}{\partial t}dt + \frac{\partial P}{\partial r}([\theta - \kappa r + X]dt + \sigma dW) + \frac{\partial P}{\partial X}(-\delta X dt + \sigma_x dW^{(x)}) \\ &\quad + \frac{1}{2}\frac{\partial^2 P}{\partial X \partial r}\sigma\sigma_x\eta dt + \frac{1}{2}\frac{\partial^2 P}{\partial r^2}\sigma^2 dt + \frac{1}{2}\frac{\partial^2 P}{\partial X^2}\sigma_x^2 dt \end{aligned} \tag{7.4}$$

which leads to a partial differential equation for the bond price $P(t,T)$

$$\frac{\partial P}{\partial t}+\frac{\partial P}{\partial r}[\theta(t)-\kappa r+X]-\frac{\partial P}{\partial X}\delta X+\frac{1}{2}\frac{\partial^2 P}{\partial X\partial r}\sigma\sigma_x\eta+\frac{1}{2}\frac{\partial^2 P}{\partial r^2}\sigma^2+\frac{1}{2}\frac{\partial^2 P}{\partial X^2}\sigma_x^2-rP=0. \tag{7.5}$$

As the considered model appears to be affine we assume a solution of the standard form [O12]

$$P(t,T)=e^{A(t,T)-B(t,T)r-C(t,T)X}. \tag{7.6}$$

Substituting this ansatz into (7.5) yields

$$\begin{aligned}\left(\frac{\partial A(t,T)}{\partial t}-\frac{\partial B(t,T)}{\partial t}r-\frac{\partial C(t,T)}{\partial t}X\right)P(t,T)-(\theta(t)-\kappa r+X)P(t,T)B(t,T)\\ +P(t,T)C(t,T)\delta X+P(t,T)B(t,T)C(t,T)\sigma\sigma_x\eta+\frac{1}{2}P(t,T)B(t,T)^2\sigma^2\\ +\frac{1}{2}P(t,T)C(t,T)^2\sigma_x^2-rP(t,T)=0.\end{aligned} \tag{7.7}$$

Separating the r and X terms gives a system of three differential equations

$$\begin{aligned}\frac{\partial A(t,T)}{\partial t}-B(t,T)\theta(t)+B(t,T)C(t,T)\sigma\sigma_x\eta\\ +\frac{1}{2}B^2(t,T)\sigma^2+\frac{1}{2}C^2(t,T)\sigma_x^2=0 &(7.8)\\ \frac{\partial B(t,T)}{\partial t}-\kappa B(t,T)+1=0 &(7.9)\\ \frac{\partial C(t,T)}{\partial t}+B(t,T)+\delta C(t,T)=0 &(7.10)\end{aligned}$$

The homogeneous solution of (7.9) is given by

$$B_{\text{hom}}(t,T)=c\,e^{\kappa t} \tag{7.11}$$

Variation of parameters gives $B(t,T)=c_B(t)\,e^{\kappa t}$ gives by substitution back into (7.9)

$$c_B(t)=\frac{1}{\kappa}e^{-\kappa t}+c_0 \tag{7.12}$$

With the boundary condition $B(T,T)=0$ we find $c_0=-e^{-\kappa T}/\kappa$ which gives finally

$$B(t,T)=\frac{1}{\kappa}\left(1-e^{-\kappa(T-t)}\right). \tag{7.13}$$

The homogeneous solution of (7.10) is given by

$$C_{\text{hom}}(t,T)=c_C\,C^{\delta t} \tag{7.14}$$

Variation of parameters gives $C(t,T) = c_C(t)\, e^{\delta t}$ gives by substitution back into the differential equation

$$c_C = \frac{1}{\kappa(\kappa-\delta)} e^{-\kappa T + (\kappa-\delta)t)} + \frac{1}{\kappa\delta} e^{-\delta t} + c_1 \tag{7.15}$$

With the boundary condition $C(T,T) = 0$ we find

$$c_1 = -e^{-\delta T}\left(\frac{1}{\kappa\delta} - \frac{1}{\kappa(\kappa-\delta)}\right) \tag{7.16}$$

and therefore

$$C(t,T) = \frac{1}{\kappa(\kappa-\delta)} e^{-\kappa(T-t)} + \frac{1}{\kappa\delta} + \frac{1}{\delta(\delta-\kappa)} e^{-\delta(T-t)}. \tag{7.17}$$

In the next step we show how the function $\theta(t)$ has to be calibrated (similar to the Ho-Lee model) so that the discount function matches the observed discount function exactly.
Integration of (7.9) gives

$$\begin{aligned}\int_0^T \frac{\partial A(u,T)}{\partial u} du &= A(T,T) - A(0,T) \\ &= \int_0^T B(u,T)\theta(u) - B(u,T)C(t,T)\sigma\sigma_x\eta - \frac{1}{2}B^2(u,T)\sigma^2 - \frac{1}{2}C^2(u,T)\sigma_x^2 du.\end{aligned} \tag{7.18}$$

With $A(T,T) = 0$ we can compute the derivative with respect to T using the Leibnitz rule

$$\begin{aligned}\frac{\partial}{\partial T}A(0,T) &= -\int_0^T \frac{\partial B(u,T)}{\partial T}\theta(u)du - B(T,T)\theta(T) \\ &\quad + \int_0^T \frac{\partial}{\partial T}\left(B(u,T)C(u,T)\sigma\sigma_x\eta + \frac{1}{2}B^2(u,T)\sigma^2 + \frac{1}{2}C^2(u,T)\sigma_x^2\right)du \\ &\quad + B(T,T)C(T,T)\sigma\sigma_x\eta + \frac{1}{2}B^2(T,T)\sigma^2 + \frac{1}{2}C^2(T,T)\sigma_x^2 \\ &= -\int_0^T \frac{\partial B(u,T)}{\partial T}\theta(u)du \\ &\quad - \left(B(0,T)C(0,T)\sigma\sigma_x\eta + \frac{1}{2}B^2(0,T)\sigma^2 + \frac{1}{2}C^2(0,T)\sigma_x^2\right)\end{aligned} \tag{7.19}$$

and another differentiation gives

$$\begin{aligned}\frac{\partial^2}{\partial T^2}A(0,T) &= -\int_0^T \frac{\partial^2 B(u,T)}{\partial T^2}\theta(u)du - \left.\frac{\partial B(u,T)}{\partial T}\right|_{u=T}\theta(T) \\ &\quad - \frac{\partial}{\partial T}\left(B(0,T)C(0,T)\sigma\sigma_x\eta + \frac{1}{2}B^2(0,T)\sigma^2 + \frac{1}{2}C^2(0,T)\sigma_x^2\right)\end{aligned} \tag{7.20}$$

with $\partial B(u,T)/\partial T|_T = 1$ and $\partial^2 B(u,T)/\partial T^2 = -\kappa \partial B(u,T)/\partial T$

$$\begin{aligned}
\theta(T) &= -\int_0^T \frac{\partial^2 B(u,T)}{\partial T^2}\theta(u)du - \frac{\partial^2}{\partial T^2}A(0,T) \\
&\quad - \frac{\partial}{\partial T}\left(B(0,T)C(0,T)\sigma\sigma_x\eta + \frac{1}{2}B^2(0,T)\sigma^2 + \frac{1}{2}C^2(0,T)\sigma_x^2\right) \\
&= \kappa\int_0^T \frac{\partial B(u,T)}{\partial T}\theta(u)du - \frac{\partial^2}{\partial T^2}A(0,T) \\
&\quad - \frac{\partial}{\partial T}\left(B(0,T)C(0,T)\sigma\sigma_x\eta + \frac{1}{2}B^2(0,T)\sigma^2 + \frac{1}{2}C^2(0,T)\sigma_x^2\right) \\
&= -\kappa\frac{\partial}{\partial T}A(0,T) - \frac{\partial^2}{\partial T^2}A(0,T) \\
&\quad - \kappa\left(B(0,T)C(0,T)\sigma\sigma_x\eta + \frac{1}{2}B^2(0,T)\sigma^2 + \frac{1}{2}C^2(0,T)\sigma_x^2\right) \\
&\quad - \frac{\partial}{\partial T}\left(B(0,T)C(0,T)\sigma\sigma_x\eta + \frac{1}{2}B^2(0,T)\sigma^2 + \frac{1}{2}C^2(0,T)\sigma_x^2\right) \qquad (7.21)
\end{aligned}$$

where we used (7.19) in the second step. With (7.6) we obtain

$$A(0,T) = \log P(0,T) + B(0,T)r_0 + C(0,T)X_0 \qquad (7.22)$$

$$\frac{\partial A(0,T)}{\partial T} = -f(0,T) + \frac{\partial B(0,T)}{\partial T}r_0 + \frac{\partial C(0,T)}{\partial T}X_0 \qquad (7.23)$$

$$\frac{\partial^2 A(0,T)}{\partial T^2} = -\frac{\partial f(0,T)}{\partial T} + \frac{\partial^2 B(0,T)}{\partial T^2}r_0 + \frac{\partial^2 C(0,T)}{\partial T^2}X_0 \qquad (7.24)$$

therefore

$$\begin{aligned}
\theta(T) &= \kappa f(0,T) + \frac{\partial f(0,T)}{\partial T} \\
&\quad - \kappa\left(B(0,T)C(0,T)\sigma\sigma_x\eta + \frac{1}{2}B^2(0,T)\sigma^2 + \frac{1}{2}C^2(0,T)\sigma_x^2\right) \\
&\quad - \frac{\partial}{\partial T}\left(B(0,T)C(t,T)\sigma\sigma_x\eta + \frac{1}{2}B^2(0,T)\sigma^2 + \frac{1}{2}C^2(0,T)\sigma_x^2\right) \qquad (7.25)
\end{aligned}$$

where we used $X_0 = 0$. Now we can integrate (7.10)

$$\begin{aligned}
\int_0^t \frac{\partial A(u,T)}{\partial u}du &= A(t,T) - A(0,T) \\
&= \int_0^t B(u,T)\theta(u)du - \int_0^t B(u,T)C(t,T)\sigma\sigma_x\eta - \frac{1}{2}B^2(u,T)\sigma^2 \\
&\quad - \frac{1}{2}C^2(u,T)\sigma_x^2 du. \qquad (7.26)
\end{aligned}$$

which yields with (7.22)

$$A(t,T) = \log P(0,T) + B(0,T)r_0 + \int_0^t B(u,T)\theta(u)du \\ - \int_0^t B(u,T)C(t,T)\sigma\sigma_x\eta - \frac{1}{2}B^2(u,T)\sigma^2 - \frac{1}{2}C^2(u,T)\sigma_x^2 du. \tag{7.27}$$

with (7.25) the θ integral can be written as

$$\begin{aligned}
\int_0^t B(u,T)\theta(u) = &\int_0^t \left(1 - e^{-\kappa(T-u)}\right) f(0,u)du + B(u,T)f(0,u)|_0^t \\
&- \int_0^t \frac{\partial B(u,T)}{\partial u} f(0,u)du \\
&- \kappa \int_0^t B(u,T)\left(B(0,u)C(0,u)\sigma\sigma_x\eta + \frac{1}{2}B^2(0,u)\sigma^2 + \frac{1}{2}C^2(0,u)\sigma_x^2\right)du \\
&- B(u,T)\left(B(0,u)C(0,u)\sigma\sigma_x\eta + \frac{1}{2}B^2(0,u)\sigma^2 + \frac{1}{2}C^2(0,u)\sigma_x^2\right)\Bigg|_0^t \\
&+ \int_0^t \frac{\partial B(u,T)}{\partial u}\left(B(0,u)C(0,u)\sigma\sigma_x\eta + \frac{1}{2}B^2(0,u)\sigma^2 + \frac{1}{2}C^2(0,u)\sigma_x^2\right)du \\
= &- \log P(0,t) + B(t,T)f(0,t) - B(0,T)r_0 \\
&- \kappa \int_0^t B(u,T)\left(B(0,u)C(0,u)\sigma\sigma_x\eta + \frac{1}{2}B^2(0,u)\sigma^2 + \frac{1}{2}C^2(0,u)\sigma_x^2\right)du \\
&- B(t,T)\left(B(0,t)C(0,t)\sigma\sigma_x\eta + \frac{1}{2}B^2(0,t)\sigma^2 + \frac{1}{2}C^2(0,t)\sigma_x^2\right) \\
&+ \int_0^t \frac{\partial B(u,T)}{\partial u}\left(B(0,u)C(0,u)\sigma\sigma_x\eta + \frac{1}{2}B^2(0,u)\sigma^2 + \frac{1}{2}C^2(0,u)\sigma_x^2\right)du
\end{aligned} \tag{7.28}$$

where we used $f(0,0) = r_0$ and

$$\begin{aligned}
\int_0^t f(0,u)du &= -\int_0^t \frac{\partial \log P(0,u)}{\partial u}du \\
&= -\log P(0,t).
\end{aligned} \tag{7.29}$$

$A(t,T)$ can now be obtained from substituting $B(t,T)$ and $C(t,T)$ and straightfor-

ward but long calculation leads to

$$
\begin{aligned}
A(t,T) &= \log\frac{P(0,T)}{P(0,t)} + B(t,T)f(0,t) \\
&\quad - B(t,T)\left(B(0,t)C(0,t)\sigma\sigma_x\eta + \frac{1}{2}B^2(0,t)\sigma^2 + \frac{1}{2}C^2(0,t)\sigma_x^2\right) \\
&\quad - \kappa\int_0^t B(u,T)\left(B(0,u)C(0,u)\sigma\sigma_x\eta + \frac{1}{2}B^2(0,u)\sigma^2 + \frac{1}{2}C^2(0,u)\sigma_x^2\right)du \\
&\quad + \int_0^t \frac{\partial B(u,T)}{\partial u}\left(B(0,u)C(0,u)\sigma\sigma_x\eta + \frac{1}{2}B^2(0,u)\sigma^2 + \frac{1}{2}C^2(0,u)\sigma_x^2\right)du \\
&\quad - \int_0^t B(u,T)C(t,T)\sigma\sigma_x\eta - \frac{1}{2}B^2(u,T)\sigma^2 - \frac{1}{2}C^2(u,T)\sigma_x^2 du \\
&= \log\frac{P(0,T)}{P(0,t)} + B(t,T)f(0,t) \\
&\quad + \left(-\frac{1}{4\kappa^3} + \frac{e^{-2\kappa t}}{4\kappa^3} - \frac{e^{-\kappa(t+T)}}{2\kappa^3} + \frac{e^{\kappa(t-T)}}{2\kappa^3} - \frac{e^{2\kappa(t-T)}}{4\kappa^3} + \frac{e^{-2\kappa T}}{4\kappa^3}\right)\sigma^2 \\
&\quad + \left(\frac{1}{2\kappa(\delta+\kappa)} - \frac{\delta e^{-t(\delta+\kappa)}}{\kappa\left(\delta^2-\kappa^2\right)} + \frac{e^{-2\kappa t}}{2\kappa(\delta-\kappa)} - \frac{\delta e^{2\kappa(t-T)}}{2\kappa(\delta-\kappa)(\delta+\kappa)} - \frac{e^{-\kappa(t+T)}}{\kappa(\delta-\kappa)}\right. \\
&\quad \left. + \frac{e^{-\delta t-\kappa T}}{\kappa(\delta-\kappa)} - \frac{e^{2\kappa(t-T)}}{2(\delta-\kappa)(\delta+\kappa)} + \frac{e^{(\delta+\kappa)(t-T)}}{(\delta-\kappa)(\delta+\kappa)} + \frac{e^{-2\kappa T}}{2\kappa(\delta-\kappa)} - \frac{e^{-T(\delta+\kappa)}}{(\delta-\kappa)(\delta+\kappa)}\right)\eta\sigma\sigma_x \\
&\quad + \left(-\frac{\delta^4+5\delta^3\kappa-5\delta\kappa^3+3\kappa^4}{4\delta^3\kappa^3(\delta-\kappa)^2(\delta+\kappa)} + \frac{e^{-\delta t}}{\delta^3\kappa^2} + \frac{(2\delta-\kappa)e^{-2\delta t}}{4\delta^3\kappa(\delta-\kappa)^2} + \frac{e^{-2\kappa t}}{4\kappa^3(\delta-\kappa)^2}\right. \\
&\quad - \frac{e^{-t(\delta+\kappa)}}{\kappa^2(\delta-\kappa)^2(\delta+\kappa)} - \frac{e^{\delta(t-T)}}{\delta^3\kappa(\delta-\kappa)} - \frac{e^{2\delta(t-T)}}{4\delta^3(\delta-\kappa)^2} - \frac{(\delta+\kappa)e^{\kappa(t-T)}}{2\delta^2\kappa^3(\kappa-\delta)} - \frac{e^{\kappa(t-T)-\delta t}}{\delta^2\kappa^2(\delta-\kappa)} \\
&\quad - \frac{e^{\kappa(t-T)-2\delta t}}{2\delta^2\kappa(\kappa-\delta)^2} - \frac{e^{-\kappa(t+T)}}{2\kappa^3(\kappa-\delta)^2} - \frac{e^{2\kappa(t-T)}}{4\kappa^3(\delta-\kappa)^2} + \frac{e^{-\delta t-\kappa T}}{\delta\kappa^2(\kappa-\delta)^2} + \frac{e^{(\delta+\kappa)(t-T)}}{\delta\kappa(\delta-\kappa)^2(\delta+\kappa)} \\
&\quad \left. + \frac{e^{-\delta T}}{\delta^3\kappa(\delta-\kappa)} + \frac{e^{-2\delta T}}{4\delta^3(\delta-\kappa)^2} + \frac{e^{-2\kappa T}}{4\kappa^3(\delta-\kappa)^2} - \frac{e^{-T(\delta+\kappa)}}{\delta\kappa(\delta-\kappa)^2(\delta+\kappa)}\right)\sigma_x^2.
\end{aligned}
\tag{7.30}
$$

As we now found analytic expressions for $A(t,T)$, $B(t,T)$ and $C(t,T)$ we are able to express the bond price $P(t,T)$ as a function of the model parameters.
The continuously compounded forward rate is then given by

$$
\begin{aligned}
f(t,T) &= -\frac{\partial \log P(t,T)}{\partial T} && (7.31)\\
&= -\frac{\partial A}{\partial T} + \frac{\partial B}{\partial T}r + \frac{\partial C}{\partial T}X. && (7.32)
\end{aligned}
$$

Applying Itôs lemma gives

$$\begin{aligned} df(t,T) &= \frac{\partial f}{\partial t}dt + \frac{\partial f}{\partial r}dr + \frac{\partial f}{\partial x}dx + \frac{1}{2}\frac{\partial^2 f}{\partial r^2}dr^2 + \frac{1}{2}\frac{\partial^2 f}{\partial u^2}du^2 + \frac{1}{2}\frac{\partial^2 f}{\partial r \partial x}drdx \\ &= \frac{\partial f}{\partial t}dt + \frac{\partial B}{\partial T}dr + \frac{\partial C}{\partial T}dx \\ &= \left(\frac{\partial f}{\partial t} + \frac{\partial B}{\partial T}(\theta(t) - \kappa r + x) - \frac{\partial C}{\partial T}\delta x\right)dt + \frac{\partial B}{\partial T}\sigma dW_t + \frac{\partial C}{\partial T}\sigma_x dW_t. \end{aligned} \quad (7.33)$$

Variance of the forward rate is then easily obtained

$$\begin{aligned} \mathrm{var} f(t,T) &= \left(\frac{\partial B(t,T)}{\partial T}\sigma\right)^2 + \left(\frac{\partial C(t,T)}{\partial T}\sigma_x\right)^2 + 2\sigma\sigma_x\eta\frac{\partial B(t,T)}{\partial T}\frac{\partial C(t,T)}{\partial T} \quad (7.34) \\ &= \sigma_x^2\frac{\left(e^{-\delta(T-t)} - e^{-\kappa(T-t)}\right)^2}{(\kappa-\delta)^2} + 2\eta\sigma\sigma_x\frac{e^{-\kappa(T-t)}\left(e^{-\delta(T-t)} - e^{-\kappa(T-t)}\right)}{\kappa-\delta} + \sigma^2 e^{-2\kappa(T-t)}. \end{aligned}$$

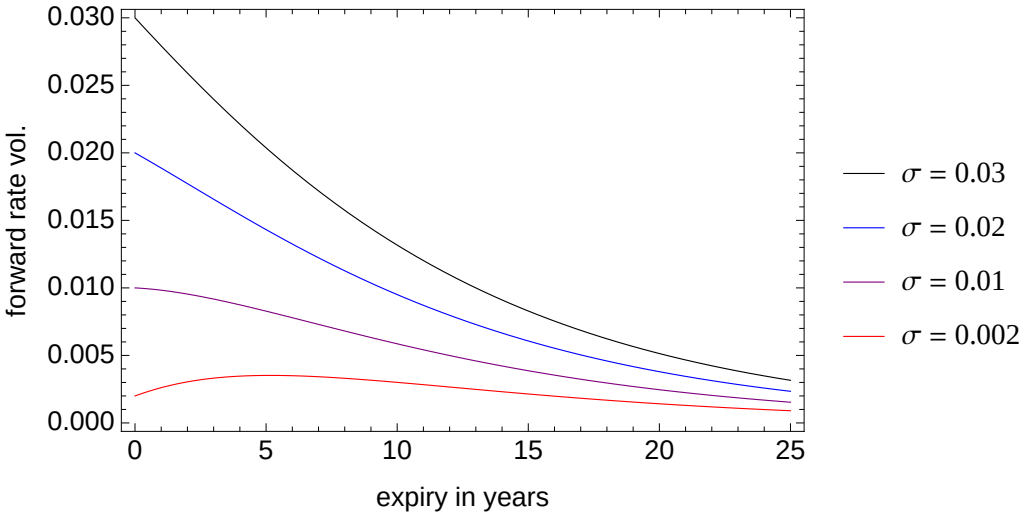

Figure 7.2: Forward rate volatility of the model for for parameters $\kappa = 0.1$, $\sigma = 0.2$,$\sigma_x = 0.001$ and $\eta = 0.9$

Now we can calculate the variance of the bond price by

$$\begin{aligned} \mathrm{Var}[P(t,T)] &= \sigma^2\int_0^t [B(u,T) - B(u,T)]^2\,du + \sigma_x^2\int_0^t [C(u,T) - C(u,T)]^2\,du \\ &\quad + 2\rho\sigma\sigma_x\int_0^t [B(u,T) - B(u,T)]\,[C(u,T) - C(u,T)]\,du \\ &= \left(-\frac{e^{-2t\kappa}}{2\kappa^3} - \frac{e^{-2T\kappa}}{2\kappa^3} + \frac{e^{-2(T-t)\kappa}}{2\kappa^3} - \frac{e^{-(T-t)\kappa}}{\kappa^3} + \frac{e^{-(t+T)\kappa}}{\kappa^3} + \frac{1}{2\kappa^3}\right)\sigma^2 \\ &+ \left(-\frac{2e^{(t-T)\delta}}{\delta\kappa(\delta+\kappa)(\kappa-\delta)} - \frac{2e^{-T(\delta+\kappa)}}{\delta\kappa(\delta+\kappa)(\kappa-\delta)} - \frac{2e^{(t-T)\kappa}}{\delta\kappa(\delta+\kappa)(\kappa-\delta)}\right. \\ &\left. + \frac{2e^{(t-T)(\delta+\kappa)}}{\delta\kappa(\delta+\kappa)(\kappa-\delta)} - \frac{2e^{-(\delta+\kappa)t}}{\delta\kappa(\delta+\kappa)(\kappa-\delta)} + \frac{2e^{-T\delta-t\kappa}}{\delta\kappa(\delta+\kappa)(\kappa-\delta)}\right) \end{aligned}$$

$$
\begin{aligned}
&+\frac{2e^{-t\delta-T\kappa}}{\delta\kappa(\delta+\kappa)(\kappa-\delta)}+\frac{2}{\delta\kappa(\delta+\kappa)(\kappa-\delta)}+\frac{e^{-2t\kappa}}{\kappa^3(\kappa-\delta)}\\
&-\frac{2e^{-(t+T)\kappa}}{\kappa^3(\kappa-\delta)}+\frac{2e^{(t-T)\kappa}}{\kappa^3(\kappa-\delta)}+\frac{e^{-2T\kappa}}{\kappa^3(\kappa-\delta)}-\frac{e^{2\kappa(t-T)}}{\kappa^3(\kappa-\delta)}-\frac{1}{\kappa^3(\kappa-\delta)}\Bigg)\eta\sigma_x\sigma\\
&+\Bigg(-\frac{e^{-2t\delta}}{2\delta^3(\kappa-\delta)^2}+\frac{e^{-(t+T)\delta}}{\delta^3(\kappa-\delta)^2}-\frac{e^{-2T\delta}}{2\delta^3(\kappa-\delta)^2}+\frac{e^{2\delta(t-T)}}{2\delta^3(\kappa-\delta)^2}-\frac{e^{t\delta-T\delta}}{\delta^3(\kappa-\delta)^2}\\
&+\frac{1}{2\delta^3(\kappa-\delta)^2}-\frac{e^{-2t\kappa}}{2\kappa^3(\kappa-\delta)^2}+\frac{e^{-(t+T)\kappa}}{\kappa^3(\kappa-\delta)^2}-\frac{e^{(t-T)\kappa}}{\kappa^3(\kappa-\delta)^2}-\frac{e^{-2T\kappa}}{2\kappa^3(\kappa-\delta)^2}\\
&+\frac{e^{2\kappa(t-T)}}{2\kappa^3(\kappa-\delta)^2}+\frac{1}{2\kappa^3(\kappa-\delta)^2}+\frac{2e^{\delta(t-T)}}{\delta\kappa(\kappa-\delta)^2(\delta+\kappa)}+\frac{2e^{-(\delta+\kappa)T}}{\delta\kappa(\kappa-\delta)^2(\delta+\kappa)}\\
&+\frac{2e^{(t-T)\kappa}}{\delta\kappa(\kappa-\delta)^2(\delta+\kappa)}-\frac{2e^{(t-T)(\delta+\kappa)}}{\delta\kappa(\kappa-\delta)^2(\delta+\kappa)}+\frac{2e^{-(\delta+\kappa)t}}{\delta\kappa(\kappa-\delta)^2(\delta+\kappa)}\\
&-\frac{2e^{-T\delta-t\kappa}}{\delta\kappa(\kappa-\delta)^2(\delta+\kappa)}-\frac{2e^{-t\delta-T\kappa}}{\delta\kappa(\kappa-\delta)^2(\delta+\kappa)}-\frac{2}{\delta\kappa(\kappa-\delta)^2(\delta+\kappa)}\Bigg)\sigma_x^2
\end{aligned}
\tag{7.35}
$$

Due to the fact that the model is Gaussian the price of an European call option (floor let) with maturity T and strike K on a zero bond with notional N and maturity S is given by the Black formula.

$$
\mathrm{ZBC}(t,T,S,N,K)=NP(t,S)\mathcal{N}(d_1)-P(t,T)K\mathcal{N}(d_2) \tag{7.36}
$$

with

$$
\begin{aligned}
d_1&=\frac{\log\frac{P(t,S)/P(t,T)}{K}+\frac{1}{2}\hat{\sigma}^2}{\hat{\sigma}}\\
d_2&=d_1-\hat{\sigma}\\
\hat{\sigma}&=\mathrm{Var}[P(t,T)].
\end{aligned}
\tag{7.37}
$$

Figure 7.3 shows the volatility term structure for the EUR market as of 09/03/2015 obtained from the Bloomberg VCUB (using Black Vol IBOR).

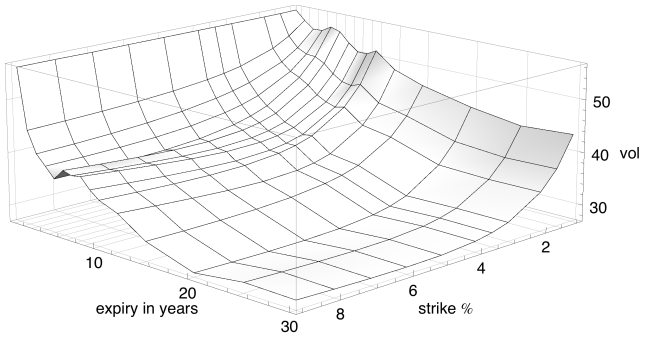

Figure 7.3: Term structure of the cap/Floor volatility for the EUR market as of 09/03/2015

To evaluate the flexibility of the model we selected volatility term structures for various pre- and post crisis dates in figure 7.4.

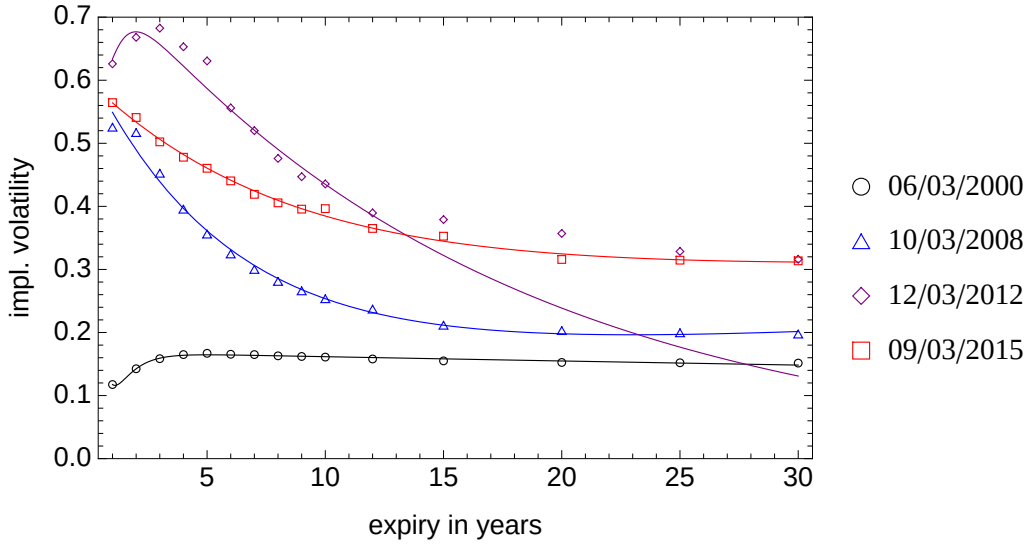

Figure 7.4: Cap/Floor volatility curves implied by the model calibrated to the at-the-money EUR cap volatility curve for various dates

The shapes of the term structure changes considerably over time. Nevertheless, the five parameters of the model allow for rather accurate fits. The obtained parameters are summarised in table 7.2.

date	κ	δ	σ	σ_x	η
06/03/2000	1.296	0.0043	0.402	0.218	-0.48
10/03/2008	0.162	0.0088	0.620	0.021	-0.81
12/03/2012	1.650	0.9810	1.261	0.026	+0.98
09/03/2015	0.094	0.0026	0.598	0.025	-0.75

Table 7.2: Fitted model parameter for volatility term structure

Conclusion

In this thesis we have presented an overview of applications of the trending Ornstein-Uhlenbeck and its extensions in mathematical finance. We gave a thorough analysis of the work of Lo and Wang [LW95] in which they showed the impact of autocorrelation in the underlying returns (predictability) on option pricing. Beginning with the trending OU process we derived and improved all analytic results which were only stated in the paper. It was shown that this models allows for a non-vanishing (negative) autocorrelation function via an additional parameter κ. Although this new underlying process does not alter the Black-Scholes formula the joint parameter estimation of κ and σ gives in general a volatility which differs from σ estimated under the assumption of a geometric Brownian motion and therefore alters the option price. The influence of predictability on option prices (via σ) was analysed.
In a next step we investigated the extension of the model to a bivariate version. This more complex model allows for a partly positive τ-return autocorrelation function. We gave a rigorous proof of the of the fair option pricing formula and studied the practical impact on the option pricing.
Furthermore we implemented a Monte Carlo Code to simulate (bivariate) trending OU processes and analysed possible issues of the parameter estimation. We found that using closing prices around 10 year of data are needed to obtain relatively stable numerical results. This almost rules out any practical use of the model. A solution could be the use of intraday ticking prices and could be subject of future investigations.
The analysis of market data for equity indices, stock and futures showed that the bivariate trending OU process in general produces lower volatilities than the standard geometric Brownian motion. Nevertheless, due to the substantial fitting errors which originated from the small data size a conclusive answer could not be given on the basis of daily closing data.
In addition we extended the trending OU process to a jump diffusion process. Although the model remained to be solvable analytically the τ-return autocorrelation

function showed no new features and remained purely negative.
Finally we used the bivariate trending OU process to build an interest rate model. The model is solvable analytically although the long analytical expressions make it rather unattractive as the intuition offered be simpler model is lost in this case.

Appendix A

Important Theorems

The following theorems are just stated informally (see Øksendal [O00], Bjork [B09] and Delbaen et.al. [DS06] for more details).

A.1 The Feynman-Kac Theorem

The Feynman-Kac theorem allows to express the solution of a given partial differential equation as the expected value of a function of a suitable diffusion process whose drift and diffusion coefficient are defined in terms of the PDE coefficients.

Feynman-Kac Theorem *Given Lipschitz continuous* $a(t,x), b(t,x), f(t,x)$ *and* $k(t,x)$ *and a smooth* $\phi(x)$*, the solution of the Cauchy problem on* $[0,T] \times \mathbb{R}$

$$\frac{\partial F(t,x)}{\partial t} + a(t,x)\frac{\partial F(t,x)}{\partial x} + \frac{1}{2}b^2(t,x)\frac{\partial^2 F(t,x)}{\partial x^2} + f(t,x) = k(t,x)F(t,x)$$

with the boundary condition

$$F(T,x) = \phi(x)$$

can be expressed as the expected value

$$F(t,x) = \widetilde{\mathbb{E}}\left[\int_t^T f(t,X_u)e^{-\int_t^u k(s,X_s)ds}du + \phi(X_T)e^{-\int_t^T k(s,X_s)ds}\middle| X_t = x\right]$$

where the diffusion process X *has the dynamics, starting from* x *at time* t*, given by*

$$dX_s = a(s,X)ds + b(s,X)d\widetilde{W}_s$$

under the probability measure $\widetilde{\mathbb{P}}$*. The process* $\widetilde{W}$ *is a standard Brownian motion under* $\widetilde{\mathbb{P}}$*.*

A.2 The Girsanov Theorem

The Girsanov theorem shows how a stochastic differential equation changes due to changes in the associated probability measure. It is based on the fact that the drift depends on the particular probability measure of the probability space $(\Omega, \mathcal{F}, (\mathcal{F}_t)_t, \mathbb{P})$ and that if the probability measure is changed, the drift of the equation changes while the diffusion coefficient remains the same. The Girsanov theorem can be thus useful when it is desired to modify the drift coefficient of a SDE.

Girsanov Theorem *Consider the stochastic differential equation*

$$dX_t = a(t, X)dt + b(t, X)dW_t$$

under $\mathbb{P}$ *and let* γ_s *be a process adapted to the filtration generated by the Brownian motion. If we define a new probability measure* $\widetilde{\mathbb{P}}$ *by*

$$L_t = \left.\frac{d\widetilde{\mathbb{P}}}{d\mathbb{P}}\right|_{\mathcal{F}_t} = e^{\int_0^t \gamma_s dW_s - \frac{1}{2}\int_0^t \gamma_s^2 ds}$$

then $\widetilde{\mathbb{P}}$ *is equivalent to* $\mathbb{P}$*. Moreover the process* $\widetilde{W}$ *defined by*

$$d\widetilde{W}_t = dW_t - \gamma_t dt$$

is a Brownian motion under $\widetilde{\mathbb{P}}$ *and*

$$dX_t = (a(t, X) + b(t, X)\gamma_t)dt + b(t, X)d\widetilde{W}_t.$$

Furthermore if X *is measurable then the expectation under* $\mathbb{P}$ *is given by*

$$\widetilde{\mathbb{E}}[X_t|\mathcal{F}_s] = \mathbb{E}\left[X_t \frac{L_t}{L_s}\middle|\mathcal{F}_s\right]$$

A.3 The Martingale Representation Theorem

Martingale Representation Theorem *Let* $\mathcal{F}_t$ *be the filtration for a Brownian motion* W *and let* M *any continuous* $\mathcal{F}_t$*-adapted martingale. Then there exists a uniquely defined* $\mathcal{F}_t$*-adapted process* ϕ_s *such that*

$$M_t = M_0 + \int_0^t \phi_s dW_s.$$

A.4 Fundamental Theorems of Asset Pricing

Consider a market model with a numeraire and N risky asset with a priori given asset price processes $S_0, S_1, ..., S_N$ under the objective measure $\mathbb{P}$.
A probability measure $\widetilde{\mathbb{P}}$ is called an equivalent martingale measure for the market model if it has the properties

1. $\widetilde{\mathbb{P}}$ is equivalent to $\mathbb{P}$ on $\mathcal{F}_t$ ($\widetilde{\mathbb{P}} \sim \mathbb{P}$)
2. all price processes $S_0/S_0, S_1/S_0, ..., S_N/S_0$ are martingales under $\widetilde{\mathbb{P}}$

First Fundamental Theorem *A market model is free of arbitrage essentially if and only if there exists a martingale measure.*
To be exact the diffuse term *essentially* means that a slightly stricter condition than no arbitrage is needed to guarantee the existence of a martingale measure. Instead there is a condition called *No free lunch with vanishing risk* (NFLVR) which is equivalent to the existence of arbitrage in a general continuous time market model [DS94].

Second Fundamental Theorem *Assume that the market is arbitrage free and consider a fixed numeraire asset S_0. Then the market is complete if and only if the martingale measure $\widetilde{\mathbb{P}}$, corresponding to the numeraire S_0, is unique.*

Bibliography

[AP10] Andersen, L.B.G, Piterbarg, V.V. (2010) *Interest Rate Modeling, Volume I: Foundations and Vanilla Models.*, Atlantic Financial Press.

[B28] Brown, R. (1828) *A brief account of microscopical observations made in the months of June, July and August, 1827, on the particles contained in the pollen of plants; and on the general existence of active molecules in organic and inorganic bodies.* Phil. Mag. 4, 161-173.

[B09] Bjork, T. R. (2009) *Arbitrage Theory in Continuous Time.* 3rd ed, Oxford University Press.

[B12] Baz, J. (2012) *Oxford Lecture Notes: Interest Rate Models* Oxford University.

[BCK92] Bollerslev, T., Chou, R.Y., Korner, K.F. (1992) *ARCH modeling in finance : A review of the theory and empirical evidence* Journal of Econometrics 52, 5-59.

[BS73] Black, F., Scholes, M. (1973) *The pricing of options and corporate liabilities.* Journal of Political Economy 81, 637-654.

[CLM97] Campbell, J.Y., Lo, A.W., MacKinley, A.C. (1997) *The Econometrics of Financial Markets.* Princeton University Press.

[C01] Cont, R. (2001) *Empirical properties of asset returns: stylized facts and statistical issues.* Quantitative Finance, 1, 223-236.

[C05] Cont, R. (2005) *Long range dependence in financial markets* In Fractals in Engineering: New Trends in Theory and Applications, Springer.

[DS94] Delbaen, F., Schachermayer, W. (1994) *A general version of the fundamental theorem of asset pricing.* Mathematische Annalen 300 463-520.

[DS06] Delbaen, F., Schachermayer, W. (2006) *The Mathematics of Arbitrage.* Springer.

[E05] Einstein, A. (1905) *Ueber die von der molekularkinetischen Theorie der Waerme geforderte Bewegung von in ruhenden Fluessigkeiten suspendierten Teilchen.*, Annalen der Physik 322 (8) 549-560.

[F09] Filipovic, D. (2009) *Term-Structure Models.* Springer.

[FF88a] Fama, E., French, K. (1988) *Permanent and temporary components of stock prices* Journal of Political Economics. 22, 3-26.

[FF88b] Fama, E., French, K. (1988) *Permanent and temporary components of stock prices* Journal of Political Economics. 22, 3-26.

[G05] Geman, H. (2005) *Commodities and Commodity Derivatives*, Wiley.

[KS87] Karatzas, I., Shreve, S.E. (1987) *Brownian Motion and Stochastic Calculus*, Springer.

[L08] Lemons, D.S., Gythiel, A. (1997) *Paul Langevins 1908 paper On the Theory of Brownian Motion [Sur la theorie du mouvement brownien, C. R. Acad. Sci. (Paris) 146, 530533 (1908)]*, Am. J. Phys. 65, 1079.

[LS01] Liptser, R.S., Shiryaev, A.N. (2001) *Statstics of Random Processes* Springer.

[L90] Lo, A.W. (1990) *When are contrarian profits due to stock market overreactions*, Review of Financial Studies 3, 175-206.

[LM88] Lo, A.W., MacKinlay, A.C. (1988) *Stock market prices do not follow random walks: Evidence from a simple specification test*, Review of Financial Studies 1, 41-66.

[LW95] Lo, A.W., Wang, J. (1995) *Implementing option pricing models when asset returns are predictably*, Journal of Finance 50, 87-129.

[M73] Merton, R. (1973) *Rational theory of option pricing*, Bell Journal of Economics and Management Science 4, 141-183.

[M76] Merton, R. (1976) *Option pricing when underlying stock returns are discontinuous*, Journal of Financial Economics 3, 125-144.

[O00] Øksendahl, B. (2000) *Stochastic Differential Equations - An Introduction with Applications*, 5th ed. Springer.

[O12] Oosterlee, C.W. (2012) *Oxford Lecture Notes: Courier Methods in Computational Finance* Oxford University.

[OU30] Uhlenbeck, G.E., Ornstein, L.S. (1930) *On the theory of Brownian motion*, Physical Review 36, 823-84.

[R03] Rebonato, R. (2003) *There-Structure Models: a Review* Oxford University.

[R14] Ruf, J. (private communication).

[RY99] Revuz, D., Yor, M. (1999) *Continuous Martingales and Brownian Motion.* Springer.

[S00] Shreve, S.E. (2000) *Stochastic Calculus for Finance - Continuous-Time Models.* Springer.

[S03] Sadr, A. (2003) *Interest Rate Swaps and Their Derivatives.* Wiley.

[T02] Tuckman, B. (2002) *Fixed Income Securities - Tools for Today's Markets.* 2rd ed, Wiley.

[T08] Thierfelder, C. (2009), Ph.D. thesis, Massey University Auckland, New Zealand

[T12] Theis, J. (2012) *Oxford Lecture Notes: Modelling Interest Rate Derivatives* Oxford University.

[W23] Wiener, N. (1923) *Differential space*, Journal of Mathematical Physics 2, 131-174.